Fibre-Reinforced Polymer Bridges Guidance for Engineers

A feasibility study of fibre-reinforced polymer and its design

Jim Sjöö Sonesson | Master Thesis | Division of Structural Engineering | Faculty of Engineering | Lund University | 2019

Fibre-Reinforced Polymer Bridges
Guidance for Engineers

A feasibility study of fibre reinforced polymer and its design

Jim Sjöö Sonesson

LUND
UNIVERSITY

Master Thesis, Report: TVBK-5270, Division of Structural Engineering, Faculty of Engineering, Lund University, Lund, 2019

Fibre-reinforced polymer bridges – Guidance for Engineers
A feasibility study of fibre-reinforced polymer and its design

Fiberarmerade polymerbroar – Rekommendationer för praktiskt konstruktörsarbete

Jim Sjöö Sonesson
2019

Report TVBK-5270
ISSN 0349–4969
ISRN: LUTVDG/TVBK-19/5270 (75p)

Examensarbete/Master Thesis
Handledare/Supervisors:
Jonas Niklewski (LTH) och Erik Olsson (ELU Konsult AB)

Avdelningen för konstruktionsteknik
Lunds tekniska högskola
Lunds universitet
Box 118
221 00 Lund

www.kstr.lth.se

Division of Structural Engineering
Faculty of Engineering, LTH
Lund University
P.O. Box 118
SE-221 00 Lund
Sweden

www.kstr.lth.se/english

ABSTRACT

The use of fibre reinforced polymers (FRP) in bridge applications have been rising over the last couple of years. The material is strong relative to its weight and is highly customisable in both form and performance. There is however no standardised design code available and the experience within the industry is limited. Henderson and Mottram (2018) recently published a guideline for the design of FRP bridges using the available design provisions given by Ascione et al. (2016). With the use of these two publications, this thesis evaluates the possibility to design an FRP bridge and the feasibility of such a bridge relative to conventional alternatives.

Three types of FRP bridges are designed using the previously mentioned available documentation and FEA in BRIGADE/Plus: glass fibre with polyester (GFRP), pultruded GFRP using the same materials as the former, and carbon fibre with epoxy (CFRP). Each bridge is designed to cover three spans as simply supported bridges. The bridges are then compared to a predesigned reference bridge. The reference bridge is continuous over the three spans and consists of stress-laminated timber. Furthermore, the reference bridge is re-designed as a simply supported bridge to enable a fair comparison. Finally, the main difficulties in applying the current guidelines are commented on and future recommendations are provided.

The FRP bridges are found to fulfil the ULS and the deflectional limitations set, but depending on the vibrational comfort limitations they may not be a good alternative to the continuous reference bridge. They do however show similar behaviour to that of the simply supported timber bridge. Improvements of the design in combination with mass tuned dampers are discussed as a solution to deal with some of the shortcomings, making FRP a viable choice.

The literature study concludes that the material offers environmental improvements to that of the more conventional materials, in particular steel and concrete. The study does however not conclude the same for the economic aspects. FRP bridges are in most cases found to be more expensive than bridges of other materials. However, as knowledge and experience on FRP in bridge applications increases, the cost is predicted to decrease.

From the literature study, it can also be concluded that the design of FRP is heavily dependent on the choice of conversion factor and the material partial factors, which are dependent on the uncertainties involved. At the extreme, material dimensions are found to vary up to 57 %. Furthermore, the conversion factors are found hard to determine. Some are not yet well defined and some environmental impacts on the material are still to be evaluated.

SAMMANFATTNING

Användandet av fiberarmerade polymerer (FRP) som material vid brobyggnad har ökat över de senaste åren. Materialet är starkt i förhållande till sin vikt och kan anpassas både form- och styrkemässigt. Det finns dock ingen standardiserad dimensioneringskod tillgänglig och erfarenheten av materialet i branschen är begränsat. Därav har Henderson och Mottram (2018) publicerat en guide för hur man ska använda de nuvarande dimensioneringsråden utgivna av Ascione et al. (2016). Baserat på dessa två publikationer ämnar sig denna rapport till att utvärdera möjligheterna till att dimensionera en FRP-bro och till att utvärdera dennas konkurranskraftighet.

Tre broar dimensioneras med tre typer av FRP med hjälp av de tidigare nämnda publikationerna och med FEM-analys i BRIGADE/Plus: glasfiber med polyester (GFRP), pultruerad FRP bestående av samma material samt kolfiber med epoxi (CFRP). Var och en av broarna är konstruerade för att täcka tre span som tre på varandra följande enkelt upplagda broar. Vidare jämförs broarna med en referensbro bestående av en kontinuerlig bro över alla tre span i tvärspänt limträ. Denna bro är dock, för jämförelses skull, omgjord till att som FRP-broarna bestå av tre enkelt upplagda broar. Utöver jämförelsen mellan dessa broar undersöks även konstruktionsprocessen av FRP-broarna.

FRP-broarna finnes uppfylla såväl dimensioneringskraven i brottsgränstillstånd som nedböjningskrav. Dock anses dem inte vara ett bra alternativ till den kontinuerliga bron då komfortnivåerna med hänsyn till vibrationer understiger vad som anses lämpligt. GFRP-broarna inses dock ha ungefärligen samma dynamiska respons som de enkelt upplagda träbroarna. Genom förbättringar av materialets struktur, brons utformning och med hjälp av justerade massdämpare anses dock alla FRP-broar kunna bli ett gångbara alternativ.

Den genomförda litteraturstudien visar på att FRP medför miljömässiga förbättringar jämfört med de mer konventionella materialen, vilket vidare styrker att FRP är ett bra alternativ i brobyggnad. Studien visar dock inte på samma fördelar när de ekonomiska aspekterna undersöks. FRP inses i de flesta studier till att vara ett dyrare alternativ jämfört med konventionella material. Det finns dock en studie som tyder på att FRP i framtiden kan bli det billigare alternativet i takt med att kunskapen om materialet ökar.

Litteraturstudien visar också på att de nödvändiga dimensionerna av FRP är starkt beroende på valet av konverteringsfaktor och materialets partialfaktorer. De erforderliga dimensionerna kan skilja med så mycket som 57 % beroende på val av faktorer. Vidare visar studien på att konverteringsfaktorerna kan vara svårbestämda. Vissa är ännu inte väldefinierade och vissa påverkningar från klimatet på materialet är ej undersökta.

PREFACE

This master's thesis was carried out during the spring of 2019 as a cooperation between the Division of Structural Engineering at Lund's Faculty of Engineering, LTH, and ELU Konsult AB. The thesis accomplishes five years of studies and comprises 30 credits for the Master of Science in civil engineering.

I would like to thank my supervisor Erik Olsson at ELU Konsult for his patience with my constant stream of questions and for his guidance throughout the whole process. I am also grateful for the valuable comments on my report and the help I have received from my supervisor Jonas Nikelewski. I would also like to thank my colleagues at ELU Konsult in Malmö for their support and for making the time more joyful.

Finally, I would like to thank my friends and family for their support through my five years at LTH. Without you this would not have been possible.

Lund, June 2019

Jim Sjöö Sonesson

NOTATIONS

Notations used in the thesis where a description is not provided in the text.

Roman letters

E	Young's modulus
E_1	Young's modulus in the longitudinal direction
E_2	Young's modulus in the transverse direction
E_{f1}	Young's modulus of fibre in the longitudinal direction
E_{f2}	Young's modulus of fibre in the transverse direction
E_R	Young's modulus of resin/matrix
G_{12}	Shear modulus in the main plane
G_f	Shear modulus of the fibre
G_R	Shear modulus of resin/matrix
Q	Stiffness
V_f	Volume fibre fraction

Greek letters

γ	Shear strain
ε	Strain
κ	Curvature
ρ	Density
ν	Poissons' ratio
ν_f	Poissons' ratio of fibre
ν_R	Poissons' ratio of resin/matrix
σ	Stress
τ	Shear stress
ω_0	Fundamental frequency

GLOSSARY

CFRP	**C**arbon **F**ibre-**R**einforced **P**olymer
CLT	**C**lassical **L**aminate **T**heory
EOTA	**E**uropean **O**rganisation for **T**echnical **A**ssessment
FEA	**F**inite **E**lement **A**nalysis
FRP	**F**ibre-**R**einforced **P**olymer
GFRP	**G**lass **F**ibre-**R**einforced **P**olymer
SLS	**S**erviceability **L**imit **S**tate
ULS	**U**ltimate **L**imit **S**tate

Contents

1 Introduction

1.1 Background

The use of fibre reinforced polymers (FRP) in bridge applications have been rising over the most recent years. The material has previously been used mostly as a complement to other materials but is now also used as the main structural elements. FRP brings several benefits over the more traditional construction materials. Henderson and Mottram (2018) mention that the most prominent benefits include its high strength to weight ratio, the high resistance to corrosion and its degree of customisability.

The strength and the density vary depending on the materials used in the composite as well as the composition of them. According to Henderson and Mottram, the weight of FRP bridges commonly end up between 30 to 50 % of that of a steel bridge and about 25 % of that of a concrete bridge.

Due to the resistance to corrosion, the need for maintenance is significantly reduced compared to bridges built with traditional materials. In turn, the FRP alternative remains a viable option even though its initial costs are high (Daniel 2003, Henderson & Mottram 2018 and Patljak 2018). Furthermore, costs can be reduced in other aspects such as during the installation of the bridge. The bridges can be prefabricated, shipped to the site and lifted into place, hence reducing the traffic interference and the associated costs which tend to be relatively high.

The shape of the material can be chosen practically without limitations, allowing for unique architectural expressions and structural optimisation. Due to its directional properties, the material can be optimised for the specific stress distribution at hand (Henderson & Mottram 2018, Nijssen 2015 and Agarwal & Broutman 1990).

The material also suffers from several drawbacks. The costs of raw materials and processing are high, recycling is not yet well developed and the knowledge on structural behaviour concerning details and connections is limited (Nijssen 2015). The largest obstacle to use the material in bridge engineering is however the lack of experience in the industry in combination with the absence of a standardised design code. A design code in the form of a Eurocode is in development, but in the meantime a pre-normative document has been released by Ascione et al. (2016). This document is however not yet considered final and can in some instances be hard to interpret, which is the reason for a guideline being published by Henderson & Mottram (2018). The two publications have not yet been integrated and adopted by the industry where design guides made by the manufacturers, such as Fiberline Composites A/S (2002), are used instead.

1.2 Objective

The main objective of this thesis is to investigate the feasibility of using FRP as a material in bridge design. This is done by answering the following questions:

1. Is it possible to make a preliminary design of an FRP bridge using the documentation provided by Ascione et al. (2016) and Henderson and Mottram (2018)?
2. How will design assumptions linked to environmental factors and material production affect the final design?
3. Could an FRP bridge be a viable alternative to bridges made out of more conventional materials such as steel, wood or concrete?
4. How would the use of different types of FRP affect the final design?

1.3 Scope and Limitations

The scope of the report is limited to simply supported pedestrian FRP bridges, subject only to vertical forces. The analysis is made both for the serviceability limit state (SLS), analysing deflection and vibration, and the ultimate limit state (ULS), analysing strength and local stability. Fatigue will however not be considered since the fatigue load cycles are not expected to exceed 5000, nor are the considered bridges assumed to be very sensitive to wind (Ascione et al. 2016 and Henderson & Mottram 2018).

The design of the bridge does not include any critical details, connections or joints. Furthermore, the analysis is limited to first-ply failure theories, not considering crack propagation and ductility of the material. Finally, no impact loads are considered.

1.4 Method

To give an understanding of the material, a literature study covering the main aspects of FRP as a material, its production process, its failure mechanisms and the theories linked to its structural behaviour is made. The literature study lay the foundation on which the analytical part of the report is based.

Three bridges consisting of different types of FRP are designed using finite element analysis (FEA). The FEA is performed using the software BRIGADE/Plus version 6.1, developed by Scanscot Technology AB. The software is based on Abaqus FEA, developed by Simulia, but with the addition of frequently used functions required in bridge engineering. Apart from using the design codes provided by Ascione et al. (2016) and guideline provided by Henderson and Mottram (2018), the analysis is made according to the European standards, Eurocode (Swedish standards institute, 2002 A & 2002 B).

Two of the three types of FRP materials employed consists of glass fibre in combination with a polyester matrix (GFRP). In one of these cases the GFRP is produced using a layup production method and in the other case pultrusion. The final bridge consists of carbon fibres in combination with epoxy (CFRP) constructed using a layup production method. These three bridges are compared to each other as well as to a predesigned reference bridge designed from stress-laminated timber. In order to compare the FRP bridges to the reference bridge, the designs are made as similar as possible.

2 The Material

2.1 Overview

A composite material consists of at least two macroscopically identifiable materials, creating a new homogeneous material with optimised properties. FRP composites consist of fibre reinforcement mixed within a polymer resin, called matrix, creating a material with properties exceeding that of the resin alone (Nijssen 2015). However, these properties can vary depending on the composition of the material and on the production method used. This makes the material versatile with a high ability to be engineered to a specific cause. However, it also means that the material is difficult to cover with one set of structural codes.

2.2 Structure of the Material

FRP is usually made up by several layers, plies, which are usually about 0,5 mm thick and stacked in a specific arrangement creating a laminate. The individual layers usually contain a single layer of fibre, either unidirectional or multidirectional. The fibres of the plies are stronger in axial loading compared to loading perpendicular to the fibres, hence creating orthotropic mechanical behaviour of the composite. This property may be used to "tailor" the laminate so that the stronger direction of the plies are oriented in parallel to the load paths (Clyne & Hull 1996, Nijssen 2015, Henderson & Mottram 2018).

To easily describe the laminate stacking sequence, a laminate orientation code has been developed (Agarwal & Broutman 1990, Clyne & Hull 1996 and Nijssen 2015). This report is limited to laminates consisting of plies with identical thickness and properties, thus the code that is described below only applies to such laminates. Agarwal and Broutman define the FRP component using four standard elements:

1. Each ply is denoted by the angle of its fibres relative to the main direction of the laminate.
2. The plies are separated by a slash if their angles are different.
3. The plies are listed from the first ply laid up in sequence.
4. Plies of the same direction in succession are denoted by a numerical subscript.

This creates a code in the following format:

$$[angle\ of\ layer\ one/\ angle\ of\ layer\ two/\ angle\ of\ layer\ k/\ .../\ .../angle\ of\ layer\ n]$$

Laminate	Code	Laminate	Code
90º		90º	
+45º	$[90/\pm45/0_2]_S$	+45º	$[(90/\pm45/0)_2]$
-45º		-45º	
0º		0º	
0º		90º	
0º		+45º	
0º		-45º	
-45º		0º	
+45º			
90º			

Figure 2.1: Example of layups with corresponding codes.

Positive (+) and negative (-) signs are used to distinguish angles having the same absolute magnitude. Furthermore, the subscript S implies symmetry of laminate orientations around the midplane. Examples of the codes can be seen in Figure 2.1.

2.3 Fibres

The fibres in a composite act as the reinforcement, adding strength and stiffness, and the fibre type and direction will greatly affect the properties of the composite. The contribution of fibre reinforcement to the mechanical properties of the composite is affected by four main factors (Clyne & Hull 1996, Nijssen 2015):

1. The strength and stiffness of the fibres
2. The orientation and array of the fibres
3. The volume/ weight fraction of the fibres
4. The bonding strength between the fibres and the matrix.

Table 2.1: Mechanical properties of fibres.

Fibre type	Tensile strength [MPa]	Tensile modulus of elasticity [GPa]	Typical density [kN/m^3]	Specific modulus [m]
E-glass	2400	69	25	28
S2-glass	3450	86	25	34
CR-glass	3400	80	27.2	29
Low modulus (LM) aramid	3600	60	14.5	40
High modulus (HM) aramid	3100	120	14.5	80
Ultra-high modulus (UHM) aramid	3400	180	14.7	120
High strength (HS) carbon	3500	160-270	18	90-150
Intermidiate modulus (IM) carbon	5300	270-325	18	150-180
High modulus (HM) carbon	3500	325-440	18	180-240
Ultra-high modulus (UHM) carbon	2000	440+	20	200+
S355 steel	355	210	77-78.5	27

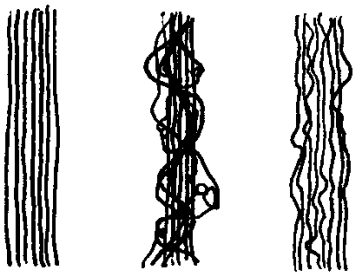

Figure 2.2: Types of roving. From the left: 1. Unidirectional 2. Spun 3. Mock.

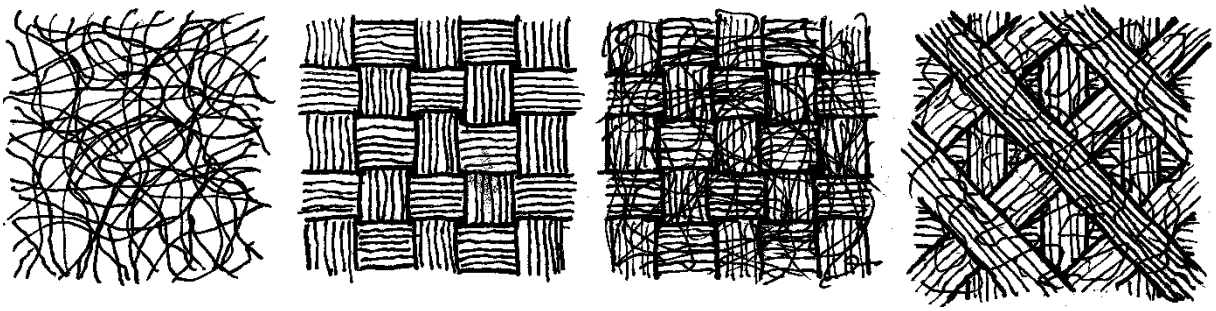

Figure 2.3: Types of mat. From the left: 1. Continuous mat 2. Weave 3. Complex mat 4. Bidirectional complex mat.

Many types of fibre can be used in FRP, the commonly used being glass, carbon and aramid fibres. Glass fibre is the most common type with good all-around properties, whereas carbon fibre provides high strength and stiffness, and aramid is favourable in situations when high impact resistance is required (Fiberline Composites A/S 2002). Mechanical properties of these fibres are presented in Table 2.1 together with structural steel for comparison (Henderson & Mottram 2018). The fifth column is obtained by dividing column three with column four.

Depending on the production method employed, different arrays, as illustrated in Figure 2.2 and Figure 2.3 (inspired by Fiberline Composites A/S (2002)) are used. The fibres of each ply may be lain into a unidirectional pattern consisting of different types of roving. The roving may also be woven into different mats or weaves. Each fibre-structure will yield different properties, allowing for a highly customisable material.

The volume/weight fraction of the fibres depend on the structure of the fibres and the production method used. Methods using fabrics with tightly packed fibres yield a higher fraction. The strength and stiffness of the FRP will increase with the fraction of fibres in the same direction (Henderson & Mottram 2018). This is true for volume fractions up to 55-70 %, where the strength peaks and then decreases with increasing amounts of fibre. However, the tensile stiffness will continue to increase even above volume fractions of 55-70 %. Henderson and Mottram describe the reason for this decrease as being the result of insufficient bonding between the fibres and the matrix.

The interfacial bond strength between the fibres and the matrix is required to transfer the load between the two components, transferring the loads from the weaker resin to the stronger fibres. Consequently, the interfacial bond greatly affects the composite strength (Agarwal & Broutman 1990). Furthermore, Agarwal and Broutman mention the importance of good interfacial condition in order to prevent micro cracks from propagating along the length of the fibres, thus making the fibres effective even after they break. The bonding strength is dependent on several parameters, including the type of textile used, the surface finishing of the fibre, the matrix used and the degree of impregnation.

Table 2.2: Resin properties.

Resin	Stiffness [GPa]	Ultimate strength [MPa]	Ultimate strain [%]	Density [kg/m^3]	Curing shrinkage [%]
Polyester	2.4-4.6	40-85	1.2-4.5	1150-1250	6-8
Vinylester	3-3.5	50-80	5	1150-1250	5-7
Epoxy	3.5	60-80	3-5	1150-1200	<2

2.4 Matrix

The matrix in the FRP consists of an isotropic polymer resin mixed together with various additives. The matrix works as an adhesive to the fibres and binds them together, enabling load transfer between the fibres through shear stress. In addition, it stabilises the fibres during compression by supporting the fibres in the weak direction. Equally important is the ability to protect the fibres from and to withstand the climate (Agarwal & Broutman 1990).

The polymers can be categorized into either thermoplastics or thermosetting polymers. The thermoplastics are characterized by melting on heating. This property is not desirable in bridge engineering, hence only thermosets are usually used (Agarwal & Broutman 1990 and Henderson & Mottram 2018). Thermosets cannot liquify after being cured, although their properties may change with temperature. The glass transition temperature, T_g, is often used as the point when the properties of the polymer become sensitive to changes in temperature (Nijssen 2015), although the properties are affected even below this limit. If exceeded, the polymers modulus of elasticity, compressive and shear strength will drop, hence the glass transition temperature being an important aspect when utilising FRP. Examples of the glass transition temperature of commonly used resins can be found in Section 4.3.

Henderson and Mottram (2018) mention that other than the glass transition temperature, several other material characteristics are to be considered in the design of FRP. The most important ones are the adhesive properties, the mechanical properties and the long-term degradation due to climate effects. Three polymers that fulfil these requirements and are therefore often used in the design of bridges include polyester, vinylester and epoxy. Nijssen (2015) presents some material properties of these polymers which are displayed in Table 2.2, although the exact properties depend on the specific chemical composition of the polymer in question.

Nijssen further compares the resins beyond the properties listed in Table 2.2. Generally, epoxy has the best overall performance but is also the most expensive. The cheaper polyesters are more sensitive to water damage, whereas epoxies are particularly durable. Finally, the curing of the mentioned resins is exothermic. In bridge design, epoxy is the most common choice, but other resins (including resins not discussed in this chapter) may be chosen due to specific requirements of the bridge (Henderson & Mottram 2018).

2.5 Production Methods

Several production methods of FRP exist. The methods can be divided into two groups: open or closed-mould methods. Open-mould methods are based on the product being placed onto a mould that will not be covered by a second mould during impregnation (Nijssen 2015). On

the contrary, the closed-mould methods use a second mould covering the existing one. This allows for the pressure to be increased in order to improve the impregnation and the penetration of resin into the fibre. According to Nijssen, this allows for a reduction of both superfluous resin and air inclusions. Furthermore, the emission of volatile substances is mentioned to be more controlled with the closed-mould production methods. Both open and close-mould methods do however allow for virtually any shape to be conserved. The production methods relevant in this report are pultrusion and fibre placement methods.

Pultrusion and fibre placement methods are two inherently different methods of achieving the desired shape of the FRP. Pultrusion as a term is a combination of the verb pull and the noun extrusion. Nijssen (2015), as well as Agarwal & Broutman (1990), explains that the method works as extrusion but instead of pushing the material through a mould it is pulled and is hence an open-mould method. The material consists of fibre bundles and mats led through a resin batch to thereafter be drawn through preforming and finally through the mould. The pultruded parts are cut into the desired length and cured in high temperature. A schematic drawing of the process is shown in Figure 2.4.

Fibre placement methods work with fibre bundles or mats being laid on a mould. These methods allow for the fibres to be oriented in desired directions within the plane. The method can be both open and closed-moulded and several methods exist. Open-moulded methods often use pre-impregnated mats or bundles and close-moulded methods may use autoclaves or similar to, with vacuum, impregnate the fibres with resin. A schematic drawing of the closed-moulded fibre placement method is visualised in Figure 2.5.

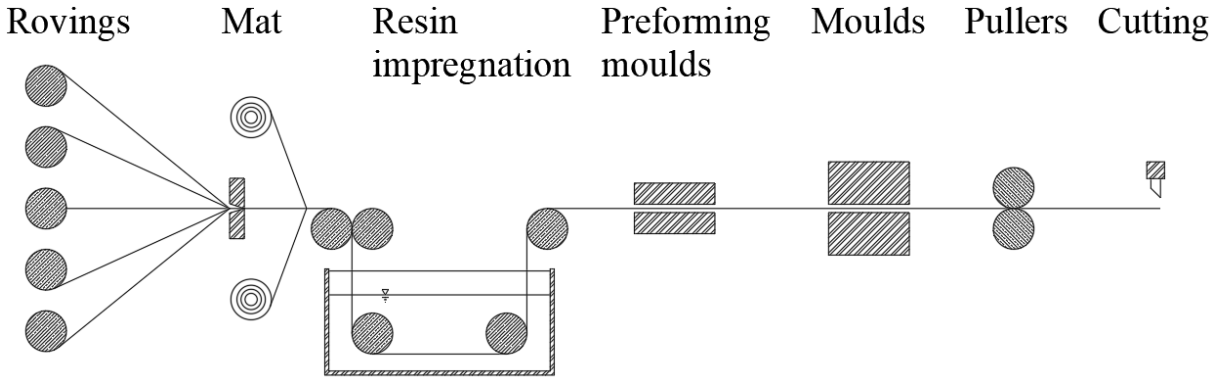

Figure 2.4: The pultrusion process.

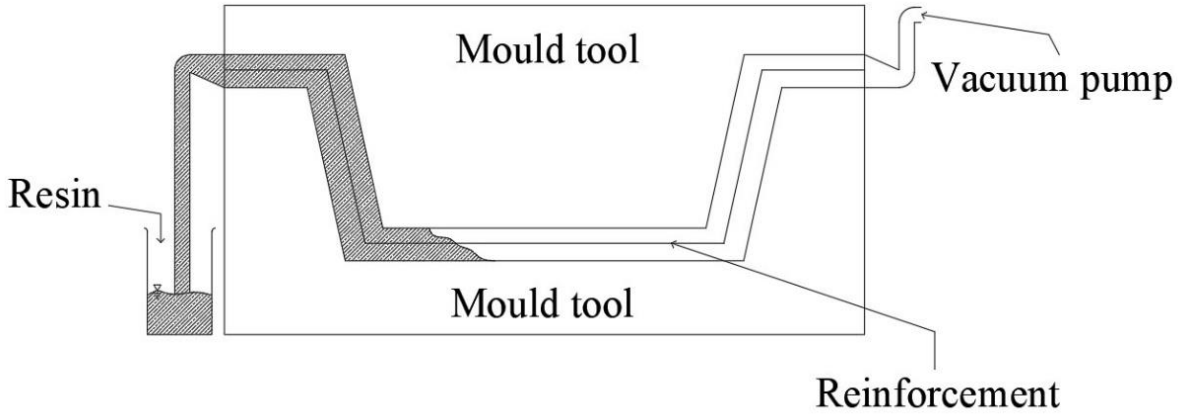

Figure 2.5: Closed-moulded fibre placement.

2.6 Failure

Failures in composites can occur due to both mechanical and other mechanisms. The mechanical mechanisms of composites differ from those of conventional materials due to the laminate structure and loading. The most important failure modes are splitting, delamination, fatigue, impact damage and creep (Nijssen 2015). Other potential failure mechanisms that are important to consider include osmosis, UV-radiation damage and damage due to temperature and fire. In order to prevent failure, the materials and design of the structure have to be considered.

2.6.1 Mechanical Failure Mechanisms

Splitting is a mechanism causing cracks parallel to the fibre direction throughout the whole thickness dimension. Splitting is an issue linked to inadequate strength of the composite transverse to the main fibre direction and may be caused by in-plane-bending or by wedge effects in connections. In order to prevent this mechanism, the fibre orientation can be altered to add strength to the transversal direction (Nijssen 2015).

Delamination consists of the same mechanism as splitting, but in this case between the individual plies. Delamination occurs due to high shear stress between the plies, especially if there is a large difference in stiffness between the two plies. Although uncommon, it is possible to increase the resistance to delamination by reinforcing fibres in the direction transversal to the plies (Agarwal & Broutman 1990 and Nijssen 2015).

The mechanism involved in fatigue failure is similar to that of steel, however, the outcome is different. Instead of one crack forming, several cracks may form at once and then propagate in several different directions. These cracks may interfere with each other, forming even larger cracks. Another difference is that composites gradually lose stiffness and strength due to fatigue. Fatigue may be prevented by orienting the fibres to the load directions or by some means reducing the stress of the component (Agarwal & Broutman 1990 and Nijssen 2015).

Impact damage in composites is hard to detect due to their elastic behaviour. Visual inspection may not reveal lasting damage as the material tend to recover its form while cracks remain hidden behind the visible surface layer. Therefore, it is recommended that the structure should be designed so that inspection can be performed from both sides of the laminate (Nijssen 2015), if the risk of impact loading persists.

Creep in composites is similar to creep in other material but is dependent on the materials used and what part of the composite that is subjected to the load. The creep is most prominent in cases when the resin is heavily loaded. However, even though fibres often are insensitive to creep, some materials such as aramid can be (Ascione et al. 2016 and Nijssen 2015).

2.6.2 Other failure mechanisms

Most resins are prone to osmosis in the form of water absorption. The osmosis may lead to damage to the structure by disrupting the bonding between the polymer chains causing blisters. If deeper penetration occurs, it can also lead to frost wedging. Preventing osmosis is most easily done by choosing a resin less sensitive to water, such as epoxy, or by applying a coating (Agarwal & Broutman 1990, Ascione et al. 2016 and Nijssen 2015).

UV-radiation may cause degradation of the resin and thus reducing the strength of the composite. The reinforcement is usually persistent against radiation, but in some cases it can cause damage. Protective paint or coating may be applied to protect the composite from exposure. Furthermore, pigment or UV-absorbers can be added to the resin (Ascione et al. 2016).

The resin is also often sensitive to high temperatures and fire. As previously mentioned, the stiffness and strength of the composite will decrease if the temperature exceeds that of the resins glass transition temperature. At even higher temperatures the resin will start to burn, destroying bonding between fibres and will eventually lead to failure. Structures subjected to compressive stress are especially vulnerable. Other than fire prevention, fire-resistant layers may be added to the structure for protection. Another solution is adding additives to the resin, such as chlorine, bromide or aluminium trihydrite. Unfortunately, these compounds are toxic when burning and are not environment-friendly (Henderson & Mottram 2018).

2.7 Sustainability

The environmental impact of FRP in bridge applications can be studied in several ways. The most practical parameter to study is energy consumption. Other factors may also be of interest, such as impact related to water, air and fertilisers. This section will however focus on the former. The production of the matrix and fibres of the FRP is discussed by Song, Young and Gutowski (2009). The authors mention that the energy consumption of the materials is strongly dependent on the production methods and the scale of production. They also present some key figures of energy consumption, as seen in Table 2.3. However, it should be mentioned that the energy intensity of the polymers does not include any additives. Furthermore, the energy usage of the manufacturing processes of FRP is discussed, where some of the energy intensities are presented in Table 2.4. It should however be noted that the figures presented are linked only to the process and not to that of the materials employed.

Finally, Song, Young and Gutowski (2009) discuss the end-of-life aspect of FRP. They mention that several recycling methods exist, but that they are currently limited to a low level of recycling. One of the main challenges is the inability to recover the long fibres with the desired properties. Today, mainly chopped off short fibres can be recovered. These fibres may be used as fillers in moulded components but may not be used as replacements to the virgin materials. It is further mentioned that recycling requires considerable processing steps before the materials may be used, making the option less desirable. Song, Young and Gutowski draw the conclusion that the end-of-life phase stands as an obstruction against an environmentally friendly large-scale production due to the inability to recycle the material properly.

A more niched study towards the application of FRP in bridge engineering is discussed by Henderson and Mottram (2018). They present some case studies made on the environmental

impact of real-life pedestrian bridges. One of these case studies evaluates the energy consumption associated with the placement of a pedestrian footbridge in a Dutch harbour using five different materials for the superstructure (Daniel, 2003). The bridge to be replaced consists of two 13,5 m spans with a width of 1,6 m. The evaluation was based on the preliminary design of each bridge proposal where the designs were used to collect data directly from the market when possible. Daniel does however mention that the uncertainty related to the input data was in many instances large, especially where rough estimates had to be made. He further mentions that the parties involved in the bridge replacement process were, nevertheless, satisfied with the data. The results of the evaluation, presented in Table 2.5, show that the pultruded FRP alternative has a lower environmental impact than the other alternatives.

A second study, by IStructE (2014), performs a cradle-to-grave analysis of an 8 m long and 1 m wide footbridge. As for the previous case, this study was based on similar designs with different materials. The study evaluated the embodied energy and carbon of the bridges with the results presented in Table 2.6. It should be noted that effects stemming from the maintenance of the bridges were not included. As for the study made by Daniel (2003), the FRP alternative exhibited the lowest energy consumption. FRP and timber exhibit similar results with regards to embodied carbon, which is likely due to the longer projected service life of FRP.

As a comparison to the conventional materials used, and more specifically to the reference bridge introduced in section 4.2, the energy consumption of glue-laminated timber is of interest. However, the energy consumption of glue-laminated timber is highly dependent on the source of energy used and where the forest and production plant are located. Bowers et al. (2017), Laurent et al. (2013) and Puettmann, Oneil & Johnson (2013) do al present different energy consumption of the material. Taking the mean if the consumptions presented, a value of 3550 MJ/m^3 is obtained. The value should however be higher as some steel is included in the bridge.

Table 2.3: Energy content of materials (Song, Young & Gutowski, 2009).

Material		Energy intensity [MJ/kg]
Polymers	Polyester	63-78
	Epoxy	76-80
Fibres	Glass fibre	13-32
	Carbon fibre	183-286
Metals	Aluminium	196-257
	Steel	30-60
	Stainless steel	110-210

Table 2.4: Energy intensity of manufacturing processes (Song, Young & Gutowski, 2009).

Manufacturing methods	Energy intensity [MJ/kg]
Autoclave moulding	21.9
Spray up	14.9
Vacuum assisted resin infusion	10.2
Pultrusion	3.1
Prepreg production	40.0

Table 2.5: Energy consumption and environmental impact of pedestrian bridges (Daniel, 2003).

Material	Mass [ton]	Initial energy [GJ]	Maintenance energy [GJ]	Total energy consumption [GJ]	Critical volume of polluted water [m^3]	Critical volume of polluted air [$m^3 \cdot 10^6$]
Painted structural steel	6.0	222	72	294	697.4	7.09
Stainless steel	5.6	300	30	330	Not investigated	Not investigated
Pultruded GFRP	4.0	96	24	120	85.8	7.92
Aluminium	3.2	215	54	269	565.3	41.10
Concrete	28.0	252	25	277	341.9	31.04

Table 2.6: Embodied energy and carbon of alternative designed bridges. IStructE (2014).

Material	Embodied energy [GJ]	Embodied carbon [ton CO_2]
Timber	30	0.93
Steel sections	84.3	6.36
Hybrid steel beams with timber deck	47.6	3.04
FRP deck and handrail	19.5	0.92

2.8 Costs

The costs efficiency of FRP bridges in comparison to bridges constructed out of conventional materials is one of the most important aspects to cover when considering an FRP bridge. However, since the number of produced FRP bridges are limited and their need for maintenance remains largely unknown, the costs are hard to predict. The predictions presented in this chapter should therefore be viewed with some degree of scepticism.

The study presented in Section 2.7 by Daniel (2013) makes a cost evaluation of several different bridge materials for a three-span, simply supported bridge in a Dutch harbour. The results, presented in Table 2.7, points to the alternative using pultruded FRP being considerably more expensive than that of structural steel and concrete. A different study by Patljak (2018) compares three different types of FRP solutions to more conventional alternatives (in this case concrete and steel/concrete composite) using life cycle cost analysis (LCC). The bridges compared are pedestrian bridges spanning 15 m with a width of 2,5 m. The most viable option of the FRP is presented along the other two bridges in Table 2.8. The analysis arrives at the same conclusion as Daniel (2013), however at a smaller cost difference between the alternatives. The discrepancy in their results may be due to several reasons, such as the production methods involved.

A different approach is made by Henderson and Mottram (2018) who presents a comparison between an FRP and a steel pedestrian bridge regarding an assessment of their financial viability. The study made regards a perfectly constructed FRP bridge, using the optimal design solutions, hence highlighting the potential of the cost efficiency of an FRP bridge. It is important to mention the fact that the numbers presented in Table 2.9 are indicative and strongly dependent on the specific conditions of the bridges. However, Henderson and Mottram highlight that some conclusions can still be drawn. The initial cost of a pedestrian bridge would be about 10% higher than that of the conventional materials, and 25% higher for road bridges. However, when it comes to the operational costs the FRP bridge is significantly cheaper if designed properly, hence FRP remains a viable alternative in the long term.

What is not mentioned in the studies presented above is whether the cost of the bridge substructure is included or not. The lower permanent load of the FRP bridge superstructure could reduce the cost of both groundworks and substructure. Furthermore, significant cost savings can be made if a fast installation is needed. The prefabricated FRP bridges have a reputation of being easy and fast to install, hence reducing the time for shutdown of traffic.

Comparing the cost of different sorts of FRP is not easily done. Carbon fibres are known to be the more expensive sort of fibre, as epoxy is considering polymers. However, these materials are in many aspects superior to that of cheaper alternatives, allowing for a reduction of FRP needed. Hence, it is hard to say what alternative is the more expensive and thus should the cost be evaluated for different FRP in case to case. Furthermore, the choice of production method affects the cost as well, complicating the cost comparison further. However, generalising the situation, FRP containing carbon fibre will initially almost always be the more expensive alternative compared FRP containing glass fibre.

Table 2.7: Costs of pedestrian bridges (Daniel, 2003).

Material	Initial costs [EUR]	Maintenance costs [EUR]	Total costs [EUR]
Painted structural steel	40 000	30 000	70 000
Stainless steel	110 000	6 000	116 000
Pultruded GFRP	70 000	17 000	87 000
Aluminium	77 000	19 000	96 000
Concrete	30 000	10 000	40 000

Table 2.8: LCCA for different bridges (Patljak, 2018).

Bridge type	Category	Net Present Value [SEK]
Concrete slab	Construction	769 000
	Maintenance	73 000
	End-of-life	3 400
	Total cost	**845 400**
Concrete and steel composite	Construction	595 000
	Maintenance	152 000
	End-of-life	2 600
	Total cost	**749 000**
GFRP	Construction	920 000
	Maintenance	26 000
	End-of-life	700
	Total cost	**946 700**

Table 2.9: Indicative values for the total cost of ownership (Henderson & Mottram, 2018).

Indicative costs assuming 15 m footbridge 2m wide (120-year design life)		FRP £	Steel £
Acquisition cost	Design and certification	12 000	9 000
	Product fee	100 000	70 000
	Transportation	3 000	5 000
	Install/commission	3 000	6 000
Operational cost	Inspections	132 000	260 000
	Coatings	30 000	240 000
	Joints	20 000	20 000
	Surfacing	25 000	25 000
	Major maintenance	-	20 000
	Traffic management	54 000	86 000
	Project management	20 000	30 000
Disposal	Decommissioning	25 000	25 000
	Disposal	10 000	5 000
Salvage	Material recycling	-	-5 000
	Total cost of ownership	**434 000**	**796 000**

3 Theory

3.1 General Considerations

The properties of composites are generally determined through experimental testing, which is required in the final design stages of a bridge (Ascione et al. 2016 and Henderson & Mottram 2015). However, in the early design stage, theoretical models may be used to estimate the material properties. This report is based on such theoretically derived values. The theories are limited to unidirectional plies with long fibres as these are the only used fibre-textile. Strength properties are however derived from tables found in Agarwal & Broutman (1990) and Fiberline Composites A/S (2002) since no rigorous theories linked to these properties have been found. All other properties have been derived using the theories presented in the following subsections.

The theories presented are strongly dependent on the material orientation of the laminate and of each individual ply. Denotations are used to specify the orientation of the properties described. The used denotations are listed below and visualised in Figure 3.1. Further, the angle θ is used to describe the angle between the global main directions of the laminate and the fibre direction of an individual ply.

- 1: The fibre direction of an individual ply.
- 2: The direction orthogonal to the fibres of an individual ply.
- x, y and z: the global main directions.

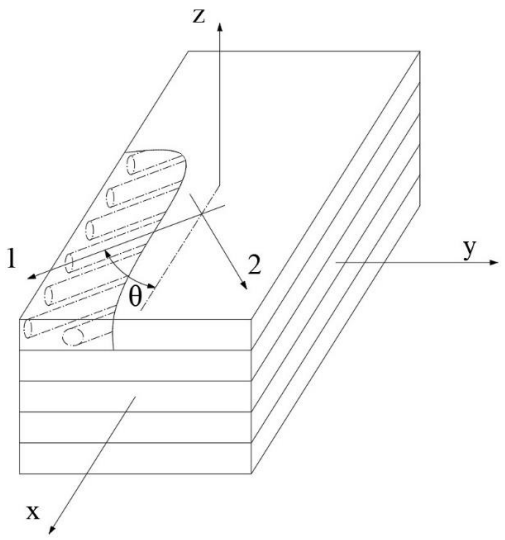

Figure 3.1: Directions of a laminate and plies.

3.2 Rule of Mixtures

The longitudinal stiffness of a unidirectional ply is derived by Agarwal & Broutman (1990) and Nijssen (2015) who arrive at the conclusion that the properties can be determined using a relation called *"the rule of mixtures"*. This applies if the fibre volume fraction exceeds a critical limit, set to 15 % by Ascione et al. (2016). Furthermore, the assumptions of good adhesion between fibres and matrix, and of the absence of damage and inclusions are made in order for the rule of mixtures to be valid.

The rule of mixtures is compared as analogous to that of electrical parallel switching (Nijssen, 2015). The method is further described by visualising the composite as a block of fibre next to a block of resin as seen in Figure 3.2. As the assumption of good adhesion applies can the strains of fibres and matrix be set as equal during loading of the block. Incorporating the volume fraction of fibres, the rule of mixtures can be written (Agarwal & Broutman 1990).

$$E_1 = \left[E_R + \left(E_{f1} - E_R\right) \cdot V_f\right]$$

The rule is suggested to be used by Ascione et al. (2016), but with the inclusion of a reduction factor, $\varphi_{UD} = 0.97$.

$$E_1 = \left[E_R + \left(E_{f1} - E_R\right) \cdot V_f\right] \cdot \varphi_{UD}$$

It is further implied that the rule of mixtures is applicable to the derivation of Poisson's ratio in unidirectional plies.

$$\upsilon_{12} = \upsilon_R - \left(\upsilon_R - \upsilon_f\right) \cdot V_f$$

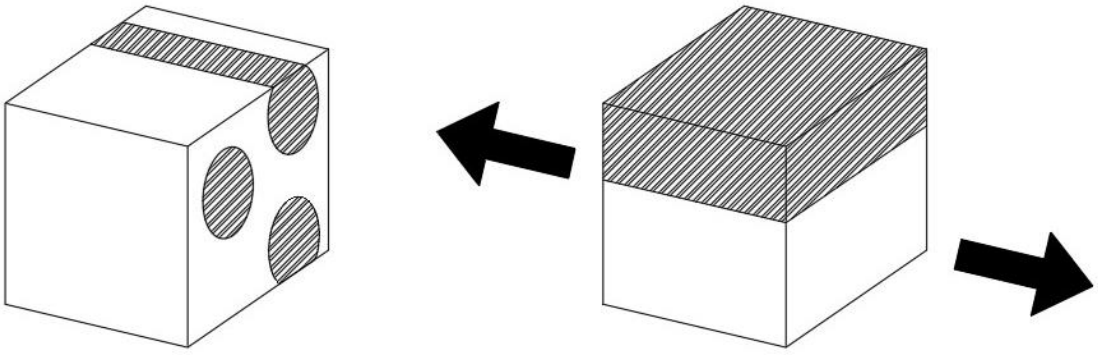

Figure 3.2: Visualisation of "rule of mixtures" inspired by Nijssen (2015).

3.3 Halpin-Tsai

The stiffness transverse to the fibre direction is difficult to predict theoretically. Several methods of predicting the stiffness have been developed. However, most of the methods consist of complicated equations or curves, making them impractical to use (Agarwal & Broutman 1990). Halpin (1969) did however derive the semi-empirical Halpin-Tsai equations which are in good agreement with the real values, making the predictions simpler. Both Agarwal & Broutman (1990) and Ascione et al. (2016) deem the equations adequate to predict the transverse and shear composite modulus in the initial design stages. The reduction factor $\varphi_{UD} = 0.97$, present in Ascione et al., is used.

$$E_2 = \left[\frac{\left(1 + \xi_2 \eta_2 V_f\right)}{\left(1 - \eta_2 V_f\right)} \cdot E_R\right] \cdot \varphi_{UD}$$

Where

$$\eta_2 = \frac{\left(\frac{E_{f2}}{E_R} - 1\right)}{\left(\frac{E_{f2}}{E_R} - \xi_2\right)}, \xi_2 = 2$$

Halpin (1969) did further derive equations similar to that of the transverse stiffness applicable for the shear modulus, thus are Halpin-Tsai used in this application as well.

$$G_{12} = \left[\frac{\left(1 + \xi_G \eta_G V_f\right)}{\left(1 - \eta_G V_f\right)} \cdot G_R\right] \cdot \varphi_{UD}$$

Where

$$\eta_G = \frac{\left(\frac{G_f}{G_R} - 1\right)}{\left(\frac{G_f}{G_R} - \xi_G\right)}, \xi_G = 1$$

3.4 Classical Laminate Theory

With the material properties of each individual ply known, the properties of the whole laminate can be determined. However, since the individual ply has properties dependent on the direction, then the stress distribution will be complicated throughout the laminate in situations when the plies are oriented differently. Following the assumption of zero slippage between plies during loading, the strain will be equal for all plies. However, since the stiffness of the individual ply will differ in the direction of the laminate, so will the stress in the plies at uniform strain, as visualised in Figure 3.3.

Classical Lamination Theory (CLT) can be used to calculate the stress and elongation of each ply under external load. Some assumptions are required in order to use CLT (Nettles, 1994 and Nijssen, 2015).

1. All fibres of a single ply are parallel and continuous. The orientation, thickness and material of different plies may however differ.
2. Constant thickness of the laminate is required.
3. The thickness of the plies are thin relative to the length and width.

4. The laminate is undisturbed: the theory is not valid in the vicinity of holes, corners, edges, etc.
5. The theory is linear elastic.
6. All plies are perfectly bonded; effects stemming from delamination are not considered.
7. Lines perpendicular to the surface of the laminate remains straight and perpendicular to the surface after deformation.
8. Smeared properties are assumed, i.e. the properties of the fibre and matrix are combined; no determination can be made on a microscopic level since the properties of each ply are smeared between the fibre and the resin.
9. Strains and stresses in the perpendicular direction to the laminae are negligible.

Nettles (1994) further derives the theory in detail. The most relevant steps will be presented below. Notations 1 and 2 refers to the main directions of the local coordinate system of a lamina and x and y to the global coordinate system as seen in Figure 3.1. The theory is based on Hooke's law, describing the properties of an elastic orthotropic material as generalised:
as generalised:

$$\sigma_i = Q_{ij}\varepsilon_j$$

The equation may instead be written on matrix form:

$$\begin{Bmatrix} \sigma_1 \\ \sigma_2 \\ \sigma_3 \\ \tau_{23} \\ \tau_{31} \\ \tau_{12} \end{Bmatrix} = \begin{bmatrix} Q_{11} & Q_{12} & Q_{13} & 0 & 0 & 0 \\ Q_{12} & Q_{22} & Q_{23} & 0 & 0 & 0 \\ Q_{13} & Q_{23} & Q_{33} & 0 & 0 & 0 \\ 0 & 0 & 0 & Q_{44} & 0 & 0 \\ 0 & 0 & 0 & 0 & Q_{55} & 0 \\ 0 & 0 & 0 & 0 & 0 & Q_{66} \end{bmatrix} \begin{Bmatrix} \varepsilon_1 \\ \varepsilon_2 \\ \varepsilon_3 \\ \gamma_{23} \\ \gamma_{31} \\ \gamma_{12} \end{Bmatrix}$$

However, the relations of the two-dimensional case are sought. Hence are all terms related to the third axis removed to form the simplified two-dimensional relation to create the reduced stiffness matrix denoted [Q].

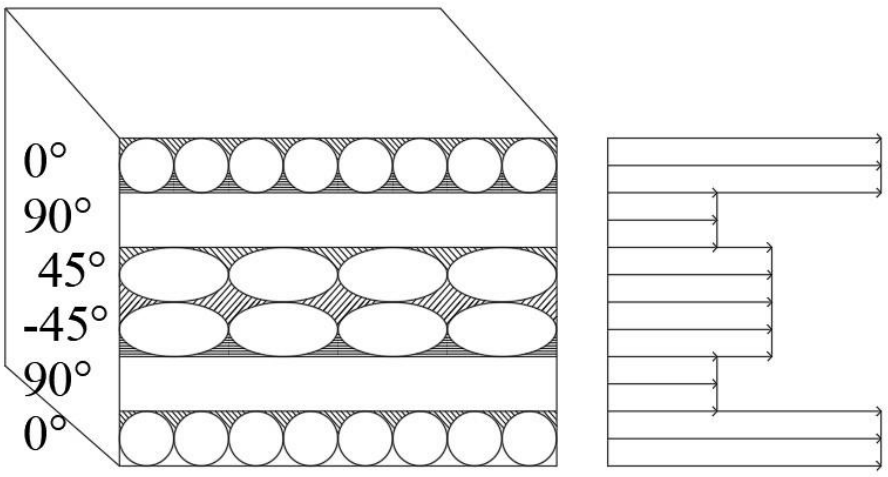

Figure 3.3: Stress distribution of a laminate subjected to uniform strain.

$$\begin{Bmatrix}\sigma_1\\ \sigma_2\\ \tau_{12}\end{Bmatrix}=\begin{bmatrix}Q_{11} & Q_{12} & 0\\ Q_{12} & Q_{22} & 0\\ 0 & 0 & Q_{66}\end{bmatrix}\begin{Bmatrix}\varepsilon_1\\ \varepsilon_2\\ \gamma_{12}\end{Bmatrix}=\begin{bmatrix}\frac{1}{1-v_{12}v_{21}}E_1 & \frac{v_{12}}{1-v_{12}v_{21}}E_2 & 0\\ \frac{v_{12}}{1-v_{12}v_{21}}E_2 & \frac{1}{1-v_{12}v_{21}}E_2 & 0\\ 0 & 0 & G_{12}\end{bmatrix}\begin{Bmatrix}\varepsilon_1\\ \varepsilon_2\\ \gamma_{12}\end{Bmatrix}=[Q]\begin{Bmatrix}\sigma_1\\ \sigma_2\\ \tau_{12}\end{Bmatrix}$$

By inverting the reduced stiffness matrix, a reduced compliance matrix denoted [S] can be written.

$$\begin{Bmatrix}\varepsilon_1\\ \varepsilon_2\\ \gamma_{12}\end{Bmatrix}=\begin{bmatrix}S_{11} & S_{12} & 0\\ S_{12} & S_{22} & 0\\ 0 & 0 & S_{66}\end{bmatrix}\begin{Bmatrix}\sigma_1\\ \sigma_2\\ \tau_{12}\end{Bmatrix}=\begin{bmatrix}\frac{1}{E_1} & -\frac{v_{21}}{E_2} & 0\\ -\frac{v_{21}}{E_1} & \frac{1}{E_2} & 0\\ 0 & 0 & \frac{1}{G_{12}}\end{bmatrix}\begin{Bmatrix}\sigma_1\\ \sigma_2\\ \tau_{12}\end{Bmatrix}=[S]\begin{Bmatrix}\sigma_1\\ \sigma_2\\ \tau_{12}\end{Bmatrix}$$

These relations are only valid for plies oriented in the main directions of the laminae. To make it applicable for plies oriented in any other direction, the stresses and strains must be transformed to the main directions. For this matter, Nettles derives a transformation matrix denoted [T] for plies rotated an angle θ counterclockwise to the main direction.

$$\begin{Bmatrix}\sigma_1\\ \sigma_2\\ \tau_{12}\end{Bmatrix}=\begin{bmatrix}\cos^2\theta & \sin^2\theta & 2\sin\theta\cos\theta\\ \sin^2\theta & \cos^2\theta & -2\sin\theta\cos\theta\\ -\sin\theta\cos\theta & \sin\theta\cos\theta & \cos^2\theta-\sin^2\theta\end{bmatrix}\begin{Bmatrix}\sigma_x\\ \sigma_y\\ \tau_{xy}\end{Bmatrix}=[T]\begin{Bmatrix}\sigma_x\\ \sigma_y\\ \tau_{xy}\end{Bmatrix}$$

However, it is desired to transform from the local system to the global. Hence is the transformation matrix is inversed.

$$\begin{Bmatrix}\sigma_x\\ \sigma_y\\ \tau_{xy}\end{Bmatrix}=[T]^{-1}\begin{Bmatrix}\sigma_1\\ \sigma_2\\ \tau_{12}\end{Bmatrix}$$

With similar steps taken for strain and concludes in the relation as follows.

$$\begin{Bmatrix}\varepsilon_x\\ \varepsilon_y\\ \frac{1}{2}\gamma_{xy}\end{Bmatrix}=[T]^{-1}\begin{Bmatrix}\varepsilon_1\\ \varepsilon_2\\ \frac{1}{2}\gamma_{12}\end{Bmatrix}$$

Nettles further describes the relation between global stress and strain using the transformation matrix and the compliance and stiffness matrices, introducing the lamina stiffness matrix $[\overline{Q}]$.

$$\begin{Bmatrix}\sigma_x\\ \sigma_y\\ \tau_{xy}\end{Bmatrix}=[T]^{-1}[Q]\begin{bmatrix}1 & 0 & 0\\ 0 & 1 & 0\\ 0 & 0 & 2\end{bmatrix}[T]\begin{Bmatrix}\varepsilon_x\\ \varepsilon_y\\ \gamma_{xy}\end{Bmatrix}=[\overline{Q}]\begin{Bmatrix}\varepsilon_x\\ \varepsilon_y\\ \gamma_{xy}\end{Bmatrix}$$

Stacking plies together to a laminate, Nettles derives the laminates response to applied external forces and moments. The response consists of elongation as well as curvature of the

plies, inducing stress. The relation is formulated with the stiffness matrix of the laminate, denoted [ABD].

$$\begin{Bmatrix} n_x \\ n_y \\ n_{xy} \\ m_x \\ m_y \\ m_{xy} \end{Bmatrix} = \begin{bmatrix} A_{11} & A_{12} & A_{13} & B_{11} & B_{12} & B_{13} \\ A_{21} & A_{22} & A_{23} & B_{21} & B_{22} & B_{23} \\ A_{31} & A_{32} & A_{33} & B_{31} & B_{32} & B_{33} \\ B_{11} & B_{12} & B_{13} & D_{11} & D_{12} & D_{13} \\ B_{21} & B_{22} & B_{23} & D_{21} & D_{22} & D_{23} \\ B_{31} & B_{32} & B_{33} & D_{31} & D_{32} & D_{33} \end{bmatrix} \begin{Bmatrix} \varepsilon_x \\ \varepsilon_y \\ \gamma_{xy} \\ \kappa_x \\ \kappa_y \\ \kappa_{xy} \end{Bmatrix}$$

The matrix may be written on compact form as below.

$$\begin{Bmatrix} N \\ M \end{Bmatrix} = \begin{bmatrix} A & B \\ B & D \end{bmatrix} \begin{Bmatrix} \varepsilon \\ \kappa \end{Bmatrix}$$

The stiffness matrix of the laminate consists of three separate 3x4 matrices related to different physical responses to the applied force and moment. The definitions of these matrices are based on a schematic sketch of the laminate indicating positions of the individual plies in relation to the geometric midplane as visualised in Figure 3.4. The definitions of the matrices are as follows:

- The extensional stiffness matrix [A]

$$A_{ij} = \sum_{k=1}^{n} \left[\overline{Q}_{ij}\right]_k (h_k - h_{k-1})$$

  These terms relate to the normal stresses and strains, with an exception of two terms, A_{16} and A_{26}, relating shear strains to normal stresses and vice versa.

- The coupling matrix [B]

$$B_{ij} = \sum_{k=1}^{n} \left[\overline{Q}_{ij}\right]_k (h_k^2 - h_{k-1}^2)$$

  The terms relate bending strains with normal stresses and vice versa, except for terms B_{16} and B_{26} relating twisting strains to normal stresses and vice versa. An important feature of the matrix is that a symmetric laminate will result in the matrix being zero in all positions, considerably reducing necessary calculations.

- The flexural stiffness matrix [D]

$$D_{ij} = \sum_{k=1}^{n} \left[\overline{Q}_{ij}\right]_k (h_k^3 - h_{k-1}^3)$$

  The flexural stiffness matrix relates the curvatures to the bending moments.

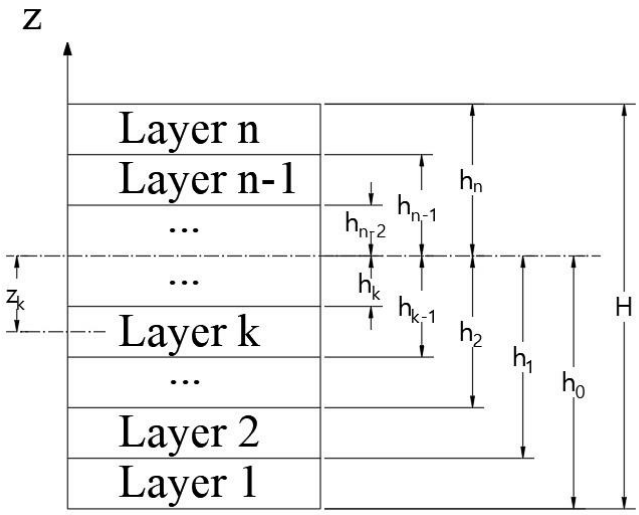

Figure 3.4: Schematic figure of a laminate where the dash-dotted line indicates the geometric midplanes position.

3.5 Design Values

The design values of a composite may be derived using the method presented by Ascione et al. (2016):

$$X_d = \eta_c \cdot \frac{X_k}{\gamma_M}$$

Where the design value, X_d, is obtained using the characteristic value of the properties, X_k, in combination with a conversion factor, η_c, and a partial factor, γ_M.

3.5.1 Conversion Factor

In order to take the environmental factors into account in the design, a total conversion factor, η_c, is introduced (Ascione et al. 2016). The total conversion factor consists of four separate factors linked to the effects of temperature (η_{ct}), humidity (η_{cm}), creep (η_{cv}) and fatigue (η_{cf}):

$$\eta_c = \eta_{ct} \cdot \eta_{cm} \cdot \eta_{cv} \cdot \eta_{cf}$$

Depending on the limit state involved, different combinations of conversion factors should be used. Ascione et al. present a table of when the different factors should be included, which is recreated in Table 3.1. However, some of these factors can be somewhat hard to determine and are to be chosen based on experience. Although recommended values are available, they can be difficult to interpret. Recommended values by Henderson and Mottram (2018), which are based on Ascione et al, are presented in Table 3.2.

It is further mentioned by Ascione et al. (2016) that if protective coating, proven to counteract temperature and humidity effects, is used, then the corresponding factor may be set to 1.0. Furthermore, other relevant conversion factors may be added to the total conversion factor if needed. One relevant factor may be linked to freeze and thaw cycles. But there is at the moment no information on the matter available, leading to uncertainties in the design.

Table 3.1: Conversion factors to be included (Ascione et al. 2016).

	Aspect being verified						
Influencing factor	Strength (ULS)	Stability (ULS)	Fatigue (ULS)	Creep (SLS)	Momentary deformation (SLS)	Vibrations (SLS)	Damage (SLS)
η_{ct}	x	x	x	x	x	x	x
η_{cm}	x	x	x	x	x	x	x
η_{cv}	x			x			x
η_{cf}	x	x		x	x	x	x

*Table 3.2: Recommended values for conversion factors (Hendersson & Mottram 2018). *) Verification needed.*

	SLS	ULS	Notes
η_{ct}	0.9	0.9	Applicable when $T < T_g - 20°C$
η_{cm}	0.8	0.8	For post-cured FRP laminates
η_{cv}	0.5	0.5	For long term effects, otherwise 1.0.
η_{cf}	1.0	*	For footbridges not sensitive to wind.

3.5.2 Partial Factors for Materials

Ascione et al. (2016) suggest that the partial material factor may be determined as a product of two sub-factors.

$$\gamma_M = \gamma_{M1} \cdot \gamma_{M2}$$

γ_{M1} corresponds to uncertainties in obtaining the correct material properties and can be set to one of three values corresponding to the level of certainty in the properties, as shown in Table 3.3. γ_{M2} corresponds to uncertainties in the properties due to the production method of the material. The factor is to be chosen depending on the variation coefficient of the production method, as seen in Table 3.4. The partial material factor is however not applied for SLS verification and may therefore be set to 1.0.

Table 3.3: Partial factor corresponding to uncertainties in obtaining the material properties.

γ_{M1} (ULS)	Method of obtaining material properties
1	Production process and quality system certified by an EOTA member
1.15	Properties derived from tests
1.35	From theoretical models or values available in technical literature

Table 3.4: Partial factor corresponding to uncertainties due to production method.

Laminate type	Variation coefficient	γ_{M2}		
		Strength verification	Local stability	Global stability
Post-cured laminates	$V_X \leq 0.10$	1.35	1.5	1.35
	$0.10 \leq V_X \leq 0.17$	1.6	2.0	1.5

3.6 SLS Design Criteria

The bridges are to be checked in the serviceability limit state of deflection as well as for vibrations. Henderson and Mottram (2018) mention that the serviceability limit state of FRP bridges usually is decisive for the design and not the ultimate limit state as is usually the case for conventional bridges. During all serviceability limit state verifications, the effects reducing the stiffness of the material are to be considered (Ascione et al. 2016), which is done through the application of the conversion factor described in Section 3.5.1.

3.6.1 Deflection

The deflection of the bridge is to be verified for all loading conditions. The bridges are also assumed to be compensating for the deflection caused by permanent loads through precamber, hence only live loads are considered.

3.6.2 Vibrations

The vibrational comfort levels of an FRP pedestrian bridge are to be considered if any of the eigenfrequencies of the bridge fall below the threshold of 5 Hz. Below this threshold, there is a considerable risk of the frequency coinciding with that produced of pedestrians crossing the bridge which may lead to resonance. The natural frequencies of the bridge are to be considered with and without ageing effects and with an assumed material damping value of 1.0 % (Mottram & Henderson, 2016). If the requirement is not met, then it is to be verified using the technical guide provided by Sétra (2006). The methodology used in this guide is described in Figure 3.5.

The input needed for the guide consists of categorisation of the bridge into one of four bridge classes and into one of three comfort levels. The bridge classes are defined by the amount of expected traffic.

- Class 1: Urban footbridge in an area with high pedestrian density.
- Class 2: Urban footbridge in a populated area that may occasionally be loaded over its entire loading surface.
- Class 3: Footbridge for standard use that may occasionally be crossed by a large number of people, but never over its entire loading surface.
- Class 4: Seldom used footbridge, built in sparsely populated areas.

The comfort levels of the bridge are to be decided by the owner of the bridge. The levels should be set so that it suits the bridge users and whether the duration of the stay on the bridge is long or not. If the users are elderly, disabled, or children, then the comfort should be higher. If the bridge is short, then the comfort may be set lower. The levels are defined as follows:

- Maximum comfort: Accelerations undergone by the structure are practically imperceptible to users.
- Average comfort: Accelerations undergone by the structure are merely perceptible to users.
- Minimum comfort: Under loading configurations that seldom occur, accelerations undergone by the structure are perceived by the users, but do not become intolerable.

Corresponding to the chosen comfort level, a range of suitable accelerations may be chosen as shown in Table 3.5. The accelerations are however given in terms of ranges and not thresholds, hence leaving some room for flexibility. To further evaluate the dynamic response of the bridge, the risk of resonance is to be determined using the frequencies of the eigenmodes according to Table 3.6. The risk is to be used in combination with the previously determined bridge class to determine what dynamic load case that is to be applied to the structure according to Table 3.7. The three load cases are in turn dependent on the assumed density d of pedestrians and the corresponding number of pedestrians N calculated using the bridge's total surface S as follows:

$$N = S \cdot d$$

Furthermore, the density of pedestrians can be linked to an equivalent number of pedestrians. The equivalent number is the number of pedestrians that are assumed to walk the bridge with the same frequency and in phase. The density and the corresponding equivalent number can be found in Table 3.8.

The dynamic load cases, presented in Table 3.9, are to be placed at the positions and directions corresponding to the worst case. The load cases are further dependent on the critical damping ratio ξ and a reduction factor ψ considering the risk of resonance. The reduction factor included in load case 1 and 2 is to be determined using Figure 3.6 and the reduction factor included in load case 3 is to be determined using Figure 3.7.

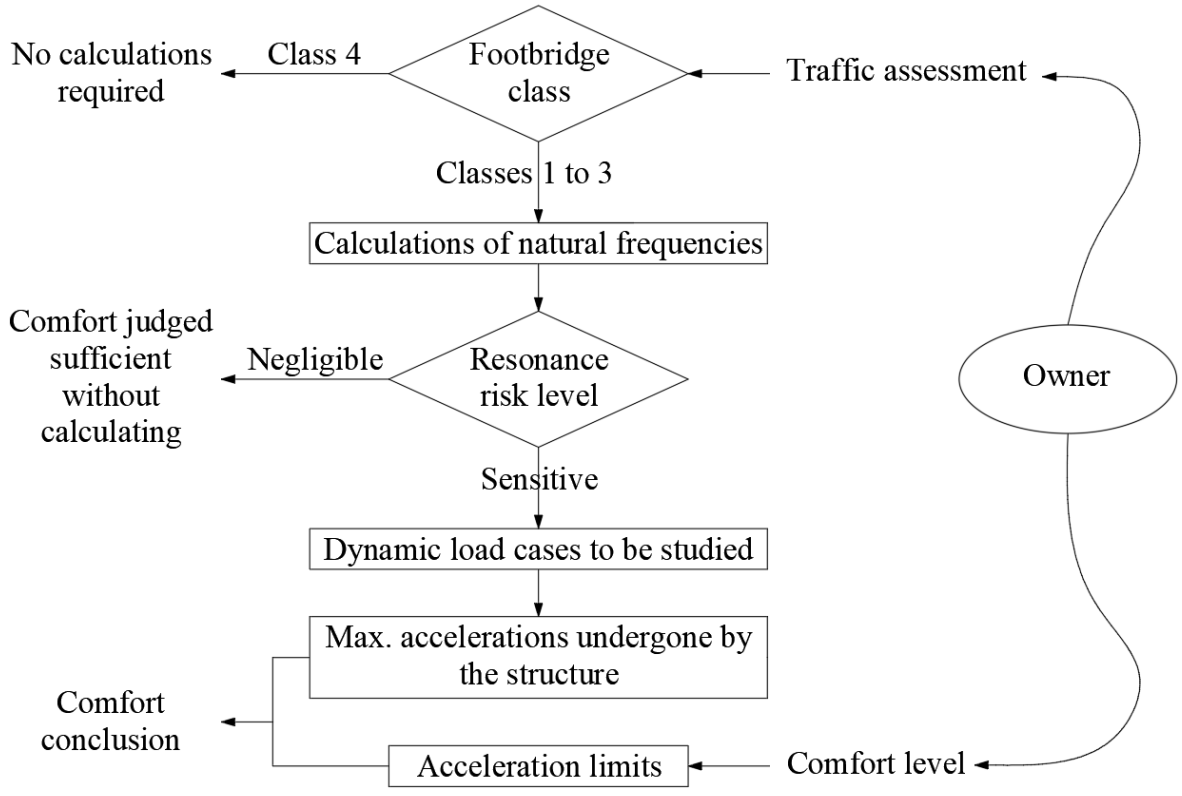

Figure 3.5: Methodology organisation chart, inspired by Sétra (2006).

Table 3.5: Acceleration ranges in m/s² for vertical and horizontal vibrations (Sétra, 2006).

	Comfort level			
	Maximum	Average	Minimum	Unacceptable
Vertical	0.0 – 0.5	0.5 – 1.0	1.0 – 2.5	> 2.5
Horizontal	0.0 – 0.15	0.15 – 0.3	0.3 – 0.8	> 0.8

Table 3.6: Frequency ranges (Hz) of the vertical and horizontal vibrations (Sétra, 2006).

	Risk of resonance				
	Negligible	Medium	High	Medium	Low
Vertical	0.0 – 1.0	1.0 – 1.7	1.7 – 2.1	2.1 – 2.6	2.6 – 5.0
Horizontal	0.0 – 0.3	0.3 – 0.5	0.5 – 1.1	1.1 – 1.3	1.3 – 2.5

Table 3.7: Dynamic load cases to be used (Sétra, 2006).

	Risk of resonance		
Bridge class	High	Medium	Low
1	Case 2	Case 2	Case 3
2	Case 1	Case 1	Case 3
3		-	-

Table 3.8: Pedestrian density equivalent number (Sétra, 2006).

Bridge class	Density *d* of the crowd	Equivalent number of pedestrians
1	1.0 pedestrians/m²	$1.85 \cdot \sqrt{(1/N)}$
2	0.8 pedestrians/m²	$10.8 \cdot \sqrt{(\xi \cdot N)}$
3	0.5 pedestrians/m²	$10.8 \cdot \sqrt{(\xi \cdot N)}$

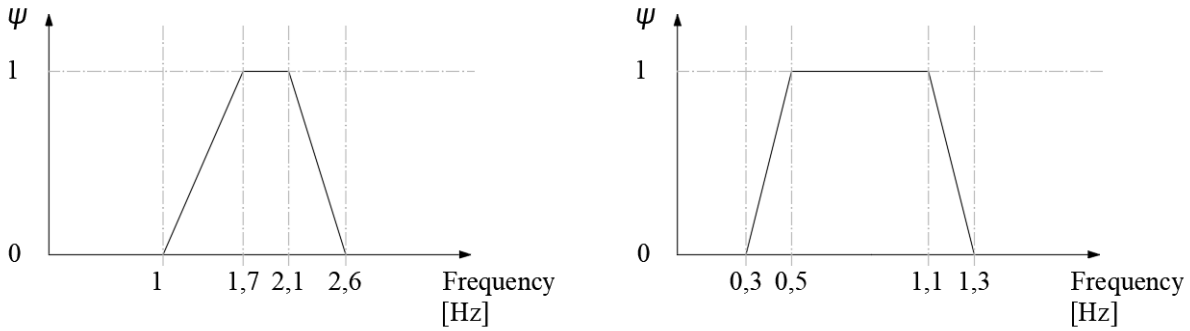

Figure 3.6: Reduction factor ψ included in load case 1 and 2. Vertical and longitudinal vibrations to the left and lateral vibrations to the right.

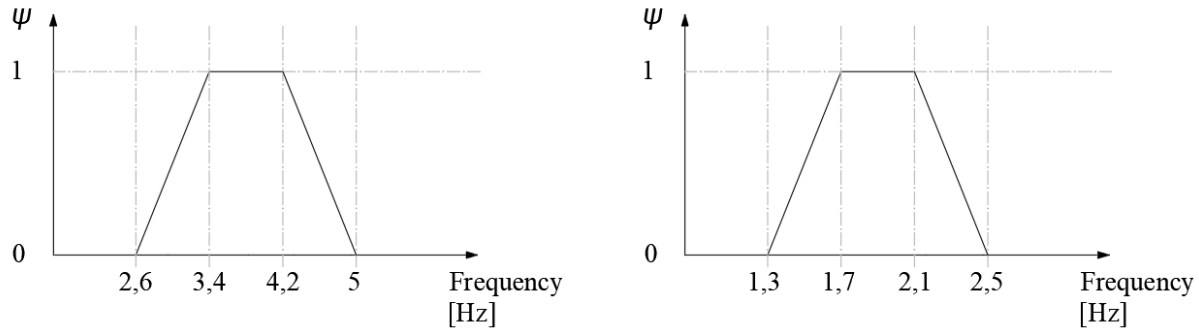

Figure 3.7: Reduction factor ψ included in load case 3. Vertical and longitudinal vibrations to the left and lateral vibrations to the right.

Table 3.9: Dynamic load cases (Sétra, 2006).

	Direction	Load per m^2
Case 1: sparse and dense crowds	Vertical (v)	$d \cdot (280) \cdot 10.8 \cdot \cos(2\pi f_v t) \cdot \sqrt{(\xi/N)} \cdot \psi$
	Longitudinal (l)	$d \cdot (140) \cdot 10.8 \cdot \cos(2\pi f_v t) \cdot \sqrt{(\xi/N)} \cdot \psi$
	Transverse (t)	$d \cdot (35) \cdot 10.8 \cdot \cos(2\pi f_v t) \cdot \sqrt{(\xi/N)} \cdot \psi$
Case 2: very dense crowds	Vertical (v)	$d \cdot (280) \cdot 1.85 \cdot \cos(2\pi f_v t) \cdot \sqrt{(1/N)} \cdot \psi$
	Longitudinal (l)	$d \cdot (140) \cdot 1.85 \cdot \cos(2\pi f_v t) \cdot \sqrt{(1/N)} \cdot \psi$
	Transverse (t)	$d \cdot (35) \cdot 1.85 \cdot \cos(2\pi f_v t) \cdot \sqrt{(1/N)} \cdot \psi$
Case 3: effect of 2nd harmonic	Vertical (v)	Same as for case 2 but 280 is reduced to 70
	Longitudinal (l)	Same as for case 2 but 140 is reduced to 35
	Transverse (t)	Same as for case 2 but 35 is reduced to 7

3.7 ULS Failure Criteria

In strength analysis of composites, the definition of failure can be defined either as a first-ply failure or a last-ply failure (Nijssen 2015), where the first-ply failure is the more conservative of the two. As the name suggests, failure is defined at the point when the first ply of the composite fails. Nijssen mentions that this does not necessarily lead to total failure of the laminate, as the laminate as a whole may have some residual strength. In order to utilise this residual strength, last-ply failure can be used instead. The failure will then occur when the last ply fails, allowing for progressive failure. However, Henderson and Mottram (2018) suggest that progressive last-ply analysis should only be used by experienced FE-analysts. Moreover, since serviceability requirements are generally more decisive for the design of FRP bridges, the definition of ULS failure is unlikely to affect the design. Other than the strength check an analysis of the maximum buckling load should be performed for the relevant parts of the structure.

3.7.1 First-Ply Failure

There have been several criterions developed predicting the strength of a ply loaded along multiple axes. These multiaxial criterions can either be independent or dependent. The independent criterion implies that the strength in one direction is not influenced by the stress in another, and the opposite is true for the dependent criterion (Nijssen 2015).

BRIGADE/Plus incorporates four different stress-based failure theories as listed below. Each theory is based on the tensile and compressive stress limits, X_t and X_c and the shear stress limit S in the X-Y plane. The material directions are denoted by 1 and 2, where 1 indicates the direction of the fibres and 2 the direction transverse to the fibres. The following applies to each theory:

$$i = 1,2: \begin{cases} \sigma_{ii} > 0 \rightarrow X_i = X_{t,i} \\ \sigma_{ii} < 0 \rightarrow X_i = X_{c,i} \end{cases}$$

Furthermore, each criterion is defined so that if the failure index I_F exceeds 1.0, failure occurs.

1. Maximum stress theory
   The maximum stress criterion is an independent criterion that states that failure will occur if the principal stress in one direction exceeds that of the strength in that direction.

$$I_F = \max\left(\frac{\sigma_{11}}{X_1}, \frac{\sigma_{22}}{X_2}, \left|\frac{\sigma_{12}}{S}\right|\right) < 1.0$$

2. Tsai-Hill theory
   The Tsai-Hill is a dependent failure criterion derived by Tsai (1968) based on Hill (1950) includes stress and strength interactions in the plane, thus the predicted strength will be slightly less than the predicted one by the maximum strength theory and requires that:

$$I_F = \frac{\sigma_{11}^2}{X^2} - \frac{\sigma_{11}\sigma_{22}}{X^2} + \frac{\sigma_{22}^2}{Y^2} + \frac{\sigma_{12}^2}{S^2} < 1.0$$

3. Azzi-Tsai-Hill theory
   The Azzi-Tsai-Hill failure theorem (Azzi & Tsai 1965) is a generalisation of Tsai-Hill theory with the difference that the absolute value of the cross-product term is used:

$$I_F = \frac{\sigma_{11}^2}{X^2} - \frac{|\sigma_{11}\sigma_{22}|}{X^2} + \frac{\sigma_{22}^2}{Y^2} + \frac{\sigma_{12}^2}{S^2} < 1.0$$

4. Tsai-Wu theory
   The Tsai-Wu failure criterion (Tsai & Wu 1971) is a special case of the Tsai-Hill criterion and requires that:

$$I_F = F_1\sigma_{11} + F_2\sigma_{22} + F_{11}\sigma_{11}^2 + F_{22}\sigma_{22}^2 + F_{66}\sigma_{12}^2 + 2F_{12}\sigma_{11}\sigma_{22} < 1.0$$

   Where the Tsai-Wu coefficients are defined as follows:

$$F_1 = \frac{1}{X_t} + \frac{1}{X_c}, \qquad F_2 = \frac{1}{Y_t} + \frac{1}{Y_c}, \qquad F_{11} = -\frac{1}{X_t X_c}, \qquad F_{22} = -\frac{1}{Y_t Y_c}, \qquad F_{66} = \frac{1}{S^2}$$

   The last coefficient F_{12} is dependent on whether the equibiaxial stress, σ_{biax}, is known or not. If known the coefficient may be calculated as below:

$$F_{12} = \frac{1}{2\sigma_{biax}^2}\left[1 - \left(\frac{1}{X_t} + \frac{1}{X_c} + \frac{1}{Y_t} + \frac{1}{Y_c}\right)\sigma_{biax} + \left(\frac{1}{X_t X_c} + \frac{1}{Y_t Y_c}\right)\sigma_{biax}^2\right]$$

However, if it is not known, as is the case in this report, it may be set by a varying term $-1.0 \leq \dot{f} \leq 1.0$ inserted in the expression: $F_{12} = \dot{f}\sqrt{F_{11}F_{22}}$

BRIGADE/Plus also have a strain-based failure theory incorporated in the form of maximum strain theory. The theory is based on the tensile and compressive strain limits, X_{ε_t} and X_{ε_c} and the shear strain limit, S_ε, in the X-Y plane. The denoted directions 1 and 2 are defined as for the stress-based failure theories:

$$i = 1,2: \begin{cases} \varepsilon_{ii} > 0 \rightarrow X_{\varepsilon i} = X_{\varepsilon_t, i} \\ \varepsilon_{ii} < 0 \rightarrow X_{\varepsilon i} = X_{\varepsilon_c, i} \end{cases}$$

The maximum strain criterion requires that $I_F = \max\left(\frac{\varepsilon_{11}}{X_\varepsilon}, \frac{\varepsilon_{22}}{Y_\varepsilon}, \left|\frac{\varepsilon_{12}}{S_\varepsilon}\right|\right) < 1.0$. The theory will however yield a result close to that of the maximum stress theory and is therefore not used in this report.

3.7.2 Last-Ply Failure

Due to the strength of a ply being a function of its direction and plies of a laminate being differently oriented, it is unlikely that the component fails at the same load as first-ply failures predict. Instead, plies will fail successively as the load increase, reducing the strength of the laminate but not leading to failure of the component as the stress can be redistributed (Agarwal & Broutman 1990). Agarwal and Broutman argue that the first-ply failure is too conservative, and that the laminate is in no real danger of actual failure when first ply failure occurs. However, the stiffness of the laminate will reduce as the plies progressively occur, causing a non-linear behaviour, as shown in Figure 3.8.

In this report, the last ply failure criterion will not be used. This is due to BRIGADE/PLUS not having this function included and since Henderson and Mottram (2018) suggest that the first-ply failure analysis should be used. It can be noted, however, that Abaqus allows for this kind of analysis to be performed.

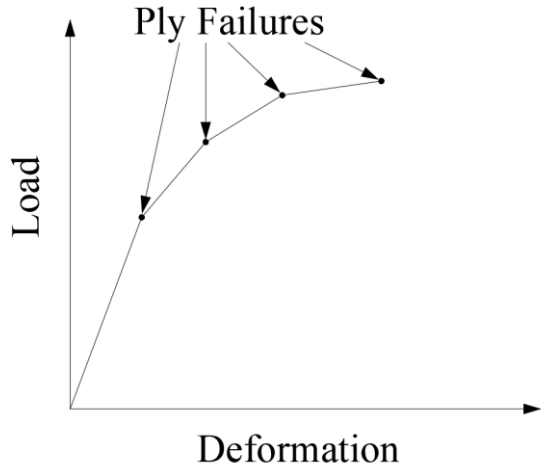

Figure 3.8: Load-deformation behaviour of hypothetical laminate (inspired by Agarwal & Broutman, 1990).

4 Bridge properties

4.1 Bridge Materials

As mentioned in Section 1.4, three FRP bridges were analysed and compared to each other and to a predesigned reference bridge made from stress-laminated timber. The three types of FRP analysed in this report were chosen based on their frequent use in the bridge industry as well as due to their availability on the market. The following materials were used:

1. GFRP laminate
2. CFRP laminate
3. Pultruded GFRP
4. Stress-laminated timber

The same design was used for each FRP bridge so as to simplify the comparison. This design was adapted to be as similar as practically possible to that of the predesigned timber bridge.

4.2 Stress-Laminated Timber Bridge

The reference bridge used in this report is a pedestrian bridge located in Skåne, Sweden. The bridge is a pedestrian, stress-laminated timber bridge, continuous over three spans. The total length of the bridge measures 60 m with a width of 3 m. The bridge deck was designed by COWI (2018) and the main drawings are presented in Appendix A.

However, due to joints being outside of the scope of the present study, the FRP bridges were designed as simply supported instead of continuous. Consequently, some alterations were necessary to enable a fair comparison to the predesigned timber bridge, and the reference bridge was redesigned as three simply supported bridges rather than a single continuous bridge. The same cross-section of the timber bridge was used since hand calculations showed that the section was still viable. Further verification was made using BRIGADE/Plus.

With the design altered, it was decided to only analyse the part of the bridge spanning the longest distance. The analysed simply supported timber bridge is visualised in figures 4.1 and 4.2. Furthermore, since the same material used in the original timber bridge was used in the new one, the properties derived by COWI (2018) could still be used, these being presented in Table 4.1. In addition to these properties, the density of the deck was set to 600 kg/m^3 and the surfacing applied linked to a weight of 2,3 kN/m^2 (COWI 2018).

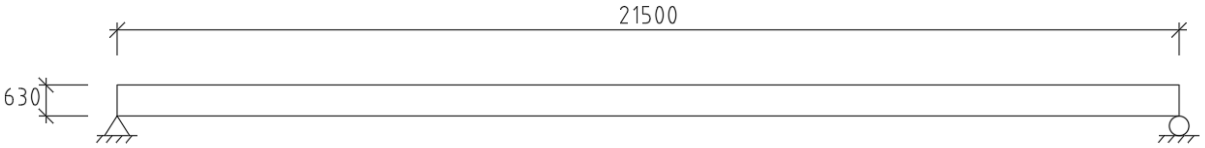

Figure 4.1: Simply supported timber and FRP bridges, measurements in mm.

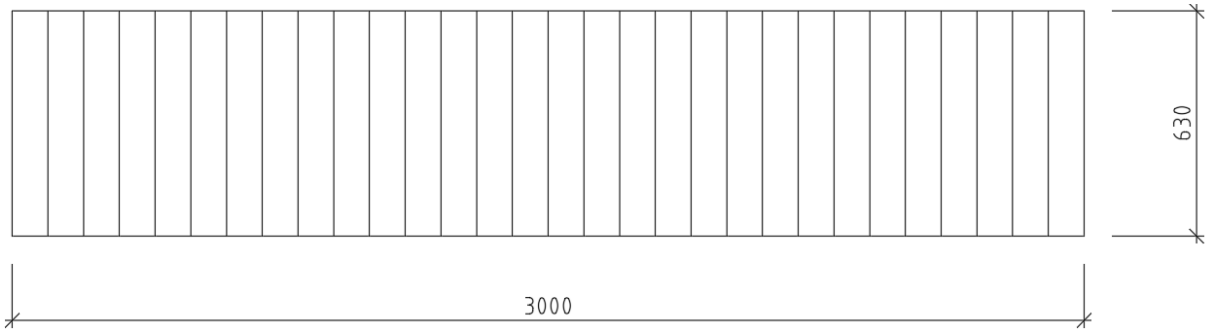

Figure 4.2: Cross section of the timber bridge, measurements in mm.

Table 4.1: Design values for material properties of the stress-laminated timber.

Material parameter		[MPa]
Flexural strength	f_{md}	17
Tensile strength	f_{td}	14
Compressive strength parallel to the fibres	f_{cd}	14
Short term compressive strength orthogonal to the fibres	f_{cd90}	1.8
Long term compressive strength orthogonal to the fibres	f_{cd90p}	1.2
Shear strength	f_{vd}	2.0
Young's modulus parallel to the fibres	E_d	10400
	$E_{0,mean}$	13000
Young's modulus orthogonal to the fibres	$E_{d,90}$	208
	$E_{90,mean}$	260
Shear modulus parallel to the fibres	G_d	624
	$G_{0,mean}$	780
Shear modulus orthogonal to the fibres	$G_{d,90}$	62
	$G_{90,mean}$	78

4.3 FRP Bridges

The design of the FRP bridges was made as close as possible to that of the timber bridge. However, since the materials are inherently different, the same exact design could not be used. The FRP bridges were designed out of mainly two materials: FRP and structural foam. The FRP was to be placed as visualised in the cross-section in Figure 4.3, where the hollow sections in the figure were to be filled with the structural foam. The structural role of the FRP is mainly to resist tension and compression in the outermost parts, and for the structural foam to resist shear forces. The vertical FRP parts of the cross sections will further support the foam by taking some of the shear force, as well as reducing the transverse lever arm of the upper and lower FRP parts.

The difference within the FRP bridges' design comes in the production methods of the material. Two of the bridges were to be constructed using a layup method, whereas the third bridge was to be constructed using pultrusion. The pultruded bridge was constructed using glass fibres in combination with polyester matrix (GFRP) as these materials are the most commonly used for the method. Of the two bridges using layup-laminates, one was to be constructed using GFRP with a composition as similar as possible to that of the pultruded bridge. The other one was constructed using carbon fibres in combination with epoxy matrix (CFRP).

There are a few differences between the two GFRP bridges. According to Fiberline Composites A/S (2002), their pultruded products contain several different types of fibre bundles and mats. In contrast, the bridge constructed using layup only uses unidirectional fibre plies, hence creating a difference in properties. Another difference stems from the lack of data concerning the fibres and matrix used in the pultrusion. The properties stated by Fiberline Composites A/S presented in Table 4.2 are that of the composite, and not for the individual components. The values stated are the minimum allowed, however, at a real project contact should be made with the manufacturer to obtain characteristic values. The only known data of the individual components were that glass fibres and polyester. As such, it is not possible to choose the exact same fibre properties and matrix for both bridges. The properties of the materials used in the layup laminates are instead based on indicative values given by Ascione et al. (2016) and Agarwal & Broutman (1990), presented in tables 4.3 and 4.4. The authors mention that these values are within the range of material properties reported in the literature, but does not state whether they are characteristic values, mean values or something else.

It should be mentioned that the pultruded FRP employed in this study may not be viable in practice. Pultruded profiles are often standardised, and not produced on demand. In this report, it is however assumed that the production of the profile employed is possible. The same applies to the FRP produced using layup production methods.

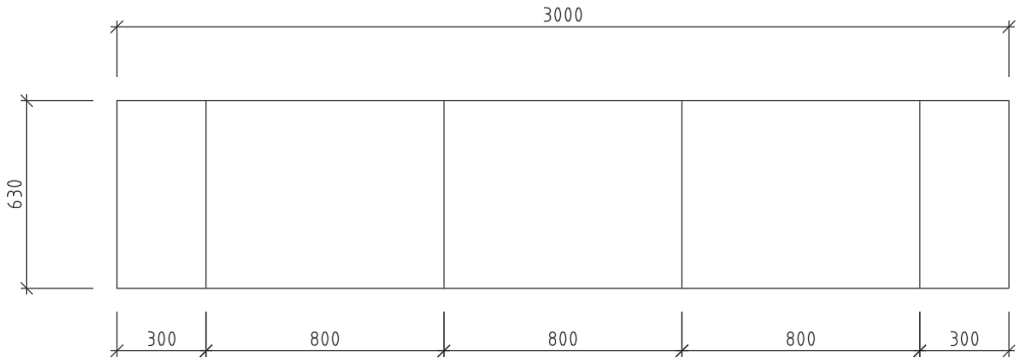

Figure 4.3: Cross section of FRP bridges. Measurements in mm.

Table 4.2: Minimum strength values of pultruded elements (Fiberline Composites A/S, 2002).

Typical strength values of pultruded elements			
		[MPa]	[-]
Flexural strength, 0º	$f_{b,1}$	240	
Flexural strength, 90º	$f_{b,2}$	100	
Tensile strength, 0º	$f_{t,1}$	240	
Tensile strength, 90º	$f_{t,2}$	50	
Compressive strength, 0º	$f_{c,1}$	240	
Compressive strength, 90º	$f_{c,2}$	70	
Shear strength	f_{τ}	25	
Young's modulus, 0º	E_1	23000-28000	
Young's modulus, 90º	E_2	8500	
Shear modulus	G	3000	
Poisson's ratio	v_{12}		0.23
	v_{21}		0.09
Density	ρ		1800 kg/m^3

Table 4.3: Indicative material properties of fibres (Ascione et al., 2016).

Indicative values fibres					
			Unit	E-glass	HS-Carbon
	Density	ρ	kg/m^3	2570	1790
	Thermal expansion	α	K^{-1} (10^{-6})	5	- 0.4
	Poisson´s ratio	v_f	-	0.238	0.3
Tension in fibre direction	Young´s modulus	E_{f1}	MPa	73100	238000
	Strain limit	ε_{f1}	%	3.8	1.5
	Strength	σ_{f1}	MPa	2750	3600
	Poisson´s ratio	v_f	-	0.238	0.02
Tension perpendicular to fibre direction	Young´s modulus	E_{f2}	MPa	73100	15000
	Strain limit	ε_{f2}	%	2.4	0.9
	Strength	σ_{f2}	MPa	1750	135
Compression in fibre direction	Strain limit	ε_{f1}	%	2.4	0.9
	Strength	σ_{f1}	MPa	1750	2140
	Modulus	G_f	MPa	30000	50000
Shear	Strain limit	γ_{12}	%	5.6	2.4
	Strength	τ_{f12}	MPa	1700	1200

Table 4.4: Indicative material properties of resin (Ascione et al., 2016).

Indicative values resin					
		Unit	Polyester	Vinylester	Epoxy
Density	ρ	kg/m^3	1200	1100	1250
Poisson´s ratio	v_{R12}	-	0.38	0.26	0.39
Young´s modulus	E_R	MPa	3550	3350	3100
Strain limit	ε_R	%	1.8	2.2	2.5
Strength	σ_R	MPa	55	75	75
Shear modulus	G_R	MPa	1350	1400	1500
Shear strain limit	γ_{12}	%	3.8	3.7	5
Shear strength	τ_R	MPa	50	65	80
Thermal expansion	α (10^{-6})	K^{-1}	50-120	50-75	45-65
Glass transition	T_g	°C	60	100	80-150

The material properties of a unidirectional ply of the layup laminate could be derived using the theory presented in Section 3. The fibre volume fraction was set to 60 % of the ply. Furthermore, the ply thickness was set to 0,5 mm for both materials using the layup laminates. The resulting characteristic properties of the plies are presented in Table 4.7. In order to further derive the design properties of the FRP material, the material partial factor along with the conversion factor applied according to Section 3.5 were used.

Since the material properties of the layup plies were derived from theoretical models, the first material partial factor, γ_{M1}, was set to the conservative value of 1,35. It was assumed that the production method used to produce the bridge was not that of hand lamination or equivalent technologies. Instead, it was suggested that the expected quality of the production methods correspond to a variation coefficient of $V_X \leq 0.10$ (Ascione et al., 2016). However, depending on whether the strength, the local instability or the global stability of the structure are to be verified, different values of γ_{M2} should be used. The actual partial factors employed are presented in Table 4.5. Since the properties given for the pultruded FRP corresponds to the minimum allowed values of the material, it is assumed that the partial coefficient γ_M can be set to 1,0. The assumption is based on

The conversion factor, η_c, of all FRP materials was evaluated as described in Section 3.5.1 with the guidance provided by Table 3.1 and Table 3.2. The bridges evaluated were assumed to not be covered by any protective coating affecting the temperature or the humidity of the material. It was further assumed that the material was fully post-cured and finally that the footbridges were insensitive to effects stemming from wind. The conversion factors presented in Table 4.6 were then derived on the basis of these assumptions.

It is unclear when and how the long-term values are to be applied in the ULS verification. The load duration affects the creep of the material and thus also the total conversion factor. However, when applying load combinations, the material will be subjected to both short and long-term loads. Since the conversion factor cannot be applied separately for the loads, one of the durations must be chosen. In this report, the short-term load duration was used. The short-term values were also used for the SLS verifications. The long-term values should still be considered when determined the precamber due to permanent loads, which was not done in this report.

Using the partial coefficient and the conversion factor of the corresponding limit state, the design material properties were derived as described in Section 3.5, presented in Table 4.7.

Table 4.5: Material partial coefficients of layup laminates.

Partial coefficient	Strength	Local stability	Global stability	SLS
γ_{M1}	1.35	1.35	1.35	-
γ_{M2}	1.35	1.5	1.35	-
γ_{M}	1.8225	2.025	1.8225	1.0

Table 4.6: Conversion factors of the FRP.

Conversion factor η_c		
Load duration	ULS Strength	SLS
Short	0.72	0.72
Long	0.36	0.36

Table 4.7: Material properties of unidirectional laminates.

		E_1	E_2	G_{12}	v_{12}	$f_{t,1}$	$f_{c,1}$	$f_{t,2}$	$f_{c,2}$	f_{12}
		[GPa]			[-]	[MPa]				
GFRP	Characteristic	43.9	14.6	4.5	0.29	1416	813	31	118	72
	ULS-Strength	17.4	5.8	1.8	0.29	559	321	12	47	28
	ULS-Local stability	15.6	5.2	1.6	0.29	-				
	SLS	31.6	10.6	3.2	0.29					
CFRP	Characteristic	139.7	7.6	5.2	0.17	1314	1220	43	168	48
	ULS-Strength	55.2	3.0	2.1	0.17	701	651	23	90	26
	ULS-Local stability	49.7	2.7	1.9	0.17	-				
	SLS	100.6	5.46	3.8	0.17					
Pultruded	Characteristic	28.0	8.5	3.0	0.23	240	240	50	70	25
	ULS-Strength	14.9	4.1	1.6	0.23	128	128	27	37	13
	ULS-Local stability	13.4	4.1	1.4	0.23	-				
	SLS	20.2	6.1	2.2	0.23					

5 Modelling

5.1 Modelling of Composite Materials

Due to the complexity of FRP as a material, the bridges were modelled in a three-dimensional FE analysis using BRIGADE/Plus. There are differences in how the different bridges have been modelled stemming from the specific material properties and structure of the bridges. Furthermore, some alterations to the program and simplifications of the bridges were made.

Composite materials may be modelled at three different levels of detail. For more detailed analysis, more information and computational power are also required. Only some mechanical properties of the material may require a high level of detail whereas a lower level is sufficient for others. The three levels of detailing to be considered in the composite analysis are presented below and are also visualised in Figure 5.1.

1. Microscopic modelling
   The fibres and matrix are analysed separately. This level of analysis is not required for the analysis at hand (Henderson & Mottram, 2018).

2. Layered modelling
   The properties of one ply are stated, where the properties of the fibres and matrix have been smeared over the ply. If possible, this ply level of analysis is required by Henderson and Mottram (2018).

3. Smeared modelling
   The whole composite is modelled as a homogeneous material with properties equivalent of the included materials. Smeared modelling is used in the global analysis or in cases when layered modelling is not possible.

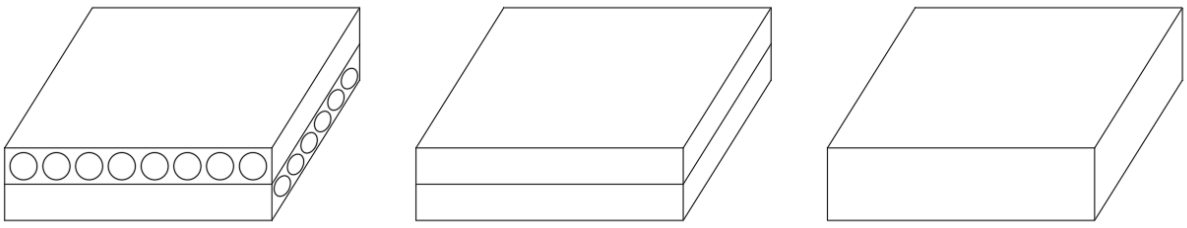

Figure 5.1: The three levels of modelling. From the left: Microscopic modelling, Layered modelling and Smeared modelling.

The bridges consisting of layup composites were modelled using layered modelling at the layers which were deemed critical. However, in order to minimise the computational time, non-critical adjacent plies, arranged in the same orientation, were modelled as a single ply. Consequently, the analysis in the present study is based on a combination of level 2 and 3, with the exception of the pultruded bridge which was modelled using smeared properties due to the unknown layering sequence and properties of the layers.

Due to the difference in modelling, the stress and strain distribution differed between the two types of production methods. The distribution through the pultruded FRP had a linear distribution due to the smeared properties, whereas the distribution through the layup composites varied as stated in Section 3.4.

5.2 Dimensions and Layups

The dimensions of the analysed bridges were based on the respective dimensions given in figures 4.1 – 4.3. The models were based on the use of shell instances, i.e. two-dimensional parts in a three-dimensional space. For the FRP bridges consisting of layup FRP, these shells were assigned three different layups at the locations shown in figure 5.2. The layups were all built symmetrically to reduce the coupling matrix and thus also the computational time, as described in Section 3.4. For the pultruded bridge, the same locations were used, but instead of layups the locations were assigned different thicknesses. Note that the layup and thickness selected for the sides of the bridge also continued on the short sides of the bridge, closing the cross section. The main direction of the FRP was set to the direction of the bridge.

The critical buckling load of the webs was analysed using a smaller model in order to reduce the computational time. The cross-section of this model was defined as shown in Figure 5.3 and with the same location of layups and thicknesses as previously shown in Figure 5.2. Furthermore, the length of the model was set to 10 m.

Figure 5.2: Layup locations seen at the cross-section of the bridge: Red: Top and bottom, Blue: Web, Green: Sides.

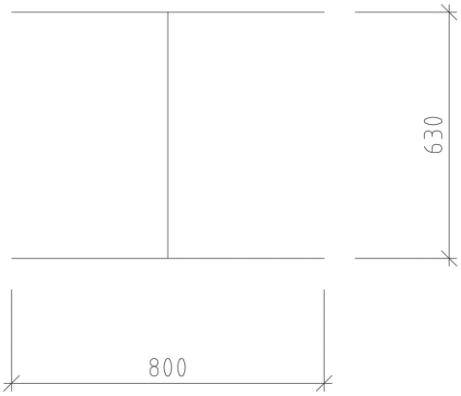

Figure 5.3: Cross section of buckle analysis cut out. Measurements in mm.

5.3 Loads and Boundary Conditions

The loads applied to the bridge were based on those applied to the reference timber bridge in the original design. However, only the vertical loads were considered due to the limited scope of this study. The vertical loads were divided into two categories: permanent and live loads.

5.3.1 Permanent Loads

The permanent loads applied consisted of the dead weights of the bridge parts. The dead weight of railings and installations were however excluded. The dead weight of the FRP and timber was based on the densities provided in Section 4 and applied as a gravity load in BRIGADE/Plus. Furthermore, the dead weight of the structural foam was based on a density of 80 kg/m^3 provided by Diab (2018). The structural effects stemming from the foam were however not modelled due to the reasons described in Section 5.5. Consequently, this load was applied as an equivalent pressure load over the bridge surface. Finally, the surfacing of the bridges was considered and estimated as shown together with the other loads in Table 5.1.

5.3.2 Live Loads

The live loads applied to the bridge were the same as for the reference bridge and consist of crowd loading and loading caused by a service vehicle, with loads as presented in Table 5.2. The loads were assumed to act separately, hence only one load was applied at a time.

As users familiar to BRIGADE/Plus know, the program will find the worst load placement of live loads through use of influence areas. The crowd load was assumed to be applicable to the whole bridge deck. This was achieved through creating the middle lane as seen in Figure 5.4 and by applying the live load as defined in BRIGADE/Plus as visualised in Appendix B. The service vehicle consists of two axle loads with a geometry described in Figure 5.5. The vehicle gave the worst effects when placed on the side of the bridge or over one of the webs of the FRP bridge. Therefore, the vehicle axle loads were applied to two lanes to find the worst placement, as shown in Figure 5.4. Due to symmetry, only lanes of one half of the bridge was modelled.

The live loads were applied differently in the buckling analysis. As the service vehicle was deemed to subject the web to the highest risk of buckling, only this load case was considered. Furthermore, it was assumed that the load effects of the two axles did not interact, due to them being far apart, hence only the larger one of them was considered in the analysis. The worst load placement was further assumed to be straight over one of the webs, where the load was applied over an area equal to that of the tire area shown in Figure 5.5.

Table 5.1: Dead weight of the bridges

Bridge material	Dead weight	Characteristic load	Load type
FRP	FRP	$\rho \cdot 9.81$ kN/m^3	Gravity
	Foam	0.5 kN/m^2	Pressure
	Surfacing	0.2 kN/ m^2	Pressure
Timber	Timber	$\rho \cdot 9.81$ kN/m^3	Gravity
	Surfacing	1.955 kN/m^3	Pressure

Table 5.2: Live loads of FRP bridges.

Load		Characteristic load	Vehicle type
Crowd load		5 kN/m^2	Lane surface load
Service vehicle	Q_{sv1}	80 kN	Vehicle load
	Q_{sv2}	40 kN	

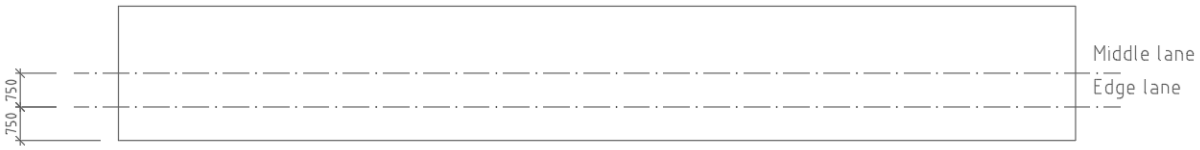

Figure 5.4: Lanes defined in BRIGADE/Plus, measurements in mm.

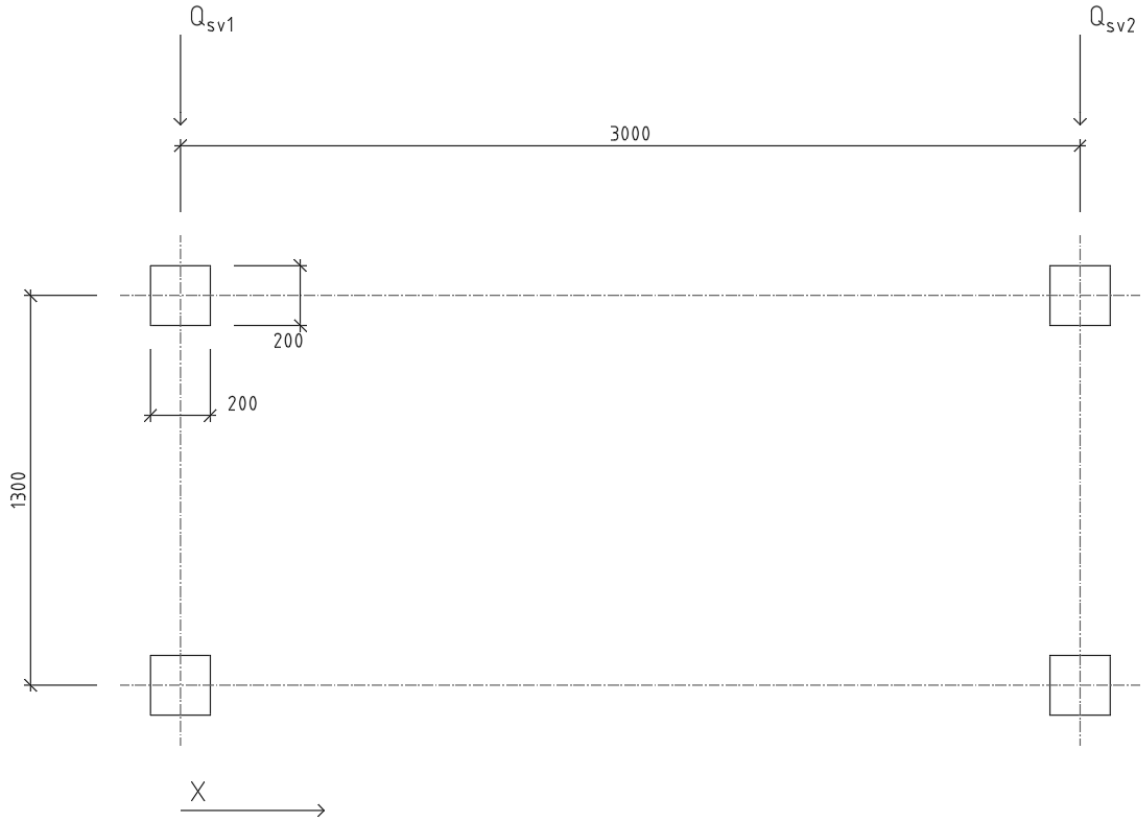

Figure 5.5: Geometry of the service vehicle, measurements in mm.

5.3.3 Boundary conditions

As previously described, the analysed bridges were considered to be simply supported over one span. The boundary conditions were therefore modelled as pinned on one side and a roller support on the other side. The supports were assumed to be acting along the lines shown in Figure 5.6.

As only a small part of the analysed bridges was considered during the buckling analysis, some boundary conditions had to be added to the cuts. All edges of the model were assumed to be locked both in the vertical and transverse directions relative to the model's main direction, as visualised in Figure 5.7. Moreover, one of the cross-sectional edges of the lower flange was locked in the longitudinal direction, making it pinned.

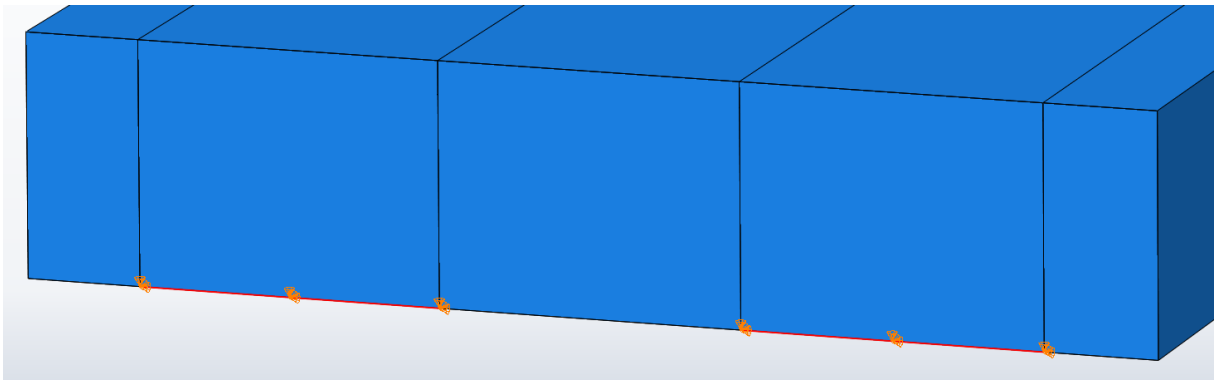

Figure 5.6: Placement of boundary conditions.

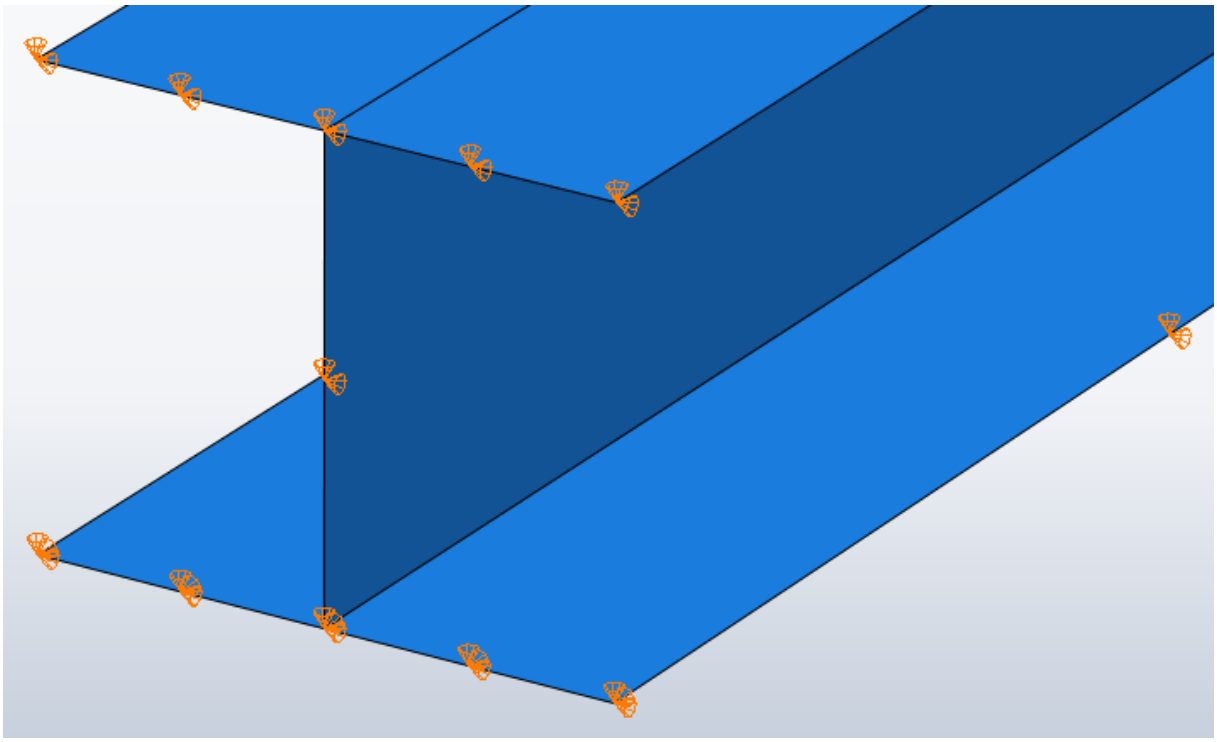

Figure 5.7: Visualisation of boundary condition placement on buckling model.

5.4 Dynamic Modelling

The dynamic response of the bridges was evaluated through an analysis of the eigenfrequencies, and when necessary the dynamic load cases, calculated according to Section 3.6.2, were applied with the corresponding frequencies.

The applied dynamic loads are, as previously described, dependent on the expected traffic density of the bridge. The expected density of the timber bridge was used as far as possible, but some alterations had to be made. According to the documentation, the crowd density of the reference bridge was assumed to be 0,5 pedestrians per square meter, which is equivalent to a bridge of class 3. The bridges analysed in this study were however considered to be placed in a more populated area corresponding to bridge class 2, and a crowd density of 0,8 pedestrians per square meter was therefore used instead. The change was made as the probability of an FRP bridge being placed in an area with low crowd density is considered low. Hence, the bridge placement was reconsidered and set to a more reasonable setting.

As the dynamic response of the bridges was to be evaluated loaded as well as unloaded, the mass of the pedestrians had to be added in the former case. This was done by adding inertia over the bridge deck equal to that of the crowd density with an assumption of the average weight of a person being 70 kg:

$$\frac{mass}{m^2} = 70 \cdot 0{,}8 = 56\ kg/m^2$$

As previously explained, the structural foam was excluded from the model and therefore the mass of the foam had to be added using inertia in the same manner as explained above.

The dynamic accelerations were evaluated using a modal dynamics step. The time period of the step was chosen so that the system had time to reach equilibrium in the analysis. Furthermore, the time increment was chosen in accordance to the following relation, linked to the largest of the relevant eigenfrequencies:

$$time\ increment = \frac{1}{10 \cdot f_{max}}$$

Finally, the damping coefficient of the system ξ was added as a direct modal through the created step. The coefficient was, in accordance to Ascione et al. (2016), set to 1 %.

5.5 Simplifications and Alterations

BRIGADE/Plus is a program based on Abaqus, which does support the analysis of composite layups. The additional functions provided in Brigade/Plus does however not support composite layup and therefore some alterations had to be made. As previously mentioned in Section 5.3.2, the live load module was used in order to assess the load effects stemming from the live loads. The composite layup output selection is not available in this module. It is however available in the step module and they can be requested by defining the domain as the composite layup, as shown in Figure 5.8. By requesting this output in the step module, the program could write the necessary output code in the .inp file linked to the module. The written code could then be copied and inserted into the .inp file written by the live load

module, hence requesting the outputs desired. An example of the code to be copied are shown in Figure 5.9, as an example of code that are to be replaced are shown in Figure 5.10. It should however be noted that the row containing "*Output, field" should be deleted from the copied code since this line already appears at a different location in the modified code. Further notion should also be made to that depending on mesh size, the procedure described above has to be made several times as the output request may be repeated in the code.

The bridges were as previously described modelled using shell elements. The use of shells does however introduce complications where the different shells interact, as visualised in Figure 5.11. On the inner side of the structure, it can be seen that the two shells interact, hence creating a stiffer corner. The opposite is true for the outer corner. The choice of offsetting the thickness from the middle is considered to yield the most realistic response. Another deviation from the real geometry is the absence of transitional radii at the corners of the model, which was not considered in the model.

The models were further simplified by excluding the structural properties of the foam from the model. This due to the doubts of its completely filling all the voids and due to difficulties in modelling the adhesive properties between FRP and foam. Instead, only the dead weight of the foam was applied in the form of a pressure load acting on the bridge. This simplification is conservative and will lead to an overestimation of the material needed. In order to make the dynamic analysis as accurate as possible, the mass of the foam was added as inertia.

Another simplification was made when applying the service vehicle to the bridge. When defining the service vehicle in BRIGADE/Plus, as seen in Appendix B, Figure 10.5, it is not possible to specify the tire area over which the load is to be applied. Instead, the program simply applies the loading as concentrated loads. This could in turn lead to unrealistic stress concentrations.

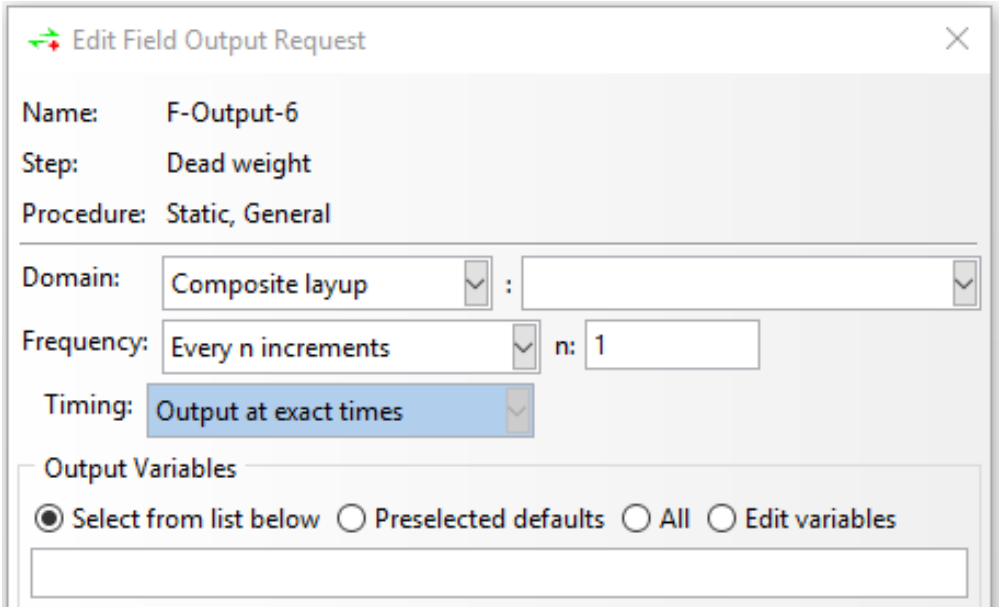

Figure 5.8: Output request.

```
**
** FIELD OUTPUT: Layup-Beambottop
**
*Output, field
*Element Output, elset=Bridge.Beambottop-1, directions=YES
1, 2, 3, 4, 5, 6, 7, 8, 9, 10, 11, 12, 13, 14, 15, 16
CFAILURE, S
*Element Output, elset=Bridge.Beambottop-1, directions=YES
17, 18, 19, 20, 21, 22, 23, 24, 25, 26, 27, 28, 29, 30, 31, 32
CFAILURE, S
**
```

Figure 5.9: Output request generated by the step-module to be copied. The numbers correspond to the requested plies.

```
*Element Output
S,
**
```

Figure 5.10: Output request generated by the live-load-module to be replaced by the code in Figure 10.

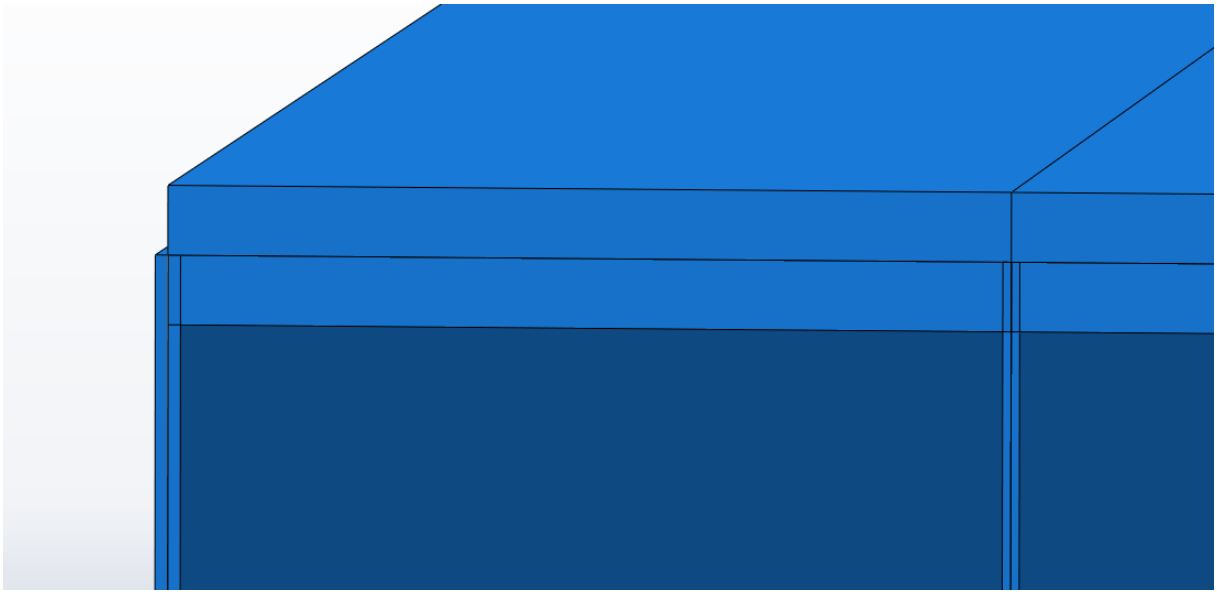

Figure 5.11: Simplified bridge model where geometry deviates from reality.

6 Results

6.1 Resulting Dimensions

The required thicknesses, corresponding layups and structural mass needed to fulfil both the ULS and the SLS results presented in the following subsection are displayed in Table 6.1. These dimensions were perceived through an iterative process, yielding, to some extension, more optimised dimensions for the requirements set. It should however be noted that these results do not need to fulfil the requirements stated for dynamic response according to Sétra (2006) as can be seen in Subsection 6.3.2. An example of a modelled layup can be seen in Figure 6.1.

Table 6.1: Layup sequences, corresponding thicknesses and structural mass of the analysed bridges. Each ply is assumed to have a thickness of 0.5 mm. Total mass includes FRP, structural foam and surfacing.

Material	Part	Location	Layup	Thickness [m]	FRP mass [kg]	Total mass [kg]
GFRP	Bridge	Top and bottom	$[(90/\pm45/0)_4/0_{43}]_S$	0.059	17100	21800
		Web	$[(90/\pm45/0)_2/(\pm45)_2]_S$	0.012		
	Sides	Sides of bridge	$[90/\pm45/0_6]_S$	0.009		
CFRP	Bridge	Top and bottom	$[90/\pm45/0)_2/0_{12}]_S$	0.02	4900	9300
		Web	$[(90/\pm45/0)_2]_S$	0.008		
	Sides	Sides of bridge	$[90/\pm45/0]_S$	0.004		
Pultruded GFRP	Bridge	Top and bottom	-	0.052	14000	18000
		Web	-	0.013		
	Sides	Sides of bridge	-	0.011		
Timber	Whole bridge	-	-	-	-	24400

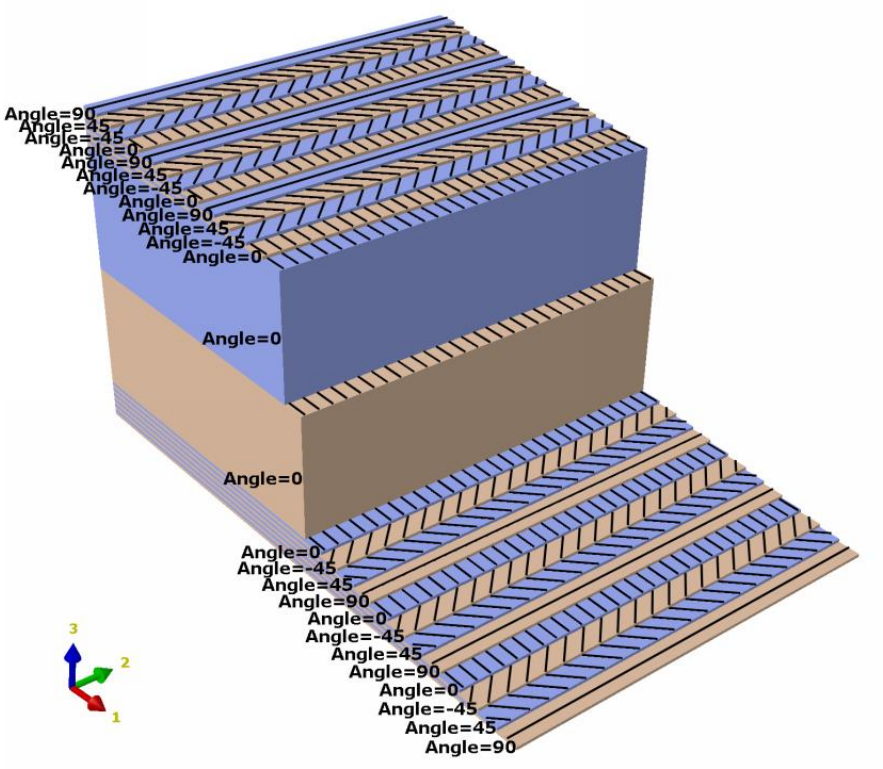

Figure 6.1: Example of a modelled layup.

6.2 ULS

All of the analysed bridges passed the requirements set in the ULS verifications. The results do however show that not all parts of the FRP bridges were used to their full potential, which is further discussed in Section 7.

6.2.1 Strength analysis

As stated in Section 3.7.1, BRIGADE/Plus use several first ply failure criteria. The result plots visualised in figures 6.2 – 6.4 have been singled out so the criterion showing the highest material usage is shown. For all bridges analysed, it was found that the Tsai-Hill criterion was decisive. The criterion is plotted in fractions of fulfilment, where 1 denotes that the criterion is fulfilled, and that failure occurs. Plots for each individual layup can be found in Appendix C. Furthermore, the strength capacity of the modified timber bridge was verified to not exceed its capacity. However, this verification is not presented in this report.

The strength verification of the layup GFRP and CFRP yielded a material usage of 98 %, Figure 6.2, and 80 %, Figure 6.3, of their capacity. This usage is found in a concentrated area in the middle of the bridge. The other parts of the bridge show low usage in comparison.

The same phenomena can be seen in the results of the pultruded GFRP, seen in Figure 6.4. The stress concentrations are however here not the decisive. Instead, the webs are subjected to stresses causing usage of 87 % of the material capacity.

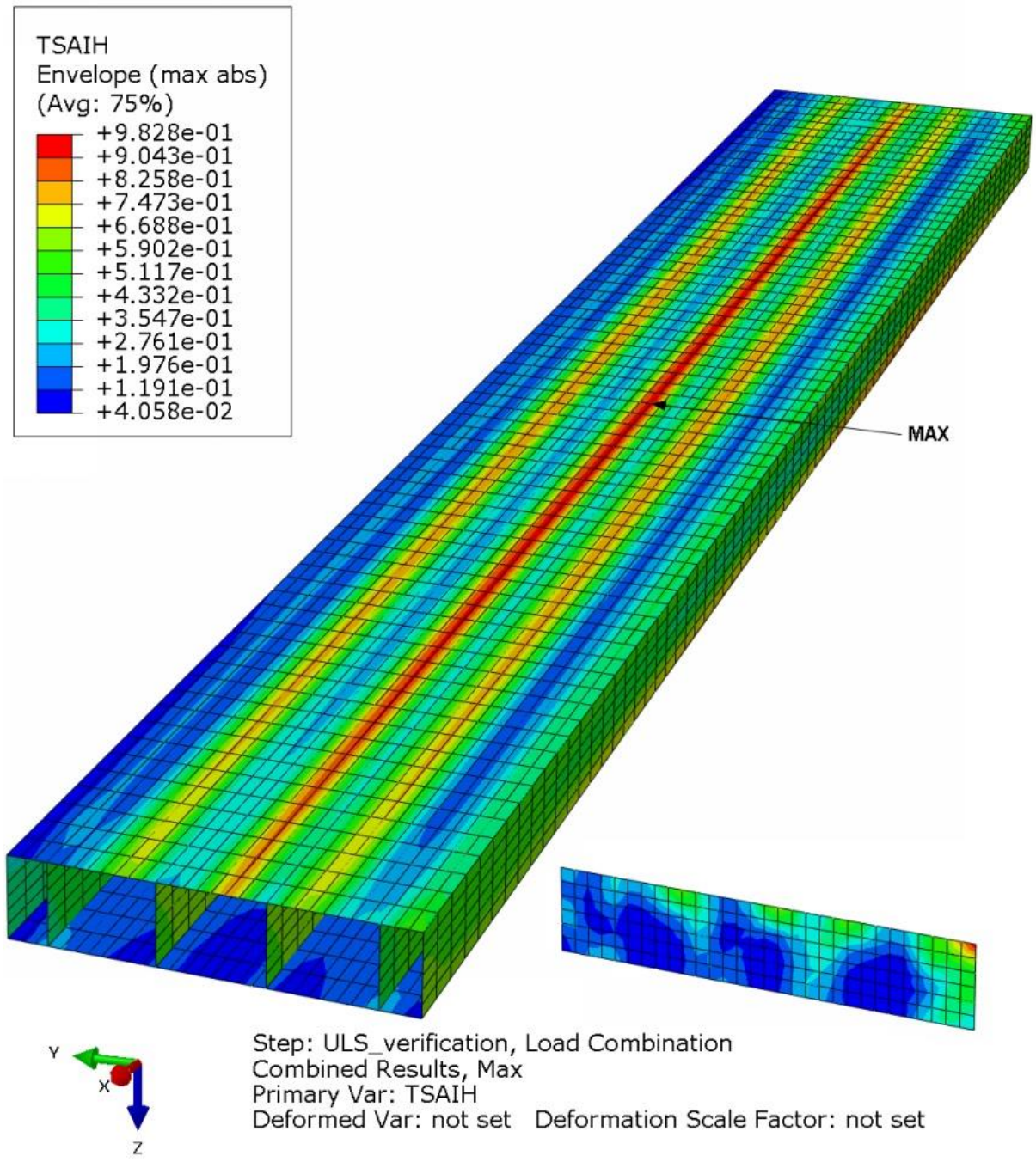

Figure 6.2: Failure criteria envelope plot of GFRP.

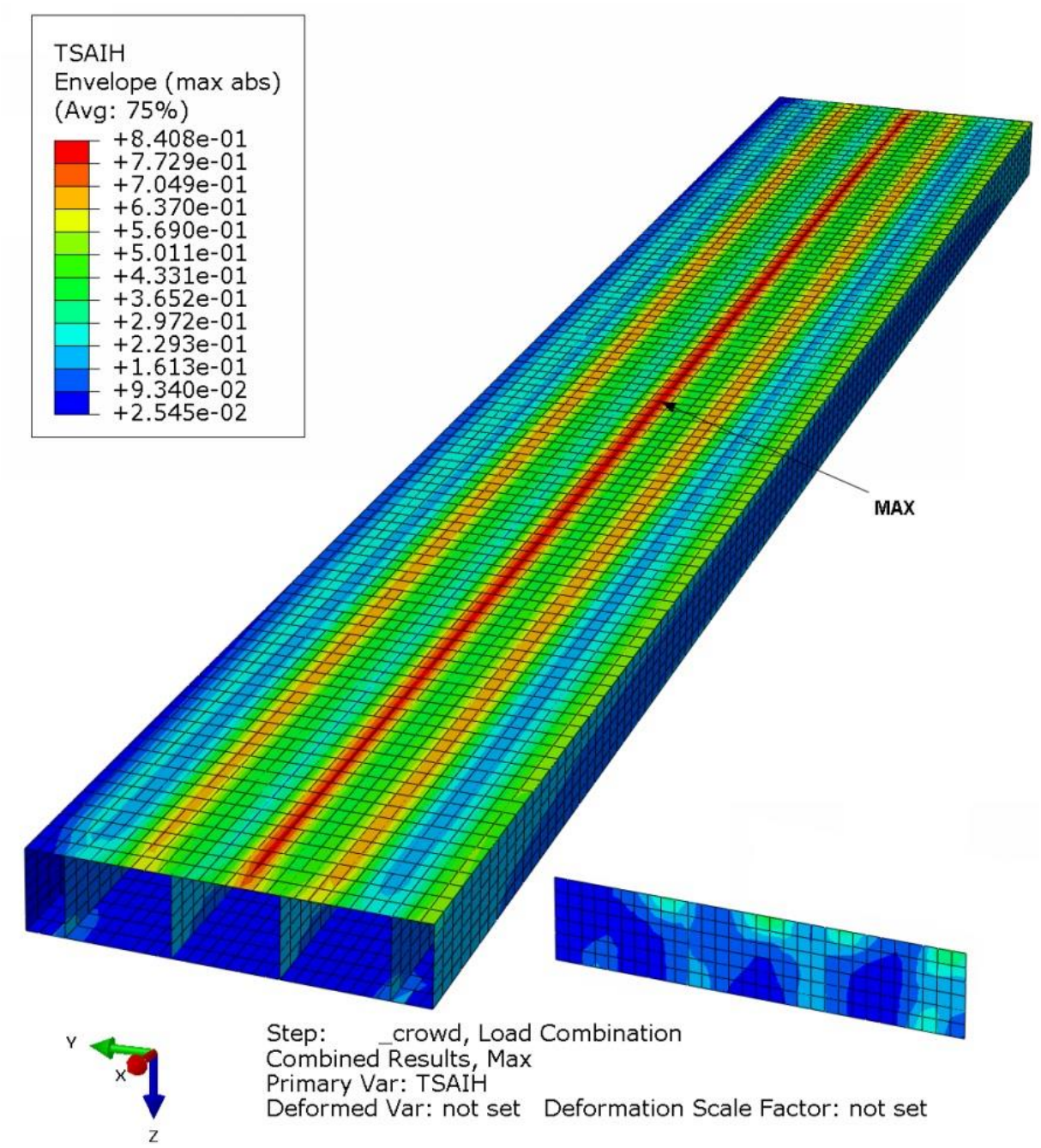

Figure 6.3: Failure criteria envelope plot of CFRP.

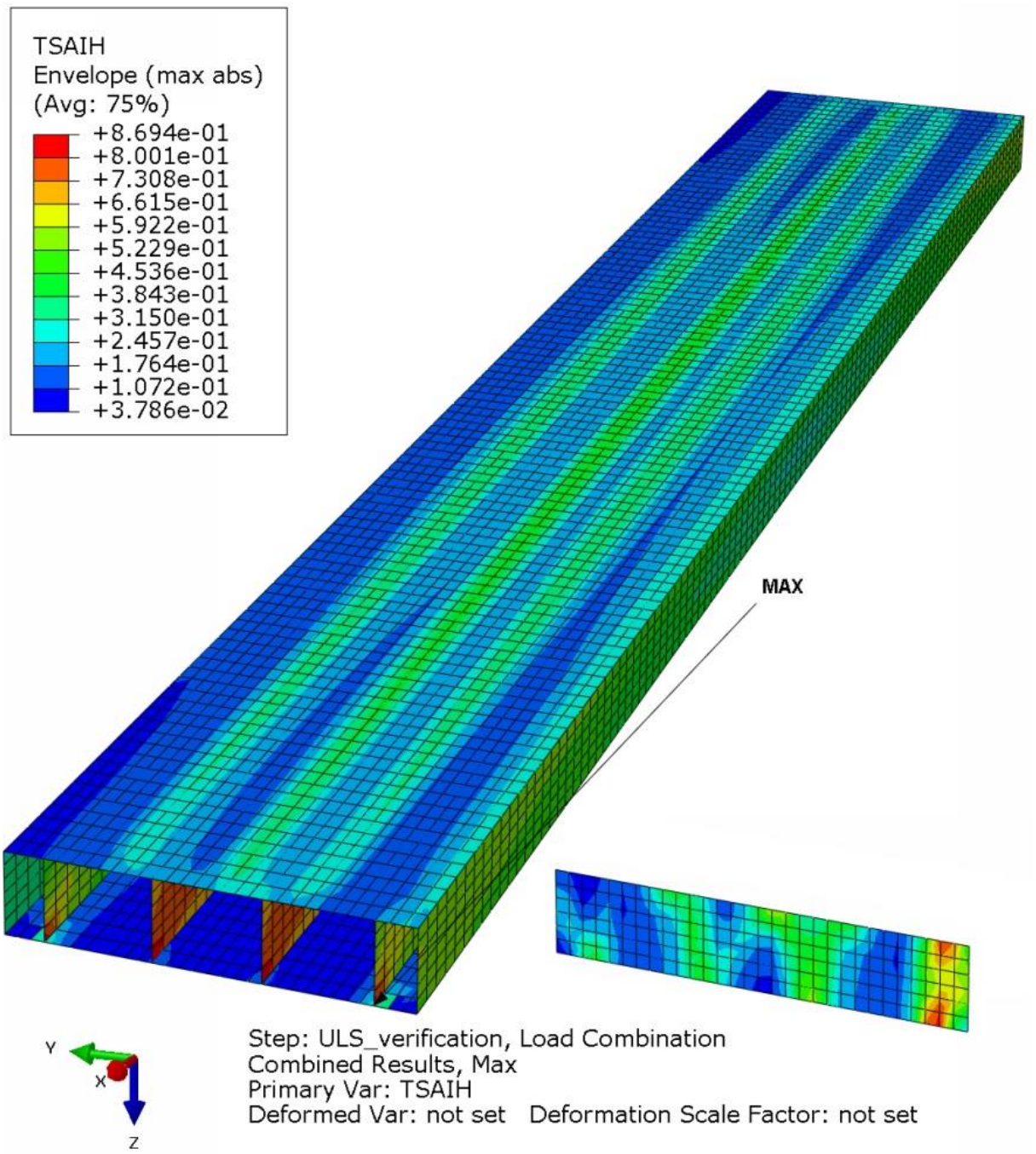

Figure 6.4: Failure criteria envelope plot of pultruded GFRP

6.2.2 Buckling analysis

The analysis of the webs confirms that they can withstand the service vehicle loading, even though the foam is assumed to not brace the web at buckling. As the load was applied as tire pressure, the axle load given in Table 5.2 must be converted into a resulting pressure. The point load at each tire may be described as:

$$P_{max} = \frac{Q_{SV1}}{2} \cdot 1.5 = \frac{80}{2} \cdot 1.5 = 60 \text{ kN}$$

Distributed over the tire area the pressure is set to:

$$Q_{max} = \frac{60}{0.2^2} = 1500 \text{ kPa}$$

Consequently, the buckling capacity of the webs should exceed 1500 kPa. The buckling capacity of the webs in all FRP bridges are presented in Table 6.2. All of the analysed webs showed the same buckling mode linked to the capacity, visualised in Figure 6.5.

Table 6.2: Buckling loads of web subjected to tire pressure.

Material	Web buckling load [kPa]
GFRP	11800
CFRP	3340
Pultruded GFRP	2480

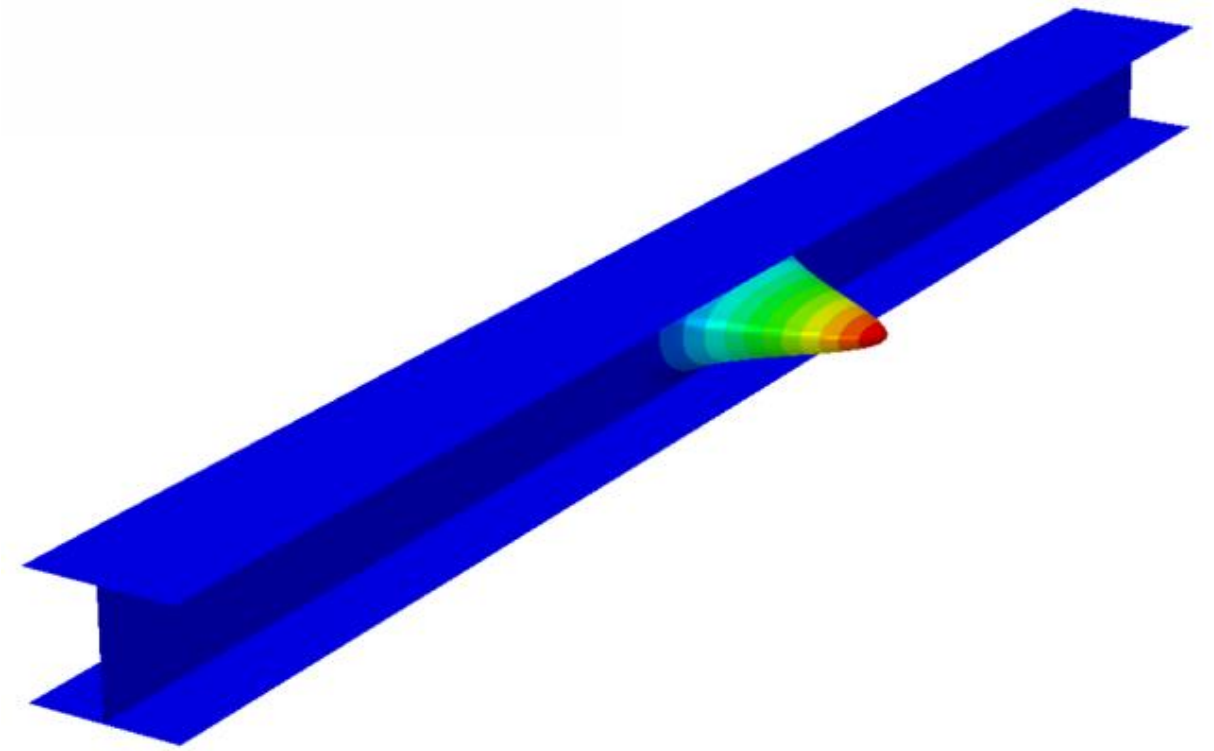

Figure 6.5: Web buckling mode.

6.3 SLS

The results of the performed SLS verifications varied depending on the bridge analysed. All of the bridges did however fulfil the deflection requirement and the difference between the results are instead found in the vibrational verifications.

6.3.1 Deflection

The maximum deflection limit was set to the bridge span length divided by 400, resulting in a limit of 54 mm. The maximum deflections were obtained as the bridges were subjected to crowd load distributed over the whole bridge deck, with values according to Table 6.3. Note that the deflections do not include that of the dead weight, as these are counteracted through precambering.

6.3.2 Vibration

The maximal allowed vertical vibrations of the analysed bridges, as stated in Table 3.5, are dependent on the desired comfort level. In this report, no specific requirement was set. The bridges performances were evaluated, and the results are presented in Table 6.4 and Appendix D. Through comparison of the comfort levels it can be seen that all of the bridges, except for the CFRP bridge, fulfil the minimum comfort requirements of 2.5 m/s^2, but none fulfil the next comfort level requirement of 0.5 – 1.0 m/s^2.

Table 6.3: Deflections of the analysed bridges

Material	Deflection [mm]
GFRP	47.0
CFRP	52.6
Pultruded GFRP	52.9
Timber	52.0

Table 6.4: Eigenfrequencies with corresponding dynamic load and maximum acceleration.

Material	Eigenfrequencies [Hz]		Dynamic load [N/m^2]		Maximum accelerations [m/s^2]
	Without crowd load	With crowd load	Without crowd load	With crowd load	
GFRP	3.1891	2.9528	10.6	6.4	2.0
CFRP	4.6610	4.1801	6.1	14.4	5.3
Pultruded GFRP	2.7934 4.6882	2.5454 4.2931	3.5 5.6	3.7 12.7	1.1
Timber	2.86	2.67	4.6	1.2	2.4

6.4 Estimated Energy Consumption

Using the structural mass of the FRP and the glue-laminated timber, presented in Table 6.1, and the energy intensity of the materials and its manufacturing methods presented in Section 2.7 were the estimated energy consumption of the bridges evaluated and presented in Figure 6.6. It can be seen that the estimated energy consumption of the timber bridge is much lower than that of the FRP bridges. However, it should be noted that the steel included in the timber bridge is not considered, nor is the structural foam of the FRP bridges.

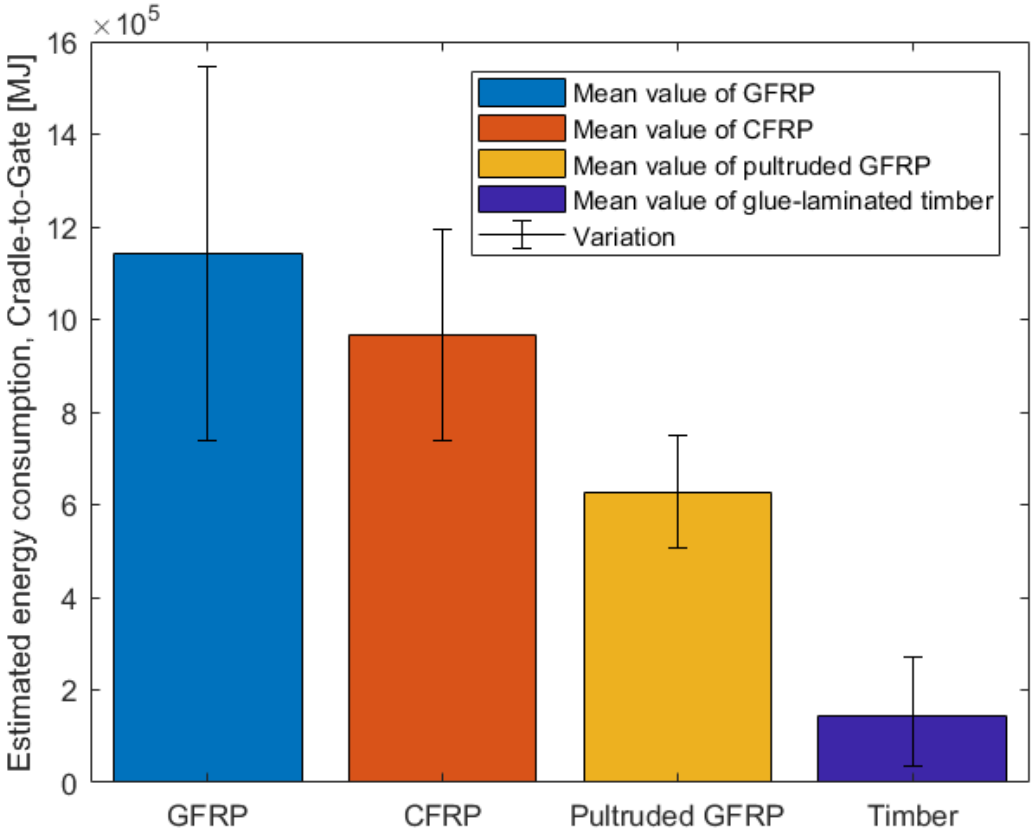

Figure 6.6: Estimated energy consumption of FRP and glue-laminated timber production.

7 Discussion

7.1 General Considerations

The results concluded in the previous section indicates that all analysed bridges fulfil the requirements set for ULS and for maximum deflection. None of the bridges does however exceed a comfort level better than the minimum allowed, and one does not reach that. Consequently, none of the bridges are suitable for replacing the continuous reference bridge. However, there are possible improvements that could render the FRP designs viable. The conceived results, design process and possible improvements are discussed in the following subsections.

The results produced in this report are as previously stated based on pre-normative documentation. The results may be altered as the actual design code is released and the results presented in this report be re-evaluated at such a release. The results produced should however not be seen as too uncertain as the documentation used are the base on which upon the standardised code are based.

The use of BRIGADE/Plus as a design tool for FRP bridges are at the writing moment not optimal due to the lack of necessary functions. The alterations made to the program are time consuming as the design process is iterative. It should further be mentioned that the computational time is multiplied with the number of plies added to the model (assuming a single section point of each layer), making the process slower than for normal analysis. Therefore, it is recommended that a more efficient program is used, if available.

The material parameters used in this study are gathered from the literature as well as through theoretical derivations. Properties derived from testing may differ from the ones produced in this report and could therefore yield other results. Furthermore, the properties used for the pultruded FRP were taken as the minimum allowed. Therefore, the actual properties are likely to exceed those employed in the present study, which would lead to different results.

The assumptions made when using classical laminate theory require that delamination is not valid or that the theory is not used in the vicinity of corners and edges. Some manufacturers claim to be able to produce layups without the risk of delamination with the use of special techniques. If these techniques are applicable or not to the designs proposed in this report is not known. As the method have been used in the vicinity or corners and edges in the report and as simplifications have been made in these areas, Section 5.5, more detailed investigations in these areas should be performed.

7.2 General Improvements

The overall performance of the bridge could be considerably improved if another overall design would have been chosen. As previously described, the design was chosen to be as similar as possible to that of the reference bridge in order to enable a fair comparison. There are however more efficient designs that should be considered, such as a truss-type superstructure. A truss would significantly improve the stiffness, and hence could less material be used. The truss-type superstructure is generally not possible when using timber due to durability concerns.

Another improvement of the overall design would have been to design the bridge as a continuous system rather than three single span structures. A continuous structure would however be more complex to design as it would have included joints, which are not covered by this report. It would further have taken more computational power as the analytical model would have been larger.

Apart from the overall design of the bridge, improvements could have been made by optimising the materials used. The optimisation would have consisted of rearranging the layup directions. This is a tedious iterative process that would take many attempts, as it is hard to predict the results beforehand. This has been done to some extent, but as seen in the ULS result plots, there are several areas where the failure criterions are not fulfilled.

Another way of optimisation would have been to use different layups for each part of the bridge. There are currently only three layups defined: for the bottom and top of the bridge, for the webs and finally one for the bridge sides. As an example, there could instead have been separate layups for each web. The biggest material savings are considered to be done if the layups of the bottom and top parts would have been separated. The bottom parts do nearly only require longitudinal fibres as these almost exclusively are subjected to longitudinal tension. On the contrary, the top does need fibres in all directions as tension will arise in other directions, hence different layups could have been used and materials saved.

To take the concept of different layups even further, the amount of fibres could have been varied in the longitudinal direction since the direction of stresses will change. This would however require more time in the design stage as well as in the actual construction of the bridge and if this would be profitable is hard to predict.

7.3 SLS

As stated in the result section, all of the bridges designed fulfilled the deflectional requirement. This was due to the design process, through iterative trial and error, finding the required layups and thicknesses of the laminates that would fulfil the limitation. The same was however not done to fulfil the vibrational comfort levels. Such a process would have taken a long time and it is doubtful if there would have been any reasonable solution to the problem.

Due to the relatively low mass of the bridges in relation to the stiffness, the first eigenfrequency will often fall below the threshold of 5 Hz, as can be seen in Table 6.4. As such, the natural frequency will coincide with the frequencies produced by pedestrians

crossing the bridge, creating resonance. The first eigenfrequency could simplified be determined through the well-known relation between stiffness *k* and mass *m* of the structure.

$$\omega_0 = \sqrt{k/m}$$

Changing the mass or the stiffness of the currently designed FRP bridges to alter the results is not considered feasible. A different solution using a tuned mass damper, counteracting the accelerations of the bridges due to the addition of mass, could however be employed. This would solve the issue at hand but would also increase costs and the need of materials for the bridges. Another solution could be to use other bridge designs with a higher stiffness relative to their mass, such as a truss.

Another aspect to be considered is the placement and usage of the bridge. In the design stage, it was assumed that the bridge was to be placed in an urban and quite populated area. If the bridge instead was to be placed in a rural area, none of the designed bridges would be required to be checked for vibrations. On the contrary, if the bridges were to be placed in a heavily populated area, effects stemming from accelerations would be even more problematic.

7.4 ULS

As previously stated in the results, all the bridges passed the ULS verifications. This result was achieved through an iterative process where the bridge designs conceived from the SLS design process were altered. The laminates were adjusted so that the stress distribution was acceptable throughout the structure and all failure criteria fulfilled.

The readjustment of plies described can although lead to several different solutions. Finding the optimal solution is possible but time-consuming. In this report, the need of plies in one direction was determined through evaluating the stresses in that direction. This was however only done using the global coordinate system, not allowing for evaluation of all ply directions. This requires some guesswork, hence it is advised to evaluate the stress in each ply using a local coordinate system.

The strength verifications of the layup laminates, shown in figures 6.2 and 6.3, show that the central area of the bridge is subjected to high stress concentrations. The stress concentrations are thought to be a result obtained through a wheel pair of the service vehicle being placed there. These stress concentrations could however be affected by the wheel pressures being simplified to concentrated loads, as previously described in Section 5.5. If that is the case, the stresses presented are likely to be conservative, and the actual stress would be lower if the concentrated loads were instead applied over an area. Another factor that could have reduced the stress concentrations would have been if the structural foam would have helped to more evenly distribute the stresses throughout the surface. If none of the reasons above would have altered the outcome, then the application of a thicker surfacing or a “buffer layer” may have been an option to increase the number of FRP laminates. A thicker surfacing may function to distribute the force applied more evenly to the structure, hence improving the results. The buffer layer suggested would have consisted of an extra layer of a lower grade FRP and foam applied between the surfacing and the structural FRP. This layer would have filled the same function as a thicker surfacing but would also protect the structural FRP when the surfacing needed replacing, acting as a buffer between the two.

7.5 Influence of Design Parameters

The results presented in the previous section are specific to the design situation at hand and are sensitive to several design parameters. Since the strength and stiffness of the material are directly proportional to the partial factor of the material as well as the conversion factors will the choice of these be crucial.

Studying Table 3.3, it can be seen that depending on whether the material property verification is certified or taken from technical literature the material partial factor will differ. A further difference may be achieved due to the production method chosen, see Table 3.4. Therefore, the partial factor of two manufacturers with different processes could range between the values presented in Table 7.1. If the ULS of the structure is decisive for the design, then this difference could lead to a 28 % increase of material needed. It is therefore advised to have close contact with a certified manufacturer during the design process and to consider the manufacturing process not only by the initial cost, but also by the impact on the final requirement of the materials.

When studying the conversion factor, similar results to those of the material partial factor can be seen. As mentioned in Section 3.5.1, the conversion factors linked to temperature and humidity may be ignored if a protective coating is applied to the structure. This modification could hence improve the properties of the material with 28 %. On the other side of the spectrum, the properties could be reduced even further due to factors not included in Ascione et al. (2016). To what extent these factors would decrease the capacity is unknown and further research is needed. It is therefore advised that protective measures such as protective coatings are evaluated and that the specific environmental impacts on the bridge are evaluated to improve the material efficiency of the structure and prevent underestimation of the materials needed.

To conclude, the impact of the design parameters is large. A combination of the two parameters discussed could, at the extremes, yield a difference of 57 % in materials needed. Hence should these factors be carefully chosen since large savings can be made.

Table 7.1: Comparison of material partial factor.

		Strength verification	Local stability	Global stability
γ_M	Minimum	1.35	1.5	1.35
	Maximum	2.16	2.7	2.025
	Difference	0.81	1.2	0.675
Difference on material parameters		28 %	30 %	25 %

8 Conclusions

8.1 Summarised Results

The designed GFRP bridges do fulfil the minimum requirements set. However, the CFRP bridge does not fulfil the vibrational requirements set. The comparable results between these bridges and the timber bridge are visualised in Figure 8.1. It can be seen that in most cases are the FRP alternatives performing better than the timber bridge. However, there are several factors of importance not compared in this report. Hence, it cannot be said with certainty whether FRP will be the better alternative.

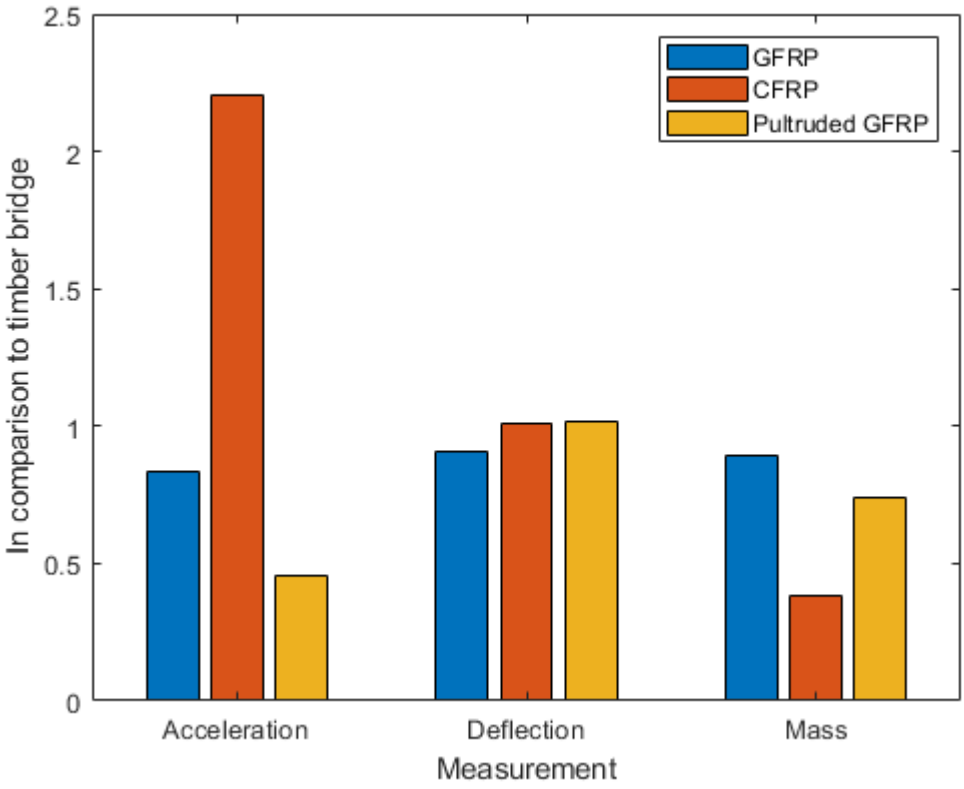

Figure 8.1: Summarised results of FRP bridges, compared to the timber bridge.

8.2 Conclusions Drawn

The use of FRP in bridge engineering, and more specifically for the design at hand, is possible and can in many situations work as an alternative to the more conventional materials. The final results are however heavily dependent on the choice of conversion factors and material partial factors. Therefore, these parameters should be considered as early as possible and with the help of manufacturers. In addition, also environmental factors particular for the area the bridge is to be placed in should be considered and investigated as they may have a large impact on the design and choice of material. Furthermore, the bridges analysed will often not fulfil the vibrational comfort levels due to their low weight and high stiffness. Tuned mass dampers may therefore be needed.

The choice of materials in the FRP is dependent on the situation at hand. There are several different products on the market, with different properties. Glass transition temperature, resistance to water damage or UV-radiation are just some critical parameters. Furthermore, if special additives need to be added, other rules of work environment etc. becomes relevant, making the whole process even more complicated. There are at the moment no guidance regarding all of these factors, hence it is recommended to contact manufacturers as they will know what kind of material may and may not work for a particular bridge.

For FRP to be a feasible option to the conventional materials it does not only have to work but also to be cost-effective. Furthermore, the feasibility will improve with a low environmental impact. As previously presented in Section 2.8, the cost-effectiveness of an FRP bridge depends on the methodology of the study in question. It is easy to characterise the results in a certain way or use data on different observations to reach a specific result. Most of the sources do however point to FRP being a more expensive alternative to the conventional materials. However, as previously presented in Section 2.8, the costs could be favourable if the design of the bridge is made to perfection and therefore it cannot be concluded whether FRP may or may not be more cost-effective than another alternative. What can be concluded is however that the costs most certainly are lower for the ground works and for the substructure as FRP bridges are lighter. Also, the need for maintenance will in most cases be lower and installation times reduced, leading to time and cost savings.

Evaluating the environmental impact of FRP, the studies presented in this report shows a clear advantage of FRP to the conventional construction materials. As seen in Section 2.7, the material is a better alternative in almost every aspect from an environmental standpoint. However, the bridges considered in this report are not the better alternative to the reference bridge, as seen in Figure 6.6. Further study of this figure reveals considerable variations due to production method and materials used. Hence, it can be concluded that the environmental impact of FRP is heavily dependent on the design, material and production method. Furthermore, the end-of-life recyclability is a major drawback of FRP. If this aspect is to be improved and as the demand for more environmentally friendly solutions increases, FRP may be a good alternative to other materials in bridge engineering.

The choice of what kind of FRP to use do affect the final product and the design process. If pultruded elements are chosen, the properties will be known and no optimisation of the material can be made, other than the thickness. In such a case, the whole process will be easier, but the material may not be as optimised. Furthermore, it is not probable that the

profile used in this report is viable due to its sheer size and due to the fact that most companies do not produce custom profiles on demand.

With the layup alternatives, the possibility to tailor the material to the needs of the bridge becomes possible. This tailoring does however consume a lot of time and the process is not as environmentally friendly as pultrusion, see Table 2.4. The choice between GFRP and CFRP is not obvious and should be decided on a case by case basis. The CFRP will be up to twice as light and can span longer distances, but at a considerably higher price. Furthermore, the production of carbon fibres is far more energy consuming than that of glass fibres.

8.3 Further Studies

There are several areas regarding the use of FRP in bridge engineering where the literature is lacking and where further research is needed. A list of subjects to be further investigated are presented below.

- The impact of horizontal forces on the bridge design.
- Joints and connections of bridge details and between bridge segments.
- Dynamic impact and design.
- FRP bridge design of road bridges.
- The impact of structural foam and its behaviour over time.
- The impact of thaw cycles on FRP material properties.
- Bridge design with last ply failure theories.
- Structural foam in FRP bridge applications.

9 References

Agarwal, B. D. & Broutman, L. J. (1990) *Analysis and Performance of Fibre Composites.* 2nd edn. New York: Wiley & Sons. ISBN: 0-471-51152-8.

Ascione, L. Caron, J.-F. Godonou, P. van IJselmuijden, K. Knippers, J. Mottram, T. Oppe, M. Gantriis Sorenssen, M. Taby, J. & Tromp, L. (2016) *Prospect for new guidance in the design of FRP*. Joint Research Center, European Commission. EUR 27666 EN. doi:10.2788/22306.

Azzi, V.D. & Tsai, S.W (1965) Anisotropic Strength of Composites. *Experimental Mechanics*. Vol. 5, Issue 9, pp 283-288. doi: 10.1007/BF02326292.

Bowers, T. Puettmann ME, Ganguly, I. Eastin, I. (2017) Cradle-to-Gate Life-Cycle Impact Analysis of Glued-Laminated (Glulam) Timber: Environmental Impacts of Glulam Produced in the US Pacific Northwest and Southeast. *Forest Products Journal*. Vol. 67. Issue 5. doi: 10.13073/FPJ-D-17-00008.

Clyne, T. W. & Hull, D (1996) *An Introduction to Composite Materials*. 2nd edn. Cambridge: Cambridge University Press (Cambridge Solid State Science Series). doi: 10.1017/CBO9781139170130.

COWI (2018) *Gångbro över Härlövsängaleden.* Job account number: A115689.

Daniel, R. A. (2003) Environmental considerations to structural material selection for a bridge. *Proc of the European bridge engineering conference*. Rotterdam: Lightweight Bridge Decks.

Diab (2018) *Divinycell PN Technincal Data*. Doc No: PN October 2018 rev. 9 SI. https://www.diabgroup.com/en-GB/Products-and-services/Core-Material/Divinycell-PN [2019-04-16].

Fiberline Composites A/S. (2002) *Fiberline design manual for structural profiles in composite materials*. 2nd edn. Kolding, Denmark. https://fiberline.com/sites/default/files/media/online-tools/190107_dm_uk.pdf [2019-02-19].

Halpin J. C. (1969) *Effects of Environmental Factors on Composite Materials*. AFML-TR 67-423.

Hashin, Z. (1980) Failure Criteria for Unidirectional Fibre Composites. *Journal of Applied Mechanics.* Vol. 47, Issue: 2 pp. 329-334. doi: 10.1115/1.3153664.

Henderson, J. & Mottram, J. T. (2018) *Fibre-reinforced polymer bridges – guidance for designers*. London: CIRIA. ISBN: 978-0-86017-794-4.

Hill, R. (1950) *The Mathematical Theory of Plasticity*. Oxford: Oxford University Press. ISBN: 978-0198503675.

IStructE (2014) *Building for a sustainable future: an engineer's guide.* London: Institution of Structural Engineers. ISBN: 978-1-906335-21-2.

Laurent, A-B. Gaboury, S. Wells, J-R. Bonfils, S. Boucher, J-F. Sylvie, B. D'Amours, S. & Villeneuve, C. (2013) Cradle-to-Gate Life-Cycle Assessment of a Glued-Laminated Wood Product from Quebec's Boreal Forest. *Forest Products Journal*. Vol. 63. Issue: 5. doi: 10.13073/FPJ-D-13-00048.

Nettles, A.T. (1994) *Basic Mechanics of Laminated composite plates.* Alabama: NASA, Marshall Flight Center. Reference Publication 1351.

Nijssen, R.P.L (2015) *Composite Materials: An Introduction.* Inholland University of Applied Sciences. ISBN: 978-90-77812-51-8.

Patljak, I. (2018) *Life cycle cost analysis of FRP pedestrian bridges*. Gothenburg: Chalmers University of Technology.

Puettmann, M. Oneil, E. Johnson, L. (2013) *Cradle to Gate Life Cycle Assessment of Glue-Laminated Timbers Production from the Southeast.*

Sétra. (2006) *Footbridges. Assessment of vibrational behaviour of footbridges under pedestrian loading.* Paris: The Technical Department for Transport, Roads and Bridges Engineering and Road Safety.

Swedish Standards Institute. (2002 A) *Eurocode – Basis of structural design*. Stockholm.

Swedish Standards Institute. (2002 B) *Eurocode 1 – Actions on structures.* Stockholm.

Song, Y. S. Young, J. R & Gutowski, T. G. (2009) Life cycle analysis of fibre-reinforced composites. *Composites Part A: Applied Science and Manufacturing.* Vol. 40, Issue: 8, pp 1257-1265. London: Elsevier. Doi: 10.1016/j.compositesa.2009.05.020.

Tsai, S. W. (1968) Strength Theories of Filamentary Structures. *Fundamental Aspects of Fibre Reinforced Plastic Composites.* Edit. Schwartz R. T. Schwartz H. S. Chap. 1. New York: Interscience. ISBN: 978-0470766033.

Tsai, S. W. & Wu, E. M (1971) A General Theory of Strength for Anisotropic Materials. *Journal of Composite Materials.* Vol. 5, Issue: 1, pp. 2-127.

Appendix

Appendix A

The most important design specifications of the continuous reference bridge made by COWI (2018) are presented in Figure 10.1 and 10.2. Furthermore, is a design overview visualised in Figure 10.3.

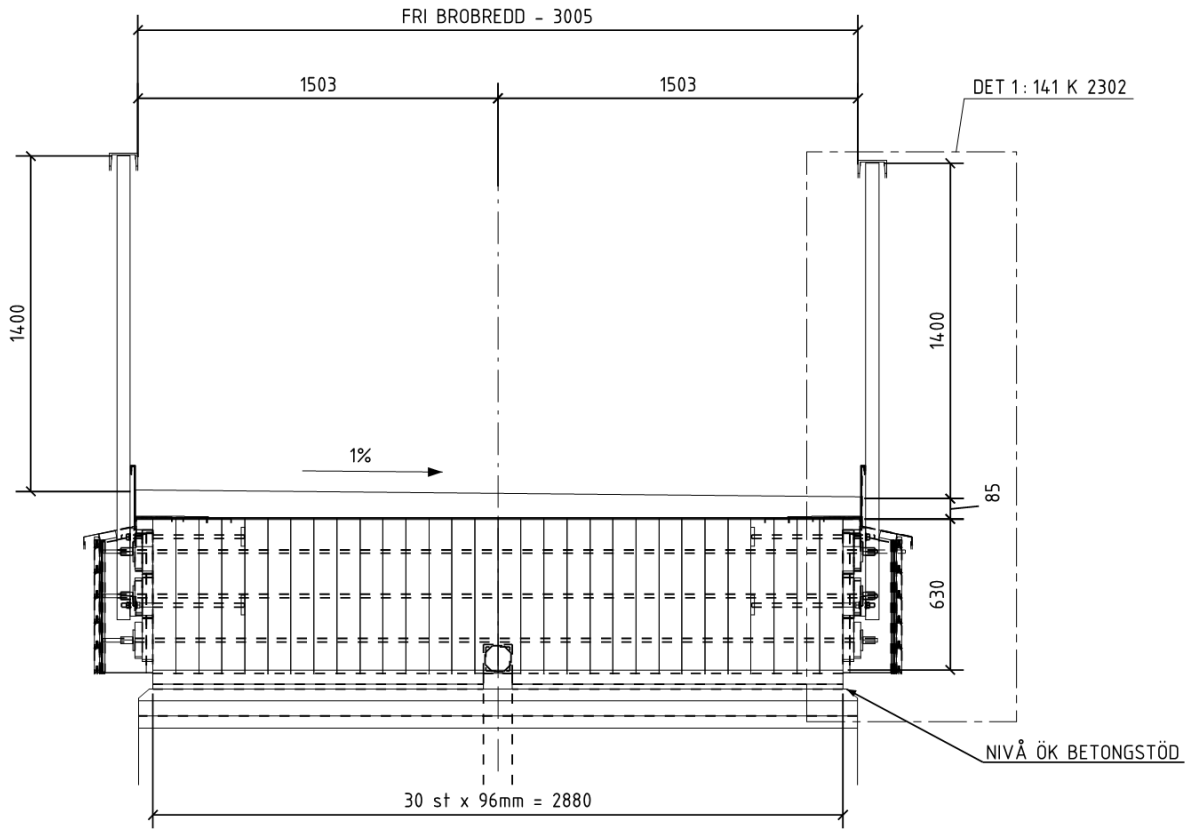

Figure 0.1: Cross section of the reference bridge.

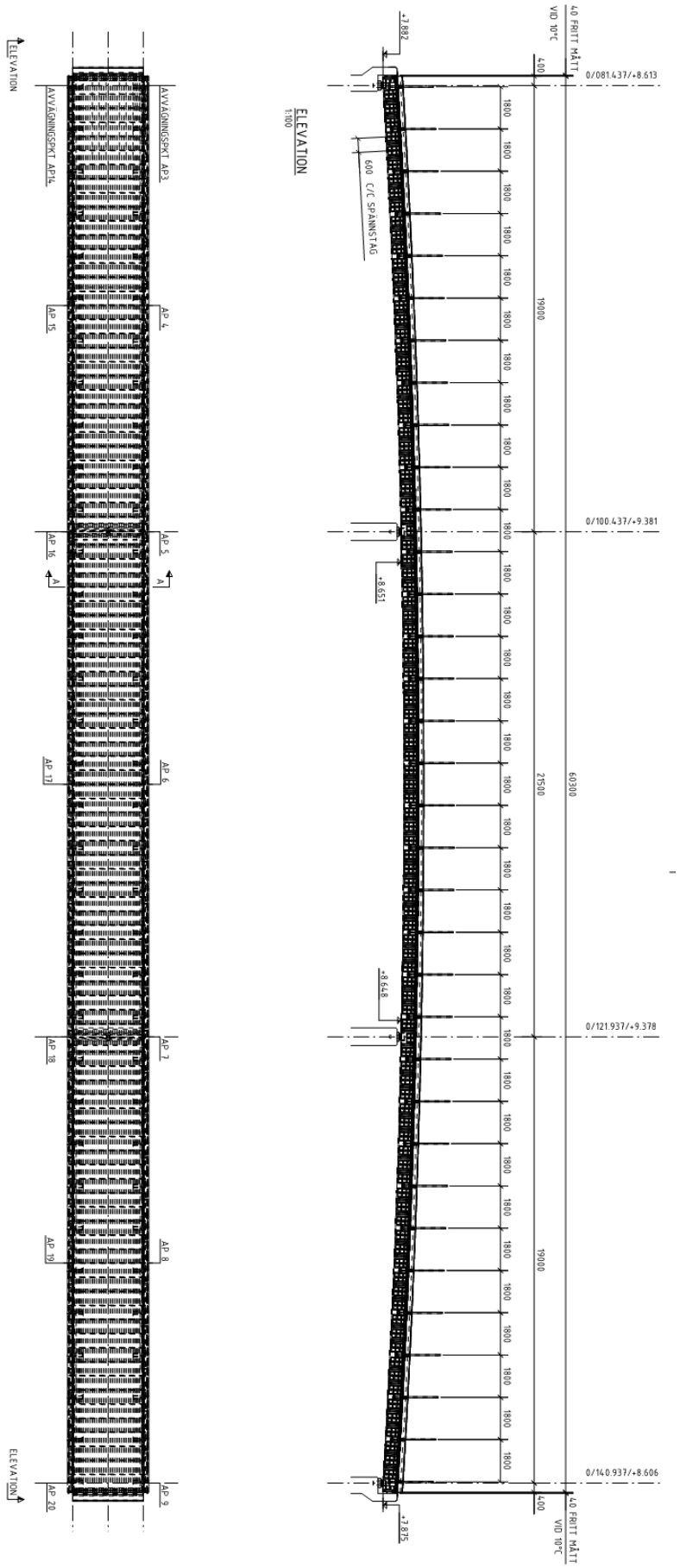

Figure 0.2: Design specification of reference bridge.

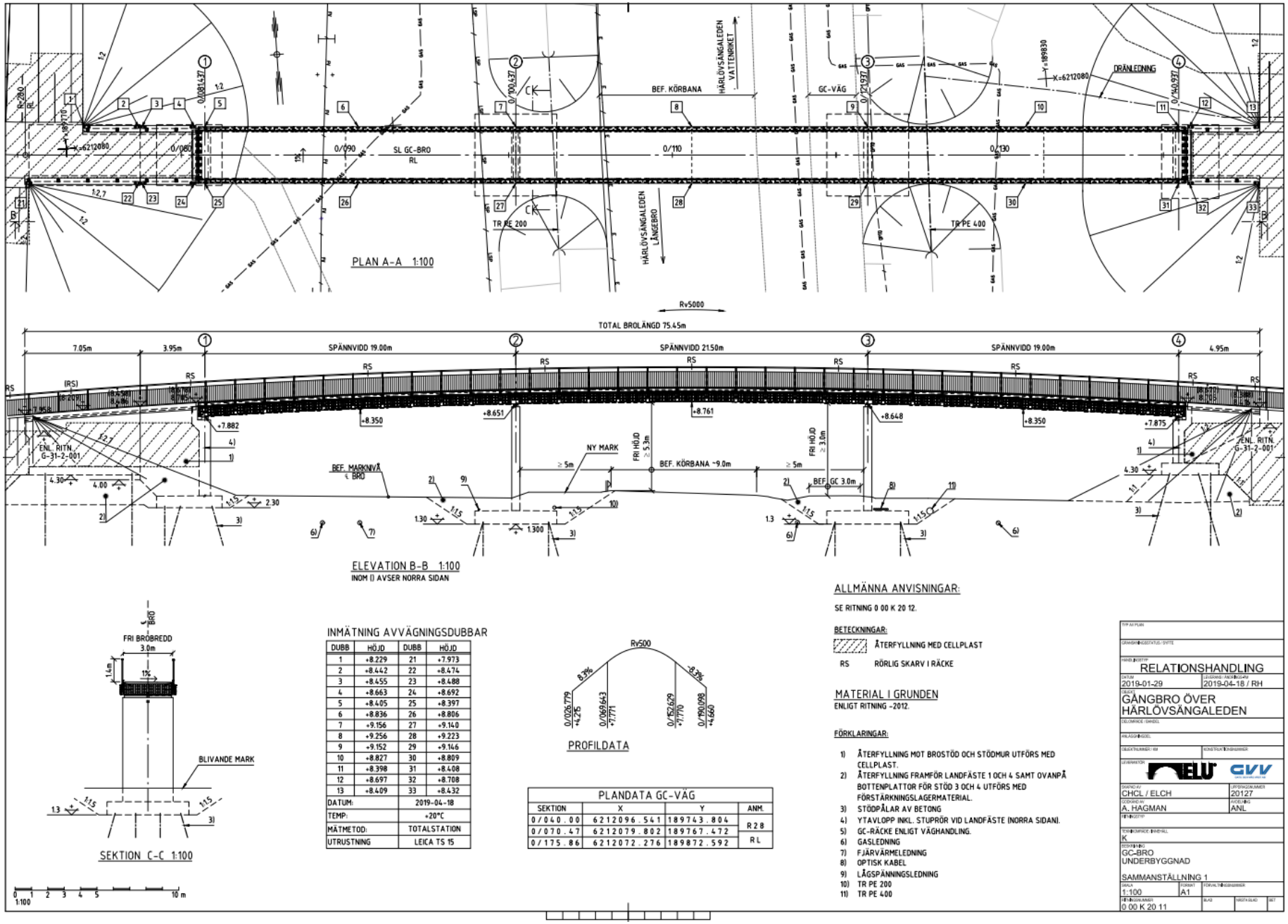

INMÄTNING AVVÄGNINGSDUBBAR

DUBB	HÖJD	DUBB	HÖJD
1	+8.229	21	+7.973
2	+8.442	22	+8.474
3	+8.455	23	+8.488
4	+8.663	24	+8.692
5	+8.405	25	+8.397
6	+8.836	26	+8.806
7	+9.156	27	+9.140
8	+9.256	28	+9.223
9	+9.152	29	+9.146
10	+8.827	30	+8.809
11	+8.398	31	+8.408
12	+8.697	32	+8.708
13	+8.409	33	+8.432
DATUM:		2019-04-18	
TEMP:		+20°C	
MÄTMETOD:		TOTALSTATION	
UTRUSTNING		LEICA TS 15	

PLANDATA GC-VÄG

SEKTION	X	Y	ANM.
0/040.00	6212096.541	189743.804	R 28
0/070.47	6212079.802	189767.472	
0/175.86	6212072.276	189872.592	RL

ALLMÄNNA ANVISNINGAR:

SE RITNING 0 00 K 20 12.

BETECKNINGAR:

ÅTERFYLLNING MED CELLPLAST

RS RÖRLIG SKARV I RÄCKE

MATERIAL I GRUNDEN

ENLIGT RITNING -2012.

FÖRKLARINGAR:

1) ÅTERFYLLNING MOT BROSTÖD OCH STÖDMUR UTFÖRS MED CELLPLAST.
2) ÅTERFYLLNING FRAMFÖR LANDFÄSTE 1 OCH 4 SAMT OVANPÅ BOTTENPLATTOR FÖR STÖD 3 OCH 4 UTFÖRS MED FÖRSTÄRKNINGSLAGERMATERIAL.
3) STÖDPÅLAR AV BETONG
4) YTAVLOPP INKL. STUPRÖR VID LANDFÄSTE (NORRA SIDAN).
5) GC-RÄCKE ENLIGT VÄGHANDLING.
6) GASLEDNING
7) FJÄRVÄRMELEDNING
8) OPTISK KABEL
9) LÅGSPÄNNINGSLEDNING
10) TR PE 200
11) TR PE 400

RELATIONSHANDLING

2019-01-29 | 2019-04-18 / RH

GÅNGBRO ÖVER HÄRLÖVSÄNGALEDEN

ELU | CVV

CHCL / ELCH | 20127

A. HAGMAN | ANL

K

GC-BRO
UNDERBYGGNAD

SAMMANSTÄLLNING 1

1:100 | A1

0 00 K 20 11

Figure 0.3: Design overview of the reference bridge.

Appendix B

Live load inputs used in BRIGADE/Plus are presented in figures 10.4 and 10.5.

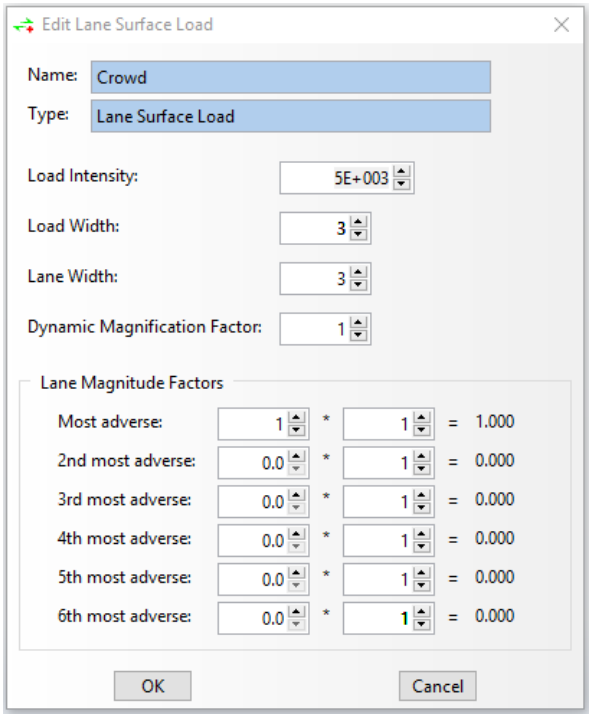

Figure 0.4: Definition of crowd load in BRIGADE/Plus.

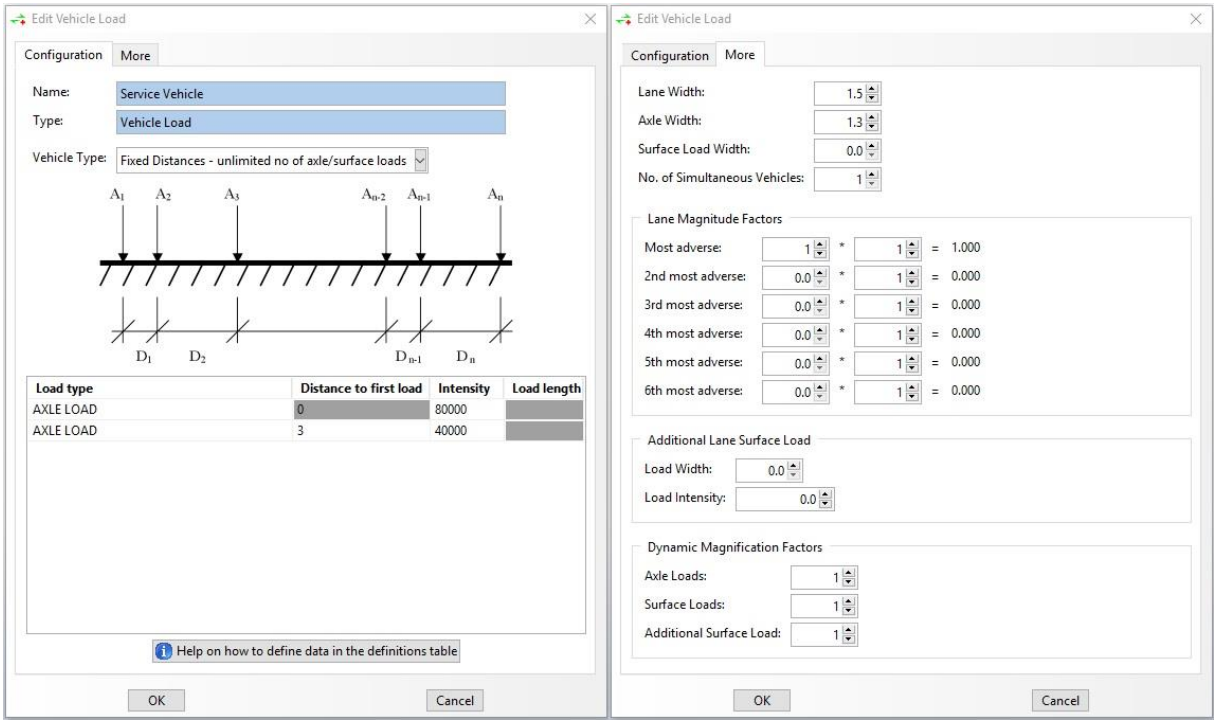

Figure 0.5:Definition of service vehicle in BRIGADE/Plus.

Appendix C

Results of strength verifications, specifically Tsai-Hill, of each FRP bridge are presented in the following subsections.

Layup – GFRP

Figures 10.6 – 10.8 show the results of the strength verification made for the GRFP produced using a layup method.

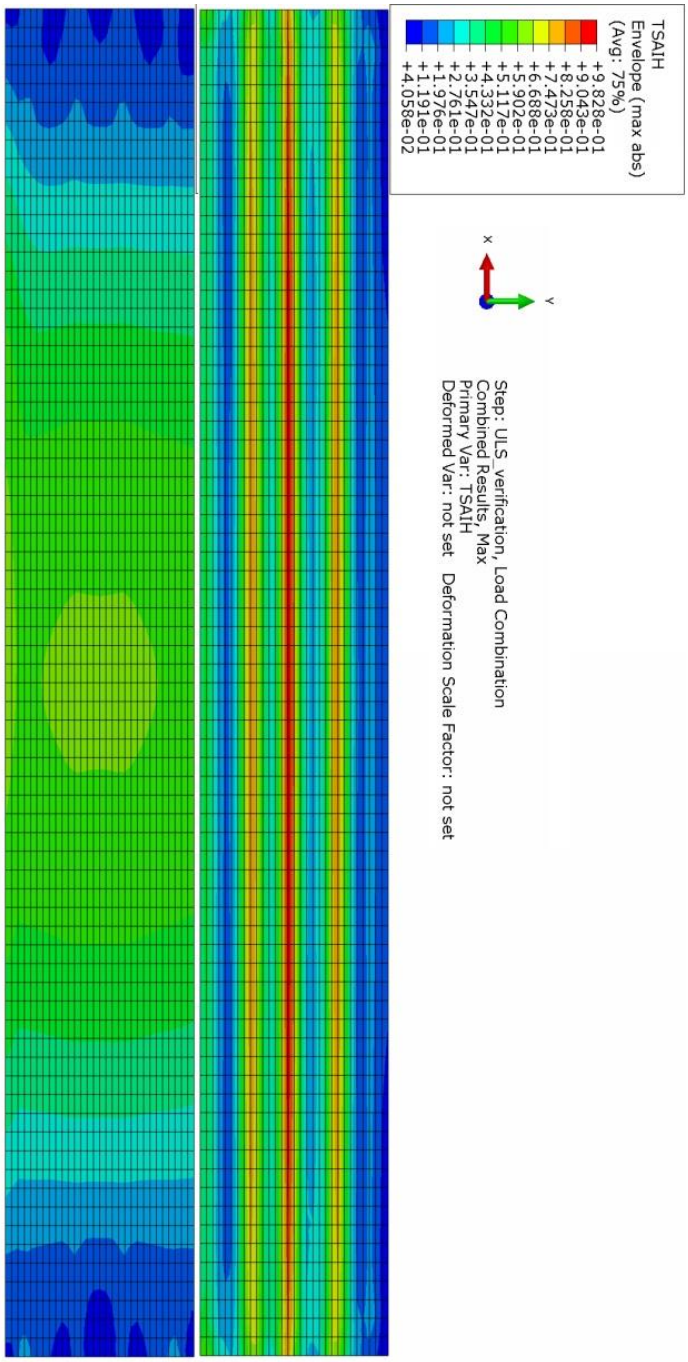

Figure 0.6: Tsai-Hill, Bottom and top-layup.

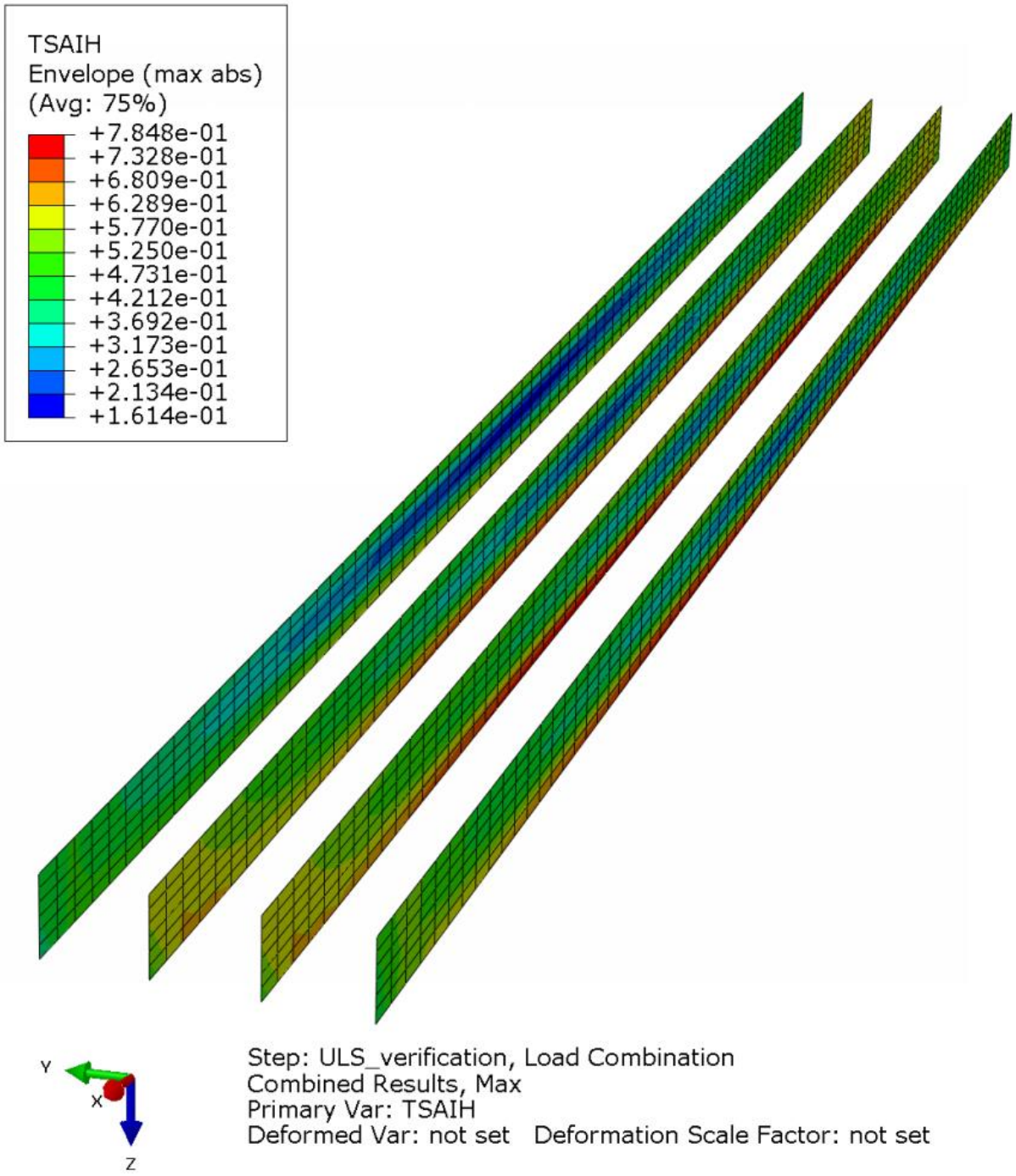

Figure 0.7: Tsai-Hill. Web-layup.

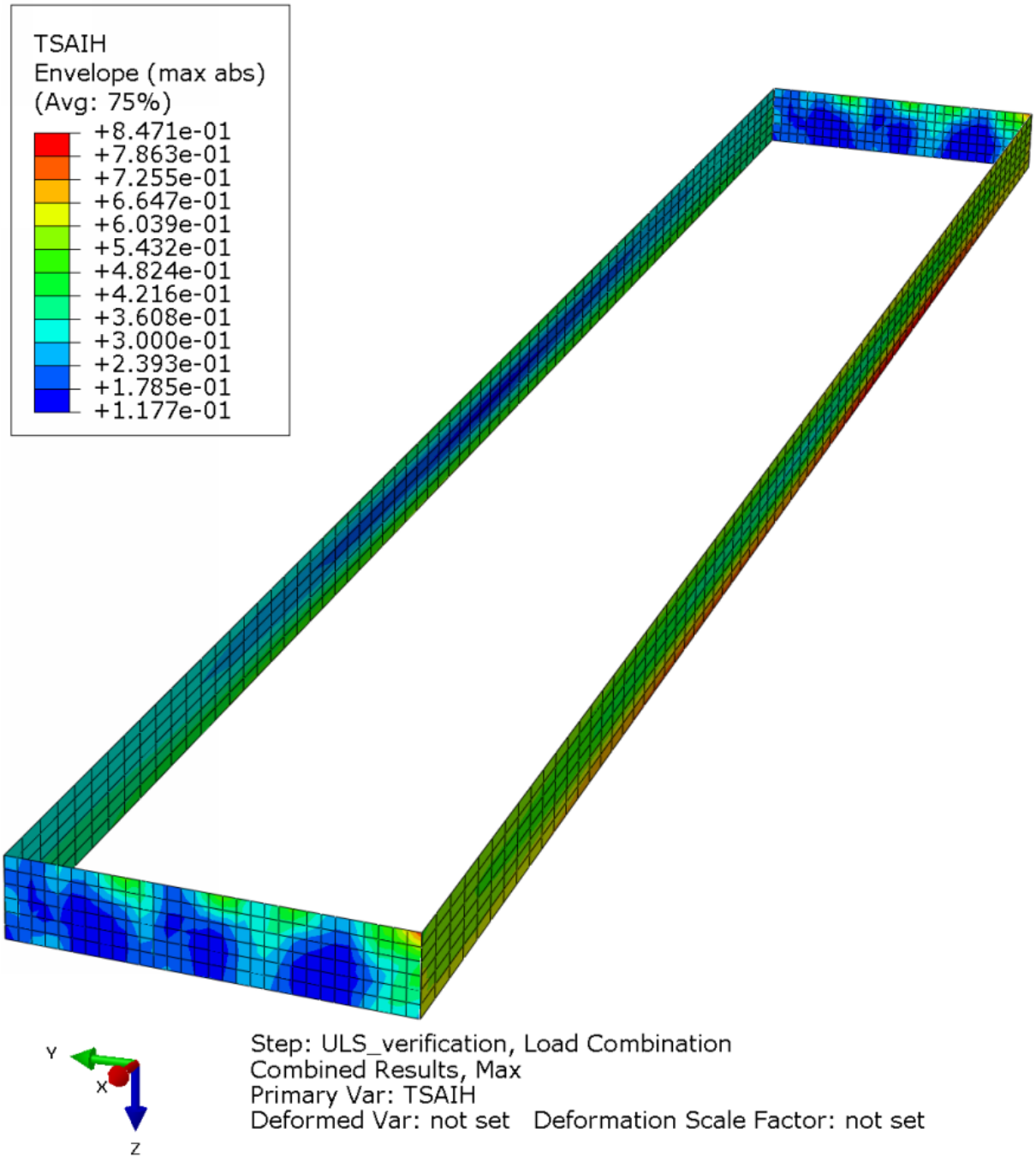

Figure 0.8: Tsai-Hill. Sides-layup

Layup – CFRP

Figures 10.9 – 10.11 show the results of the strength verification made for the CRFP produced using a layup method.

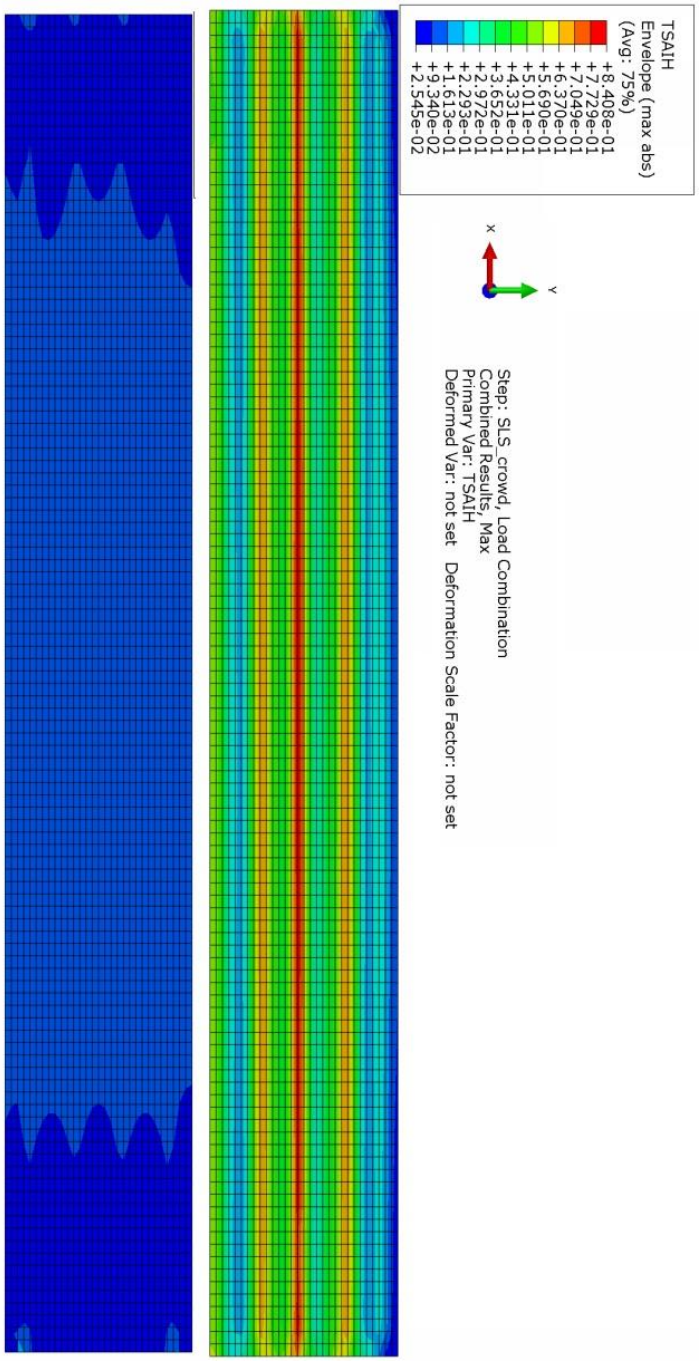

Figure 0.9: Tsai-Hill. Bottom and top-layup

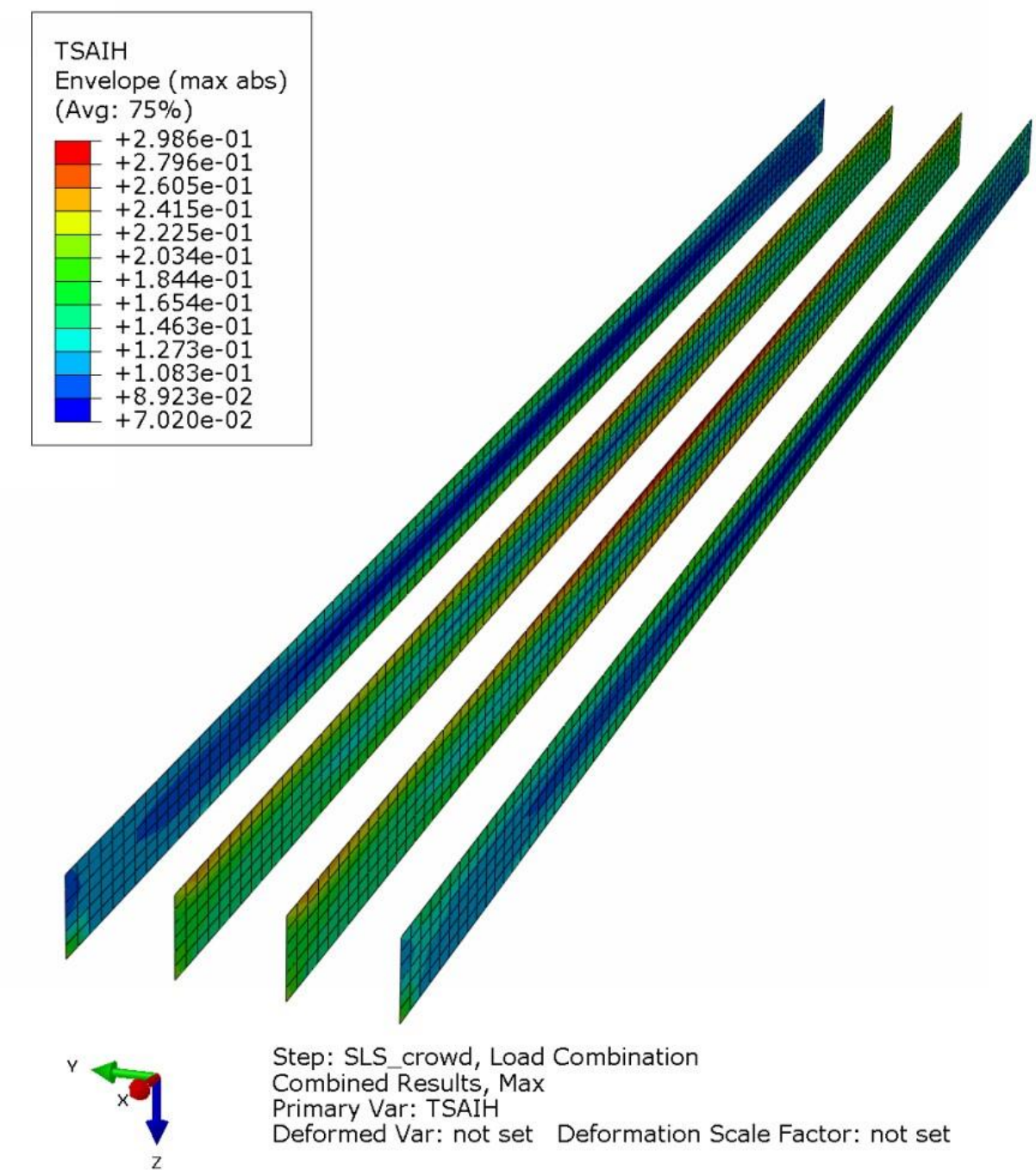

Figure 0.10: Tsai-Hill. Web-layup.

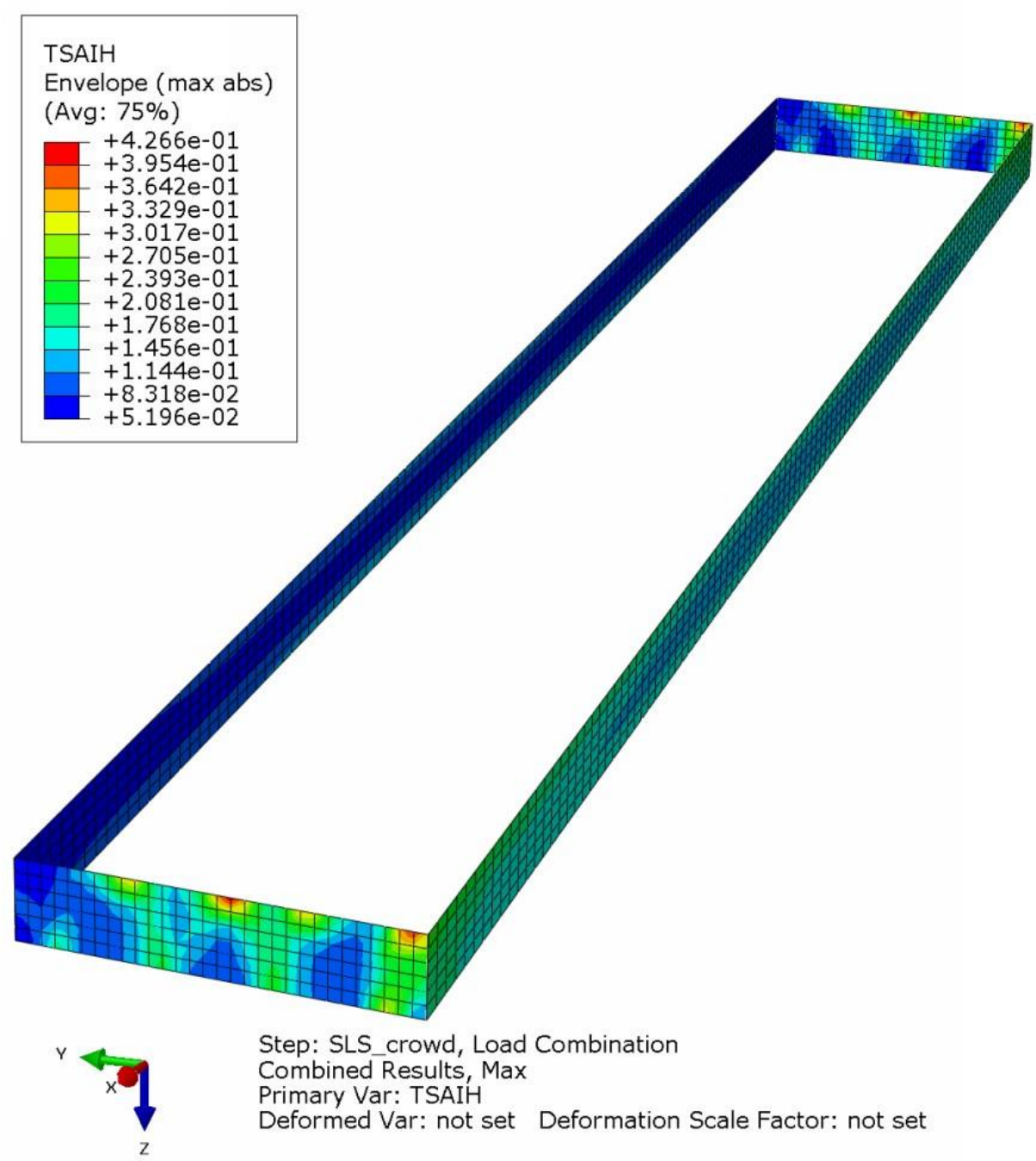

Figure 0.11: Tsai-Hill. Sides-layup.

Pultrusion – GFRP

Figures 10.12 – 10.14 show the results of the strength verification made for the GRFP produced using pultrusion.

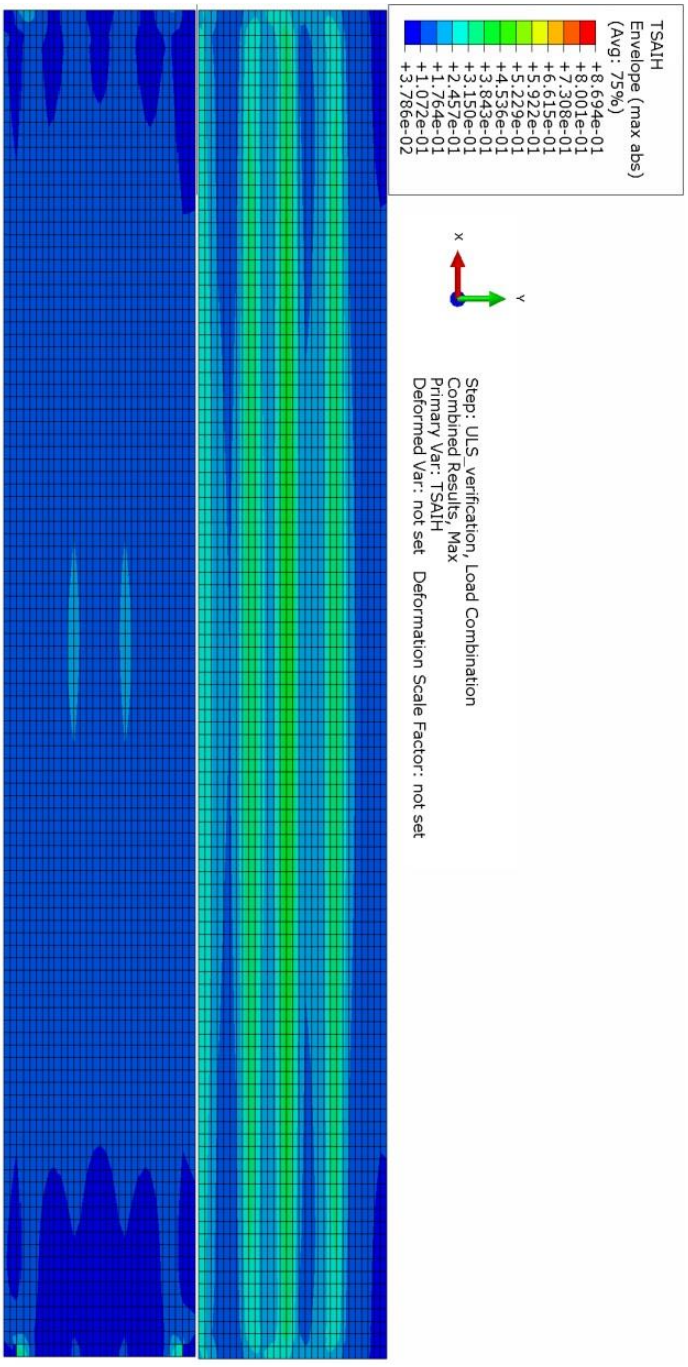

Figure 0.12: Tsai-Hill. Bottom and top-layup.

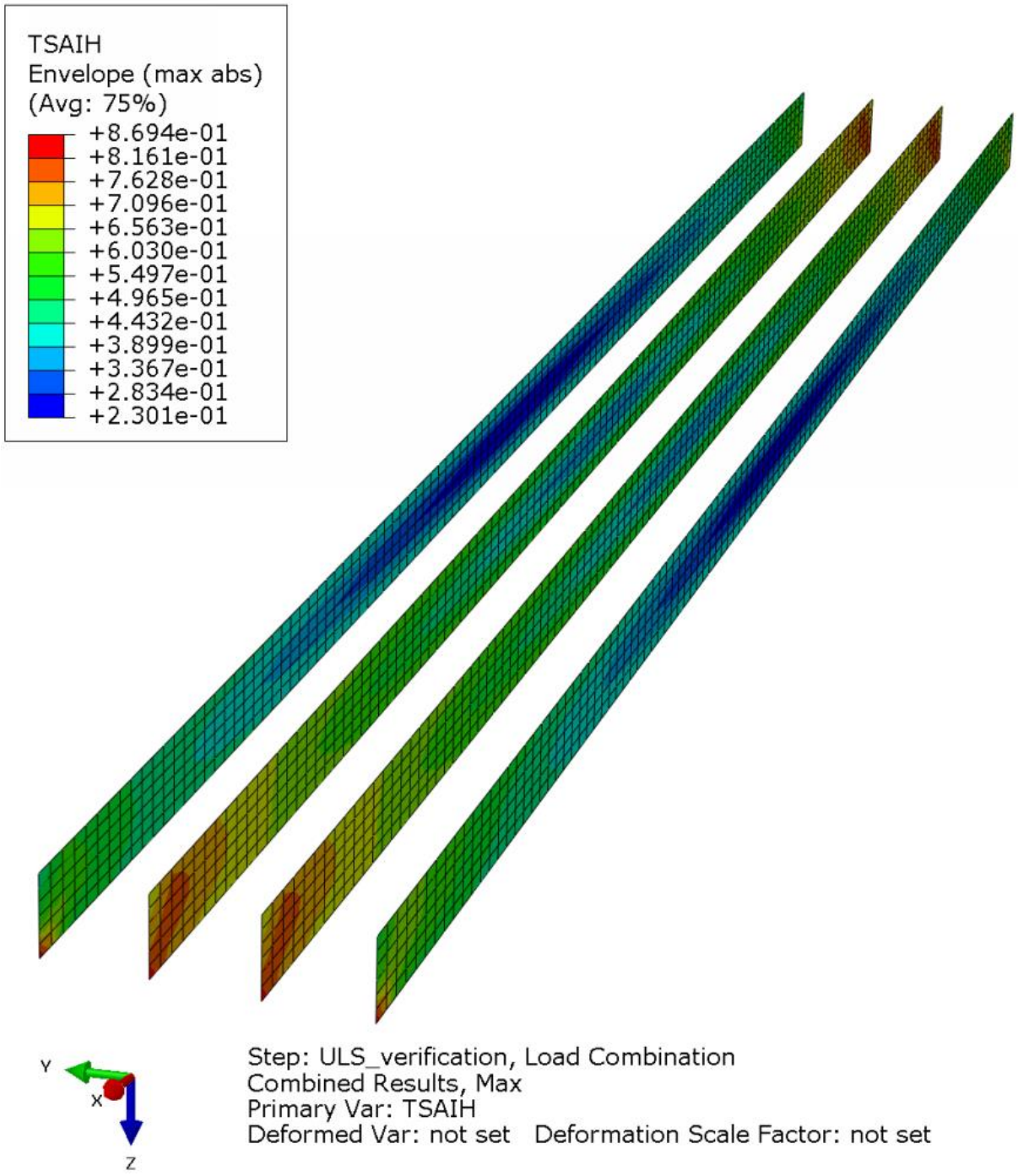

Figure 0.13: Tsai-Hill. Web-layup.

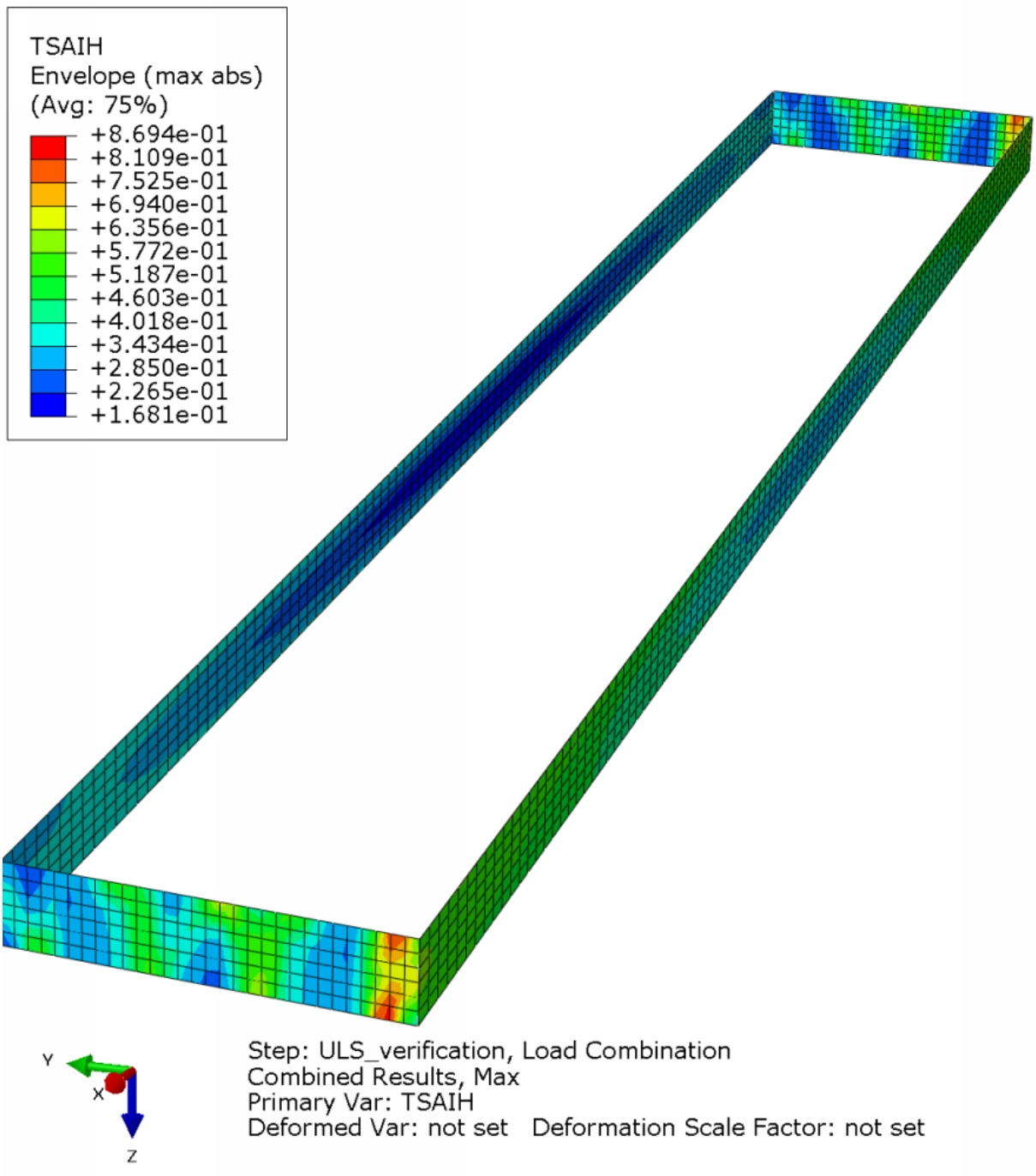

Figure 0.14: Tsai-Hill. Sides-layup.

Appendix D

Dynamic responses of Sétra analysis.

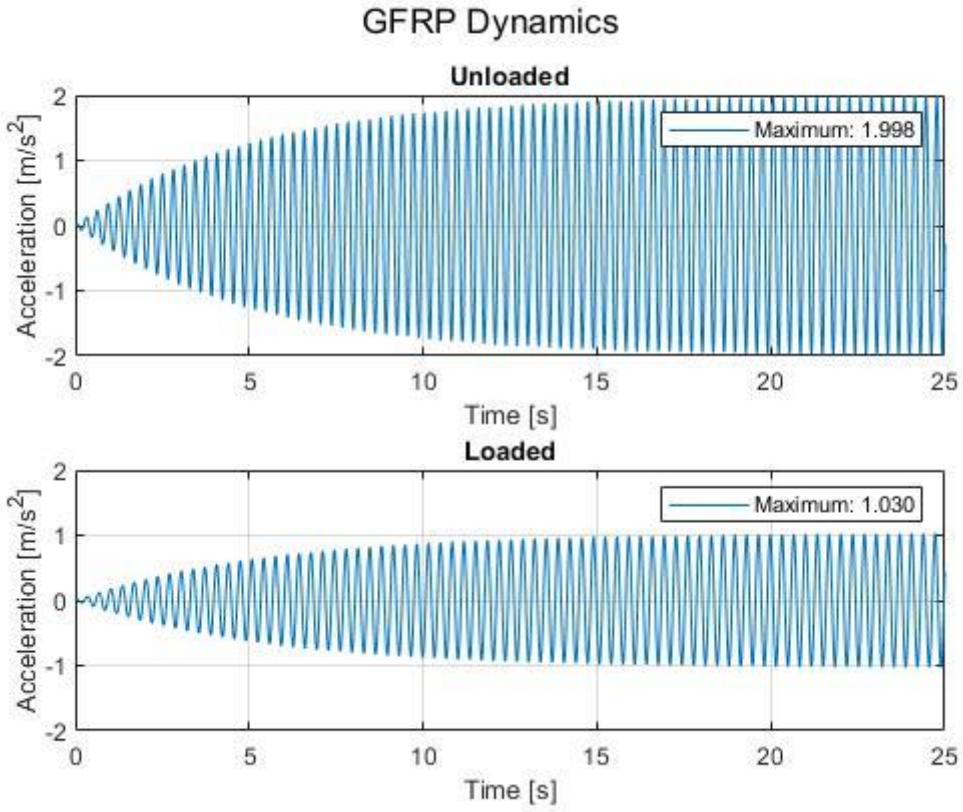

Figure 0.15: GFRP dynamic response.

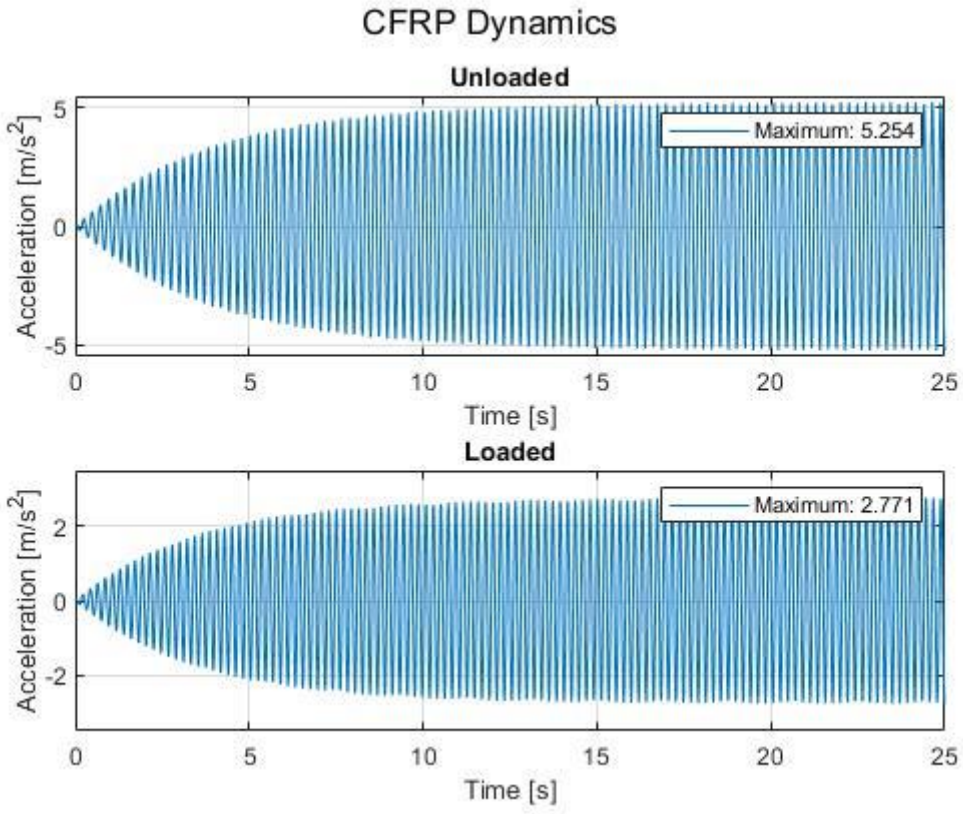

Figure 0.16: CFRP dynamic response.

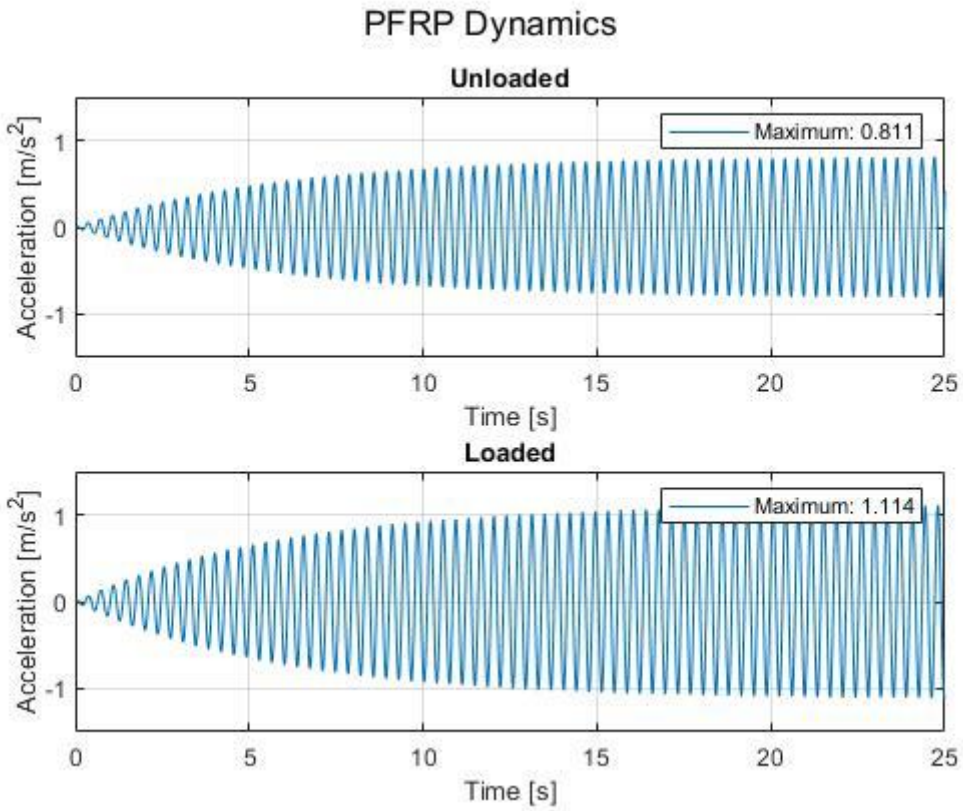

Figure 0.17: Pultruded GFRP dynamic response.

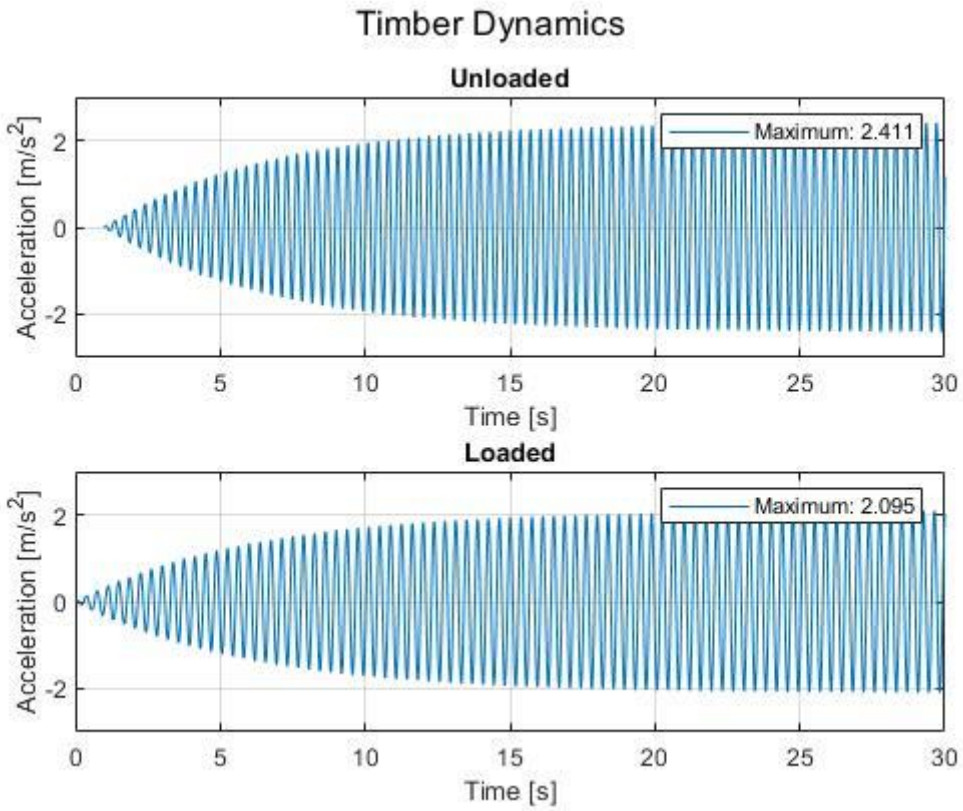

Figure 0.18: Timber dynamic response.